

UCSF

UC San Francisco Electronic Theses and Dissertations

Title

Mechanisms underlying synaptic plasticity in area of the hippocampus

Permalink

<https://escholarship.org/uc/item/1mm6r97m>

Author

Hjelmstad, Gregory O.

Publication Date

1997

Peer reviewed|Thesis/dissertation

Mechanisms Underlying Synaptic Plasticity in Area CA1 of the Hippocampus

by

Gregory O. Hjelmstad

DISSERTATION

Submitted in partial satisfaction of the requirements for the degree of

DOCTOR OF PHILOSOPHY

in

Neuroscience

in the

GRADUATE DIVISION

of the

UNIVERSITY OF CALIFORNIA

San Francisco

Approved:

David R. Copenhagen

Roger Nicoll

John B. San

Samuel J.

Robert C. Malenka

Committee in Charge

Deposited in the Library, University of California, San Francisco



Acknowledgements

It is not easy to list all of the people who have supported me over the course of my studies at UCSF. First, my graduate advisor, Rob Malenka, has created an environment where I was able to flourish. I appreciated Rob's intelligence and enthusiasm for science during our first meeting, while I was interviewing with the Neuroscience Graduate Program. What I have learned is that this enthusiasm is balanced with a true concern for the people around him. I would also like to thank Roger Nicoll, who, through his collaboration with Rob, has become a second advisor to me.

I am indebted to the members, past and present, of the lab who, on a daily basis, have been integral to my education: John "Guitar-man" Isaac, Rosel Mulkey, Saleem Nicola, Jennifer Cummings, David Selig, Reed Carroll, Dan Feldman, "Little Mario" Tzanopolous, Mike Crair, and Diane Spillane. Also, the members of the Nicoll lab (in no particular order): Stephane, Massimo, Pierre-Marie, Pablo, Paul, Gang, Carl, Chad, Matt, Albert, Steve, Christian, and Kaspar.

I would also like to thank the members of my thesis committee: David Copenhagen, Peter Sargent, and Craig Jahr; the students in the Neuroscience Program; of course, my family, whose love and support is felt across the miles; Dr. David Bodznick, who introduced me to electrophysiology; and finally, Coach K and the Blue Devils, who keep me sane during the winter and insane during March.

Most importantly, I want to thank Holly, who has been with me throughout with encouragement, understanding, humor and affection. I wouldn't be here without you.

Mechanisms underlying Synaptic Plasticity in area CA1 of the Hippocampus

Gregory Olaf Hjelmstad

Despite extensive research, the mechanisms underlying expression of long-term potentiation (LTP) have remained elusive. Specifically, it is unclear whether LTP is due to an increase in the quantal amplitude (q), the probability of release (p_r), the number of active release sites (n), or some combination of these parameters. In this study, we have taken a number of approaches using both extracellular and whole-cell recording techniques in the hippocampal slice preparation to address this issue.

We have compared the effects of LTP and long-term depression (LTD) on two subtypes of ionotropic glutamate receptor, termed α -amino-3-hydroxy-5-methyl-4-isoxazolepropionic acid (AMPA) and N-methyl-D-aspartate (NMDA) receptors. Our results indicate that LTP and LTD are not due to a presynaptic change acting on co-localized receptors.

We have also shown that activated Ca²⁺/calmodulin dependent kinase II (CaM Kinase II), when injected into the postsynaptic cell, causes an enhancement which mimics LTP. This enhancement causes a decrease in the synaptic failure rate, indicating a change in p_r or n , but also an increase in the size of spontaneous EPSCs, indicating an increase in q .

These same changes were seen with pairing-induced LTP at putative single-site recordings. Furthermore, the change in failures was more consistent with a change n than

with p_r . In contrast to some reports (Stevens and Wang, 1994; Bolshakov and Siegelbaum, 1995), we saw no evidence for a change in p_r alone accounting for LTP.

Finally, we have examine whether p_r changes with LTP using a measure that assays the proportion of synapses that are refractory following a stimulus, which should be equivalent to the mean p_r . Again, we see no evidence for a change in p_r with LTP or with LTD. Furthermore, LTP does not interact with a pharmacological manipulation that increases p_r , which would be expected if LTP were due to an increase in p_r .

In conclusion, these data indicate that LTP is associated with both a change in q and n , but not a change in p_r . These changes are consistent with a model where AMPA receptors are inserted into both functional (AMPA containing) and silent (NMDA-only) synapses.

UCSF LIBRARY

Advisors Statement

The projects presented in chapters 3-5 of this thesis were conducted in collaboration with other authors.

The data presented in Chapter 3 were collected by Greg along with two postdoctoral fellows from the laboratory: David Selig and Caroline Herron. Specifically, Greg collected the data in figures 6, 8 and 9 and made significant contributions to the discussion. This work has been published (Selig et al., 1995).

The work in Chapter 4 was performed in collaboration with Pierre-Marie Lledo, a postdoctoral fellow in Roger Nicoll's lab as well as Sucheta Mukherji, a member of Thomas Soderling's laboratory at the Vollum Institute in Portland, Oregon. Greg was responsible for the minimal stimulation experiments examining the effects on the synaptic failure rate. This work has been published (Lledo et al., 1995).

Finally the work in Chapter 5 was conducted with John Isaac, a postdoctoral fellow in the lab. Greg assisted in the data collection of standard whole-cell recordings. Both Greg and John made significant intellectual contributions to the development of this project. This work has been published (Isaac, et al, 1996).

Robert C. Malenka
11/12/97

UCSF LIBRARY

Chapter Four	CaM-kinase II and LTP enhance synaptic transmission by the same mechanism.....	60
	Summary	61
	Introduction	61
	Methods.....	62
	Results	64
	Discussion	68
Chapter Five	Long-term potentiation at single fiber inputs to hippocampal CA1 pyramidal cells	87
	Summary	88
	Introduction	88
	Methods.....	90
	Results	92
	Discussion	98
Chapter Six	Synaptic refractory period provides a measure of probability of release in the hippocampus	120
	Summary	121
	Introduction	121
	Methods.....	123
	Results	124
	Discussion	132
	Appendix	136
Chapter Seven	General conclusions	166

UCSF LIBRARY

List of Figures

Chapter Two.

- Figure 1. Image of CA1 region of hippocampus..... 21
- Figure 2. Illustration of computer-derived data set..... 23
- Figure 3. Effects of different analysis methods on the S/N ratio and r^2 for the computer-derived data sets 25
- Figure 4. Effects of different analysis methods on the S/N ratio and noise offset for recorded data sets..... 27
- Figure 5. Effects of spontaneous noise on measurements..... 29

Chapter Three.

- Figure 6. LTD of the isolated NMDAR EPSP can be induced by low-frequency stimulation and is input specific..... 46
- Figure 7. LTD of the isolated NMDAR EPSP requires a rise in postsynaptic Ca^{2+} 48
- Figure 8. The NMDAR EPSP is on average the same between two inputs..... 50
- Figure 9. Changes in the NMDAR EPSP following generation of LTD and LTP under normal conditions..... 52
- Figure 10. $1/CV^2$ of AMPAR EPSCs but not NMDAR EPSCs changes during LTD and LTP..... 54
- Figure 11. $1/CV^2$ of pharmacologically isolated NMDAR EPSCs is unaffected following generation of LTD..... 56

UCSF LIBRARY

Figure 12. Synaptic activity can depress the NMDAR EPSP without affecting the AMPAR EPSP.....	58
---	----

Chapter Four.

Figure 13. Perfusion of the Dye Fast Green occurs in 8-10 Minutes.....	71
Figure 14. The Activated Form of CaM-kinase II Potentiates Evoked EPSCs Recorded in Hippocampal CA1 Neurons.....	73
Figure 15. Individual Example showing the effects of CaM-kinase II perfusion on EPSCs evoked with minimal stimulation	75
Figure 16. CaM-kinase II induced potentiation is associated with a change in the number of synaptic failures	77
Figure 17. Postsynaptic sensitivity to AMPA is increased by CaM-kinase II....	79
Figure 18. CaM-kinase II-induced potentiation of evoked EPSCs is occluded at synapses expressing saturated LTP.....	81
Figure 19. Summary data showing occlusion of LTP by the CaM-kinase II-induced potentiation.....	83
Figure 20. Summary data from occlusion experiments examining LTP at synapses already potentiated by activated CaM-kinase II.....	85

Chapter Five.

Figure 21. LTP monitored with whole-cell recording and minimal stimulation is associated with an increase in potency.....	102
Figure 22. Summary data for eight whole-cell experiments	104
Figure 23. Example of a single axon stimulation test monitored with perforated patch recording.....	106

Figure 24. Example of LTP monitored with perforated patch recording and single axon stimulation that was associated with an increase in potency and no decrease in failure rate 108

Figure 25. Example of LTP monitored with perforated patch recording and single axon stimulation that was associated with an increase in potency and a decrease in failure rate 110

Figure 26. Paired pulse stimulation indicates an increase in n during LTP..... 112

Figure 27. Summary data for all eight perforated patch LTP experiments 114

Figure 28. LTP can be induced even when p_r is high..... 116

Figure 29. Summary graph of five experiments in 5 mM Ca^{2+} 118

Chapter Six.

Figure 30. Minimal stimulation reveals a synaptic refractory period..... 138

Figure 31. Computer simulations illustrate the sensitivity of paired pulse intervals to changes in p_r for multiple site recordings..... 140

Figure 32. Computer analysis of changes in the number of release sites..... 142

Figure 33. Actual data is fit well by the calculated curve..... 144

Figure 34. Estimate of a possible error in the calculation of p_r (p_{calc}) due to the variability in p_r from site to site..... 146

Figure 35. The potassium channel blocker 4-AP causes an increase in the calculated p_r 148

Figure 36. P_{calc} changes following application of 10 μ M CPT..... 150

Figure 37. Cadmium decreases both the EPSC amplitude and p_{calc} 152

Figure 38. Increasing the stimulus intensity has no effect on p_{calc} 154

Figure 39. Application of 200 μ M EGTA-AM, which decreases PPF causes a decrease in p_{calc}	156
Figure 40. Long-term potentiation has no effect on p_{calc}	158
Figure 41. Long-term depression has no effect on p_{calc}	160
Figure 42. Summary of all manipulations plotted as the ratio of p_{calc}	162
Figure 43. Long-term potentiation does not interact with a manipulation increasing p_r	164

UCSF LIBRARY

CHAPTER ONE
INTRODUCTION

UCSF LIBRARY

A brief survey of the history of synaptic plasticity

Towards the end of the 19th century, the pragmatist William James put forward the basic premise that “the phenomena of habit in living beings are due to the plasticity of the organic materials of which their bodies are composed.” (James, 1890). In other words, there is a biological basis underlying, and, in fact, responsible for the formation of our habits. So, too, learning processes and the formation of memory are based on similar biological plasticity. But how should this plasticity take place... and specifically where?

This question is not new and merits a historical review. Certainly, the metaphor for plasticity that James invoked, of learning as the wearing down of a pathway, was not particularly novel. As we will see, it shows up in the thinking of Descartes. What is more important was James’ materialistic localization of this metaphor to the biology of the brain.

The localization of the memory to the brain can be traced back to the 5th century BC when the Greek scholar, Alcmaeon, localized both sensory perception and thought to the brain (Finger, 1994). Plato, also, placed his “rational soul”, the part of the soul responsible for memory and learning, in the brain. For several hundred years though, this would be a minority view. Most, including Aristotle, felt that the mind was, in fact, situated around the heart.

This viewpoint dominated until the 2nd century AD, when the physician Galen wrote extensively about the brain and argued strongly against the cardiocentric view. His arguments were accompanied by compelling experimental data:

...If you press so much upon a [cerebral] ventricle that you wound it, immediately the living being is without movement and sensation, without spirit and voice, not otherwise than is seen to happen in men whose heads have been pierced. ...lest if we press the brain a little too much, the victim is rendered without sensation and without all voluntary movement; this does not happen if we press the naked heart. (in Clarke and O'Malley, 1996; p. 16)

Specifically, Galen felt that “it seems to be acceptable that the soul itself resides in the body of the brain where it produces reasoning, and the memory of sensible images is preserved there.”

Galen's teachings were preserved throughout the Middle Ages, but his conclusion that the tissue of the brain is the seat of the soul would not persist. Instead, the theory that prevailed for over a thousand years, well into the 17th century, was that the mental functions of sensation, imagination and memory are stored in animal spirits which were divided between the different ventricles of the brain.

The 17th century would see a fundamental shift in the study of the brain, due primarily to Rene Descartes. The work of Descartes played an important role in all subsequent philosophy of mind and towards the development of neuroscience. His view that the nervous system acts in a machinelike fashion was a stepping stone for the philosophies of materialism that would follow. In fact, we can see premonitions of William James in Descartes' concept regarding the recollection of memory:

Thus when the soul desires to recollect something, this desire causes the gland, by inclining successively to different sides, to thrust the spirits towards different parts of the brain until they come across that part where the traces left there by the object which we wish to recollect are found; for these traces are none other than the fact that the pores of the brain, by which the spirits have formerly followed their course because of the presence of this object, have by that means acquired a greater facility than the others in being once more opened by the animal spirits which come towards them in the same way. (Descartes, 1649/1931).

Interestingly, Descartes did not extend this materialism to the conscience experience. While he viewed animals as merely automata, his human machine required a controller, or a soul, which interacted with the brain, was influenced by the brain, but was fundamentally separate from the brain. Descartes placed this point of interaction between the mind and the brain in the pineal gland.

Thomas Willis, a second major figure from the 17th century, did not agree with Descartes' concept of the mind. Willis, who had trained as a doctor, argued that the actions of memory and the mind are situated in the cerebral cortex. Willis, though, perhaps like many in his time, acquiesced to the hegemony of the Church, and relegated to the brain only our corporeal soul, or our animal functions, leaving our higher rational thought to some higher domain (Clarke and Dewhurst, 1996).

As illustrated in the above examples, the philosophy of the mind is obviously constrained by our understanding of the biology of the brain. Over the course of the next two hundred years, considerable development in our understanding of the biology of the brain occurred. Concomitant with this increased understanding came a growing acceptance of materialist philosophies to explain the actions of the mind.

Towards the end of the 18th century, Galvani showed that nerve impulses were electrical in nature, putting an end to the concept of 'animal spirits' flowing through hollow tubes. The study of lesions in patients led to the understanding of localization of brain function (although this viewpoint was carried to an extreme by Joseph Gall and the phrenologists of the late 18th century). The development of microscopy allowed for the visualization of neurons, culminating in the work of Golgi and Ramón y Cajal. Their work, in addition to that of Charles Sherrington, who coined the term "synapse" for the gaps seen between nerves and between nerves and muscle, resulted in the neuron doctrine: the theory that the brain is composed of individual nerve cells, as opposed to a syncytium. From this theory came the concept that the site of plasticity underlying the formation of memory might occur at the site of communication between individual neurons: in other words, at the synapses.

Sherrington also provided us with the first example of synaptic plasticity. Studying the flexion reflex, Sherrington described a decrease in the reflex with repeated stimuli. Sherrington showed that there was no change in the muscle or in the motoneuron innervating it. Therefore, he concluded that the change was due to fatigue in the specific synapses onto the motoneuron that were being stimulated. (Sherrington, 1906).

A second form of synaptic plasticity was described during the 1940's at a wide variety of synapses including the neuromuscular junction (Feng, 1941), sympathetic ganglia (Larabee and Bronk, 1947), and spinal cord (Lloyd, 1949). The basic phenomenon had, in fact, been described in 1858 by J. M. Schiff (described in Hughes, 1958) prior to the discovery of the synapse. Simply, following a tetanus, or a high-frequency train of stimuli, there appeared to be a brief increase in the synaptic transmission as monitored by the excitatory postsynaptic potential (EPSP) to a single stimulus. This potentiation typically lasted on the time scale of seconds to minutes and was termed post-tetanic potentiation (PTP). It would later be shown that PTP is due to an increase in transmitter release (del Castillo and Katz, 1954b) due to an accumulation of calcium in the nerve terminal (for review see Zucker, 1989). At the time, this was considered a potential mechanism to describe learning (Hughes, 1958).

With the rise of behaviorism in the 20th century, came an increased understanding of learning processes, specifically, that of classical conditioning. Donald Hebb (1949) synthesized these developments with the current understanding of the brain, and put forward a theory for neuronal plasticity:

When an axon of cell A is near enough to excite a cell B and repeatedly or persistently takes part in firing it, some growth process or metabolic change takes place in one or both cells such that A's efficiency, as one of the cells firing B, is increased. (p. 62)

In other words, to adequately describe learning, a model mechanism should require the coincident activity of both the pre- and postsynaptic cell. While not excluding the incontrovertible relevance of both neuronal fatigue and PTP to behavior, neither possesses this property nor do they act on the time scale necessary to correlate with memory.

It was not until 1973 that a long lasting form of synaptic plasticity fitting Hebb's design was actually described in the mammalian central nervous system (Bliss and Lømo, 1973). Using a high-frequency tetanus similar to that given to elicit PTP, Bliss and Lømo found a synaptic enhancement between the axons of the perforant path and the granule cells of the dentate gyrus which could last for several hours. This form of plasticity would later be called long-term potentiation (LTP) and has remained the most plausible form of synaptic plasticity to underlie learning and memory.

Properties of Long Term Potentiation

Since LTP was first reported, it has subsequently been described at a large variety of excitatory synapses. Most of the research has focused on the synapses between the Schaffer collateral/commissural fibers and the pyramidal cells of the CA1 region of the hippocampus and many of the properties and underlying mechanisms of LTP at this synapse have been elucidated (Bliss and Collingridge, 1993; Malenka and Nicoll, 1993).

It has been shown that activation of the NMDA receptor is necessary in the triggering of LTP (Collingridge et al., 1983). Furthermore, it has been established that it is the calcium permeability of the NMDA receptor that is important, and that LTP requires a postsynaptic rise in intracellular calcium (Lynch et al., 1983; Malenka et al.,

1988). In fact, LTP can be mimicked by artificially increasing Ca^{2+} in the postsynaptic cell (Malenka et al., 1988; Neveu and Zucker, 1996).

The properties of the NMDA receptor are consistent with it being involved in a Hebbian form of plasticity. To activate, the NMDA receptor requires coincidentally, binding of glutamate and depolarization, which is required to remove Mg^{2+} from the receptor pore. Thus, the NMDA receptor will only open when the presynaptic cell fires in conjunction with depolarization of the postsynaptic cell.

An understanding of many of the properties that LTP exhibits emerges from an understanding of the function of the NMDA receptor. These basic properties include associativity, cooperativity, and input specificity (Bliss and Collingridge, 1993).

Associativity means that an small input, normally too weak to induce LTP by itself, is potentiated when it is activated simultaneously with a larger input. This occurs because the small input alone is incapable of overcoming the Mg^{2+} block on its NMDA receptors, but this can be removed when the larger input depolarizes the postsynaptic cell.

Cooperativity simply means that two sub-threshold inputs activated simultaneously become superthreshold for both inputs. Again, this is due to the voltage dependence of the NMDA receptors. Finally, LTP is input specific. In other words, an input which is not activated during the tetanus should not be enhanced, because removing the Mg^{2+} from an NMDA receptor is insufficient to activate it—the binding of glutamate to the receptor is also required. It should be noted that the notion of input specificity has come under attack. Recent work claims that following LTP, unpaired inputs onto nearby cells may also get enhanced (Bonhoeffer et al., 1989; Shumann and Madison, 1994). Even unstimulated inputs onto the same postsynaptic cell may be enhanced following LTP

(Engert and Bonhoeffer, 1997). How LTP spreads to these other synapses is unclear, as are the effects of such a phenomenon on neural processing.

The events following the induction of LTP are much less understood. It has been shown that kinase activity is necessary, for LTP is blocked by the non-specific kinase antagonist H-7 (Malenka et al., 1989). Which kinase is important is less clear. Peptide inhibitors to both PKC (Malinow et al., 1989) and calcium/calmodulin-dependent kinase II (CaM-kinase II), (Malenka et al., 1989; Malinow et al., 1989) block LTP. Phorbol esters, which activate PKC, potentiate synaptic transmission (Malenka et al., 1986), but this potentiation has properties not associated with LTP (Muller et al., 1988; Gustafsson, et al, 1988). Furthermore, LTP can be induced in mutant mice lacking the γ subtype of PKC (Abeliovich et al. 1993). On the other hand, LTP is impaired in α -calcium-calmodulin kinase II (CaM KII) mutant mice (Silva et al., 1992), although not completely absent. Furthermore, expression of a constitutively active form of CaM KII using vaccinia virus in acute hippocampal slices showed evidence consistent with an enhancement in synaptic transmission and LTP induction was impaired (Pettit et al., 1994). It is possible that both kinases may play a role in the induction of LTP (Wang and Kelly, 1995).

The final mechanism of expression has remained extremely controversial, specifically whether LTP is due to a change in a pre- or post-synaptic mechanism. One method to resolve this is the use of quantal analysis. Quantal analysis essentially attempts to fit a statistical model to synaptic transmission and is based on the principle that an EPSP is composed of a number of elementary units, or quanta. In synaptic transmission, this elemental unit is considered to be a single synaptic vesicle filled with

neurotransmitter. The basics of quantal analysis were developed by del Castillo and Katz at the neuromuscular junction (Del Castillo and Katz, 1954a), and by Katz and Miledi (Katz and Miledi, 1963) and Motoy Kuno (Kuno, 1964) at central synapses. In this theory, the fundamental components of neurotransmitter release are defined as the quantal amplitude (q) or the size of the postsynaptic response to a single quantum (or vesicle), and the quantal content (m), the number of quanta released. The quantal content can further be divided into (p_r), the probability of release of a quantum at each release site (n).

One measure that is commonly used in quantal analysis is the coefficient of variation (CV), a measure of the variability from trial to trial which gives an approximation of the quantal content ($CV=m^{-0.5}$ if $p_r \ll 1$ and is uniform between sites [del Castillo and Katz, 1954a]). Studies have shown that LTP is accompanied by a decrease in the coefficient of variation (Bekkers and Stevens, 1990; Malinow and Tsien, 1990; Manabe et al., 1993) consistent with an increase in the quantal content.

Another method to estimate the quantal content measures the occurrence of synaptic failures. A standard EPSP is a summation of the variable response of many release sites. By reducing the mean quantal content (e.g. decreasing the stimulus strength, thus lowering the number of release sites), one often observe trials where there is no detectable EPSP. Since the release process is variable, on some occasions following a stimulus, no vesicles are released. The proportion of synaptic failures, or the failure rate can then be used to calculate the mean quantal content. If only a single release is being stimulated (i.e. $n = 1$), the failure rate (p_0) will give a direct measure of p_r ($p_r = 1 - p_0$). On the other hand, if one is stimulating a large number of release sites each with a very low p_r (i.e. a Poisson distribution), then $m = -\ln(p_0)$ (del Castillo and Katz, 1954a).

Most studies agree that LTP can be associated with a decrease in the proportion of synaptic failures (Malinow, 1991; Kullmann and Nicoll, 1992), again, consistent with an increase in the quantal content. Interestingly, LTP does not appear to be exclusively due to an increase in m . There has also been evidence for an increase in the quantal amplitude (Malinow, 1991; Kullmann and Nicoll, 1992; Larkman et al., 1992; Laio et al., 1992). Consistent with this is evidence showing an increase in the amplitude of miniature EPSCs, presumptive unquantal spontaneous events (del Castillo and Katz, 1954a; Boyd and Martin, 1956), following the induction of LTP (Manabe et al., 1992).

There are many caveats about interpreting quantal analysis data, especially at central synapses where the parameters of release have not been well-established (Korn and Faber, 1991; Faber and Korn, 1991; Edwards, 1991). Specifically, difficulties arise in associating changes in quantal parameters to specific pre- or postsynaptic functions (Malenka and Nicoll, 1997). For instance, an increase in the quantal content could be due to an increase in the probability of release at a given synapse, increasing the number of synapses that release glutamate onto the postsynaptic cell (i.e., unmask presynaptically silent synapses) or by uncovering postsynaptic silent synapses. On the other hand, a change in quantal amplitude could be due to a change in the number or properties of the glutamate receptors, or to an increase in the amount of glutamate packaged into each vesicle (provided that the postsynaptic receptors are not saturated by a single vesicle). Nevertheless, a thorough understanding of the quantal changes associated with LTP can be used to narrow the possible mechanisms underlying this phenomenon.

A final property about LTP is that it can be reversed by prolonged low frequency stimulation (LFS). In addition to depotentiating previous LTP, LFS also depresses naïve

pathways in juvenile animals. This phenomenon is called long-term depression (LTD) (Malenka and Nicoll, 1993). LTD, like LTP, requires the activation of NMDA receptors and the influx of Ca^{2+} (Dudek and Bear, 1992; Mulkey and Malenka, 1992). With LTD, the Ca^{2+} influx required is smaller, and appears to activate protein phosphatases as opposed to kinases (Mulkey et al., 1993; Mulkey et al., 1994). Thus, LTD may act by dephosphorylating the same substrate which is phosphorylated during LTP. Because LTD appears to be a direct reversal of LTP, understanding the expression mechanisms of one should provide valuable information about both forms of plasticity.

UCSF LIBRARY

CHAPTER TWO

GENERAL METHODS

UCSF LIBRARY

Specific methods are provided within each chapter, but a number of the methodologies were uniform throughout this work. Therefore they are contained here.

Preparation of hippocampus

Hippocampal slices were prepared from 2-6 week old Sprague-Dawley rats or 3-5 week old male Hartley guinea pigs. The animals were anesthetized using halothane, decapitated and the brain removed into chilled ACSF saturated with 95%O₂/5%CO₂. The ACSF contained: 119 mM NaCl, 2.5 mM KCl, 2.5 mM CaCl₂, 1.3 mM MgSO₄, 1 mM NaH₂PO₄, 26.2 mM NaHCO₃, and 11 mM glucose. Each hippocampus was then isolated from the rest of the brain, placed on a piece of agar and glued to a plexiform holder. This was placed into chilled ACSF on the base of a vibratome (Ted Pella Co.). 400 micron thick transverse slices were cut, placed into a holding chamber and allowed to rest for 1-2 hours. Slices were then transferred to a standard superfusing chamber and positioned underneath a nylon net, or placed on a poly-D-lysine coated coverslip and placed onto a Axioscope microscope with infrared illumination. Slices were perfused with ACSF at approximately 2 ml/ min at room temperature or at 27-28 °C. In experiments using a GABA_A antagonist, a cut was made between the CA3 and CA1 regions to prevent epileptiform activity in the CA1 area.

Three general methods of recording were used, field recordings, whole-cell recordings and perforated-patch whole-cell recordings.

Field recordings

Field recordings were typically performed by placing a 3-5 Mohm electrode filled with normal Ringers into the Stratum radiatum roughly parallel to the stimulating electrode (bipolar stainless steel). The signal was then recorded with either an Axoclamp-2A in bridge mode or an Axopatch-1D in the $i=0$ mode (both from Axon Instruments). The initial slope of the field EPSP was measured, rather than the peak amplitude to avoid contamination from either the population spike or from inhibitory inputs (if picrotoxin was not present in the Ringer solution).

Whole cell recordings

For whole cell recordings, 2-5 Mohm electrodes were used. The contents of the internal solution varied and are provided in the specific methods for each chapter. Gigaohm (typically $\sim 10 \text{ G}\Omega$) seals were achieved using either the blind-technique or by visually patching onto a cell. The blind-technique has been well described (Blanton et al., 1989), and simply involves looking for a change in the resistance of the recording pipette while advancing through the cell body layer. To visually patch, a single pyramidal cell is localized in the cell body layer (Figure 1) and the electrode is maneuvered with its contents under positive pressure until a dimple or a discoloration of the cell is observed due to the stream of internal solution from the pipette. In general, there were no obvious differences between the two methods, although the visual method could be used only at superficial cell layers. As a result, cells obtained from this method often had higher input resistances and wash-out of LTP appeared to occur more rapidly, consistent with the idea that many of the cell's processes had been severed in the cutting procedure.

During the recordings, cells were held in voltage clamp mode using an Axopatch-1D (Axon Instruments). Cells were held at a holding potential of -60 to -75 mV. Series resistance was monitored continuously online by measuring the peak transient to a 4 mV step (filtered at 10 kHz).

Perforated patch recordings

Perforated patch recordings were made using amphotericin-B (Rae et al., 1991). For these recordings, the pipette solution contained (in mM): 117.5 Cs-gluconate, 20 HEPES, 0.2 EGTA, and 0.48 mg/ml amphotericin-B (pH 7.2). The amphotericin-B solution was prepared as described (Rae et al., 1991) and was made-up every 2-3 hours during experiments. Data collection commenced only when the series resistance had stabilized, typically 20-40 minutes after seal formation. While the series resistance of perforated patch recordings are significantly larger than standard whole cell ($38 \text{ M}\Omega \pm 4$; $n=21$), perforated patch recordings eliminate the problem of “wash-out” seen with standard whole cell where the ability to induce LTP disappears after 5-15 minutes of whole cell access, presumably due to the loss of some necessary constituent from the cell.

Data analysis

Data was filtered at 2-3 kHz, sampled at 5-10 kHz and analyzed online using software developed in the laboratory by D. K. Selig. EPSC amplitudes were measured using a window at the peak of the event (1-4 ms for AMPAR- and 4-10 ms for NMDAR-mediated events) relative to the baseline taken immediately before the stimulus artifact. Synaptic failure rates were estimated by the method employed by Liao et al. (1995).

Briefly, the failure rate was calculated as twice the proportion of events with an amplitude of greater than zero. This assumes that the failures were distributed around a mean of zero and that the signal to noise ratio of the EPSCs was large enough so that the smallest events when superimposed on the noise would always be less than zero. This method was compared with visually identifying successes and failures and gave comparable results.

Appendix – Analysis of different methods for measuring EPSCs

A number of various methods have been employed in the analysis of minimal stimulation data. These include peak measurements, integrals and template fitting. A critical analysis and comparison of these methodologies has not been undertaken. Therefore, a number of different methods of analysis were performed, first on a computer-derived data set, and then to several recordings to determine if there are any differences between these methods.

An artificial data set of one hundred trials was created by adding noise randomly taken from a gaussian distribution (mean=0; standard deviation=1) to an EPSC-shaped signal (random amplitude with mean=5) (Figure 2). The signal was measured by various methods and the noise was measured by using the same method on the underlying noise traces alone. The signal to noise ratio (S/N) was calculated by taking the mean of the signal divided by the standard deviation of the noise. As would be expected, measuring a single point at the peak of the EPSC results in an S/N of 5 (5.0 ± 0.3 ; n=3).

The first method uses a standard peak amplitude measure. This is accomplished by taking a 2 ms average at the peak of the EPSC and subtracting from this a similar

period from the baseline just prior to the onset of the EPSC. By taking an average of many points, the standard deviation of the noise is reduced, therefore increasing the S/N ratio (15.6 ± 0.5) (Figure 3A).

The second method was to take an integral measure of the EPSC, again after setting the zero point of the entire trace based on a 2 ms period in the baseline. What is immediately apparent is that the S/N of the integral measure is much lower than for the peak measurement (6.2 ± 0.1). This is obvious, since the tail of the EPSC, which has very little signal, and therefore a very small S/N, is given as much weight as the peak.

A third method that has been employed (Boshakov and Sieglebaum, 1995) is to use a roving peak finder. This method searches for the highest point in the trace, within a given window, and takes a 2 ms average around that peak. This method is advantageous when measuring a data set that has a high variability in the time-to-peak. Because we are measuring a computer-derived data set, this method results in a S/N ratio similar to that of the 2 ms peak (13.0 ± 0.7).

The final method employed in this study is to use a template matching paradigm. In this case, the covariance between the raw EPSC and the data set was determined. This method also produced a S/N comparable to the peak measurement (14.3 ± 0.4).

Since we knew that actual size of the EPSC, we were able to perform a second measure and test how well the measured values for the EPSCs correlated to the actual amplitude (Figure 3B). The peak and template methods give the highest degree of correlation, while the integral method clearly had a lower amount of correlation.

We next performed a similar analysis on a number of actual data sets. Five data sets of 100 traces each were used. Only data sets where the successes could be clearly

distinguished from the failures were used. In this case, the S/N was calculated by dividing the mean amplitude of the successes (or potency) by the standard deviation of the noise. A second parameter was also calculated, the mean of the failures as compared to the potency of the successes. This second measurement gives a measure of the potential offset of the failures peak, which could have considerable effects on the determination of failure rates.

A comparison of the S/N ratio for the various methods is shown in Figure 4. Again, it is clear that the measurement of integral is worse than the other methods ($p < 0.05$, repeated measures ANOVA with Tukey's posthoc analysis), but the other methods appear comparable. The offset analysis shows an additional point. Using a roving peak method gives a significantly worse offset than either the peak or template methods ($p < 0.05$).

There appears to be no difference between using a peak or a template measure. There is a difference though, when it comes to the effects of spontaneous noise. Figure 5 shows a trace from a data set where a spontaneous event occurred just prior to the stimulus. The peak measurement gave a value of -2.2 pA (the standard deviation of the noise was 0.43 pA), thus, this sweep would be classified as a success. The template method, though, gave a value of 0.12 (the standard deviation of the noise for this method was 0.16). Therefore, using a template, this sweep would be correctly classified as a failure.

In conclusion, while the integral and the roving peak method have obvious flaws, there appears to be little difference between utilizing a peak measurement or a template method on the S/N ratio. The template method does have the an increased ability to

identify spontaneous events that occur near the stimulus, but this can also be achieved by visually inspecting each sweep for the presence of spontaneous events.

UCSF LIBRARY

Figure 1. Image of CA1 region of hippocampus.

Digitized image of a hippocampal slice using an Zeiss Axioscope with a 40X objective and infrared illumination transferred onto a PC computer using a video capture board (ATI technologies). The paler region is the pyramidal cell body layer. Notice that individual cell bodies as well as their dendritic processes can be easily distinguished.

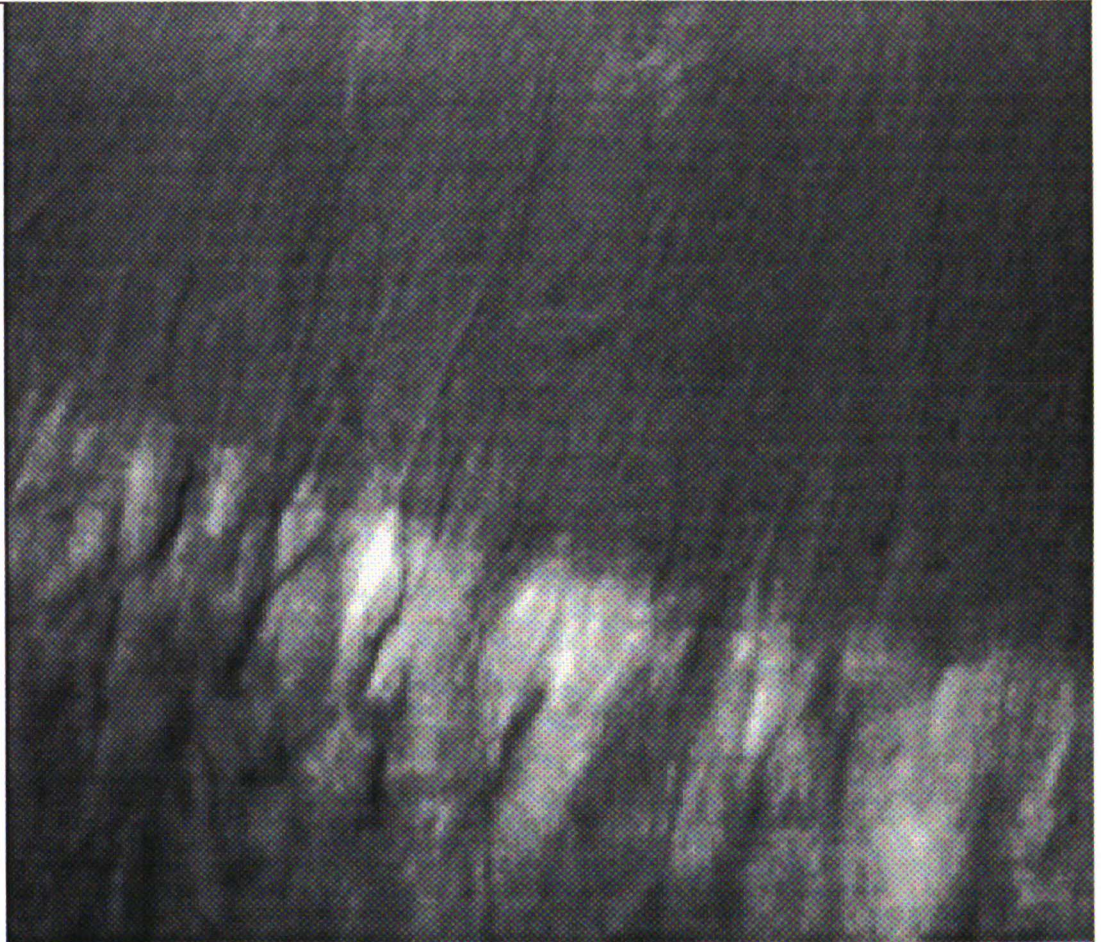


Figure 2. Illustration of a computer-derived data set.

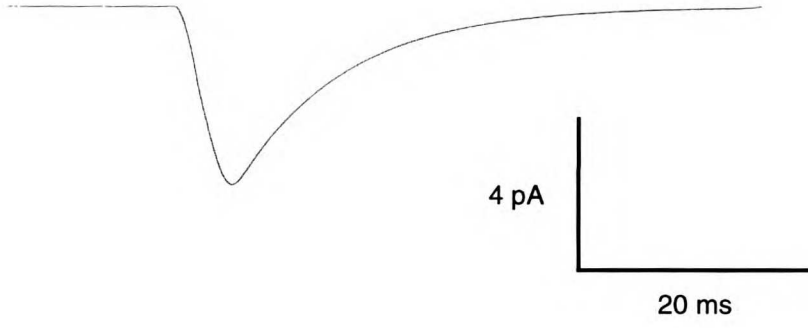
A. Computer derived EPSC before noise traces are superimposed. EPSC has an amplitude of 5 pA.

B. Sample noise trace. Each point in the noise trace was sampled from a distribution with a mean of 0 and a standard deviation of 1 pA.

C. Resulting trace after superposition of noise.

UCSF LIBRARY

A



B



C

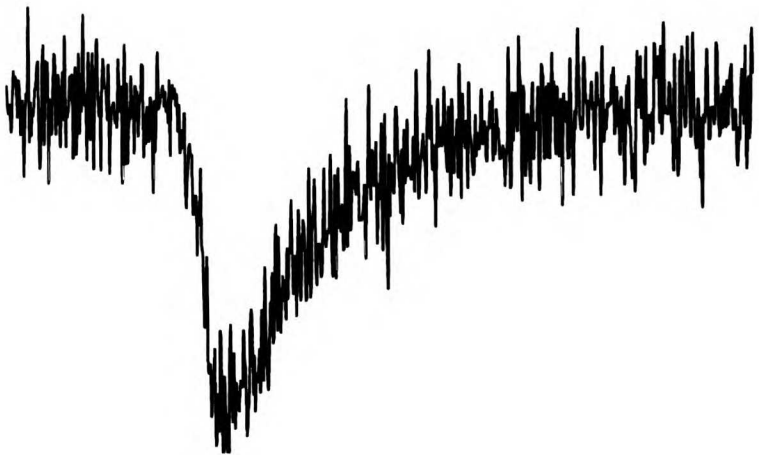
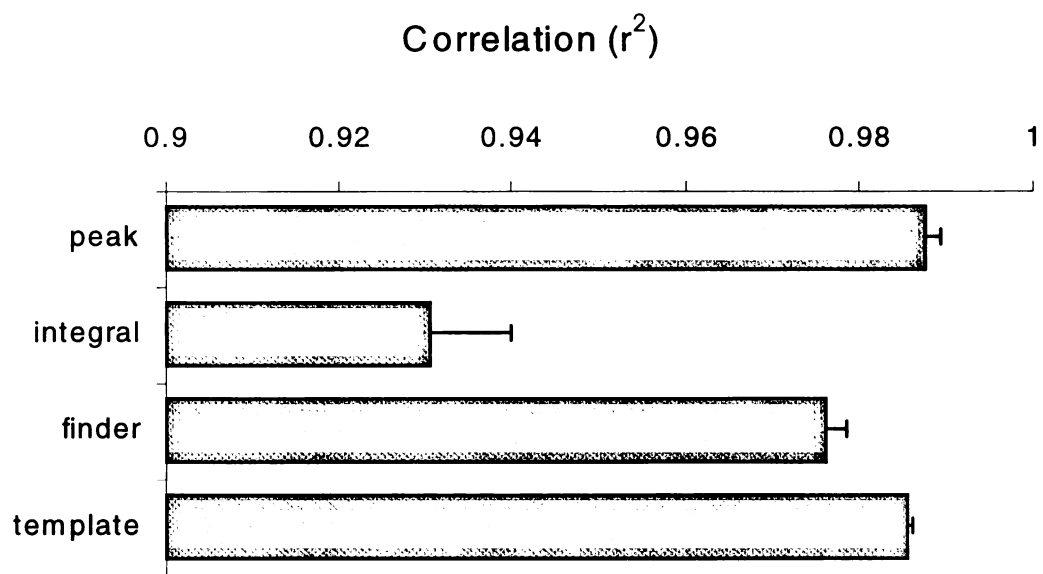
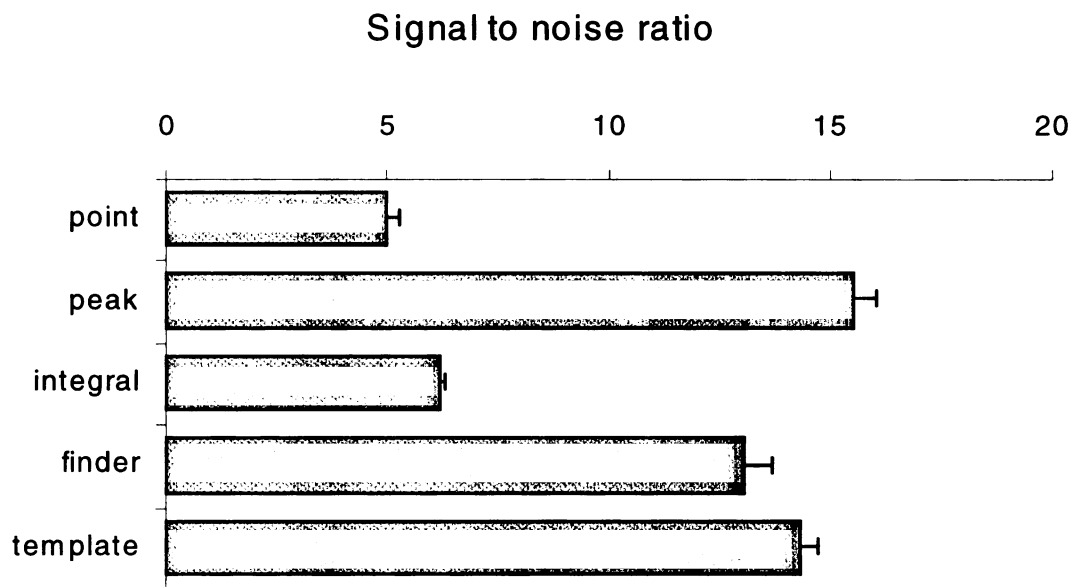


Figure 3. Effects of different analysis methods on the S/N ratio and r^2 for the data set described in Figure 2. Each analysis method was performed on the same data set of 100 traces. Error bars are s.e.m of measurements from three separate data sets.

UCSF LIBRARY



UCSF LIBRARY

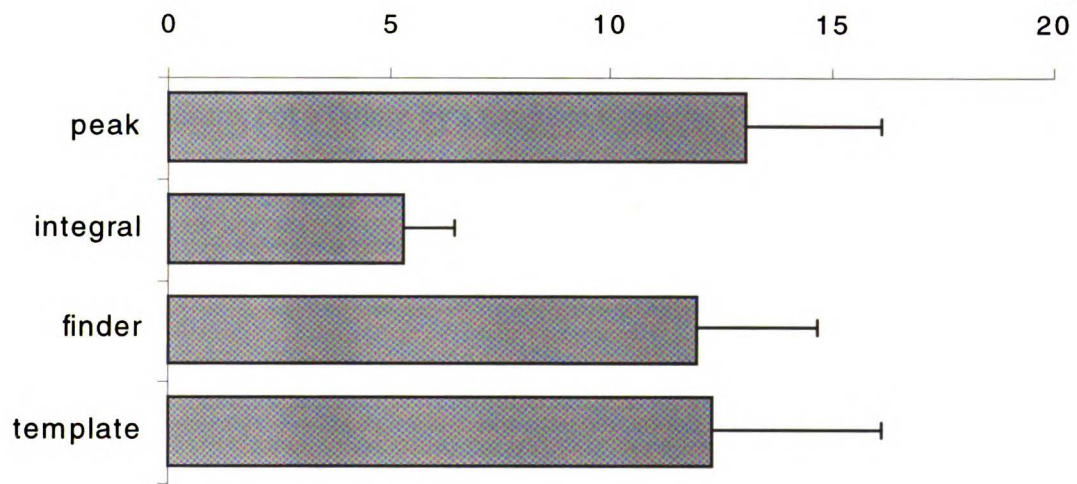
Figure 4. Effects of different analysis methods on the S/N ratio and noise offset for recorded data sets.

A. Signal to noise ratio for different methods is calculated as the potency of the events divided by the standard deviation of the noise.

B. Noise offset is calculated as the average of the noise as a percentage of the potency. A large noise offset will make it more difficult to accurately assess the true failure rate.

UCSF LIBRARY

Signal to noise ratio



Failure offset (% of potency)

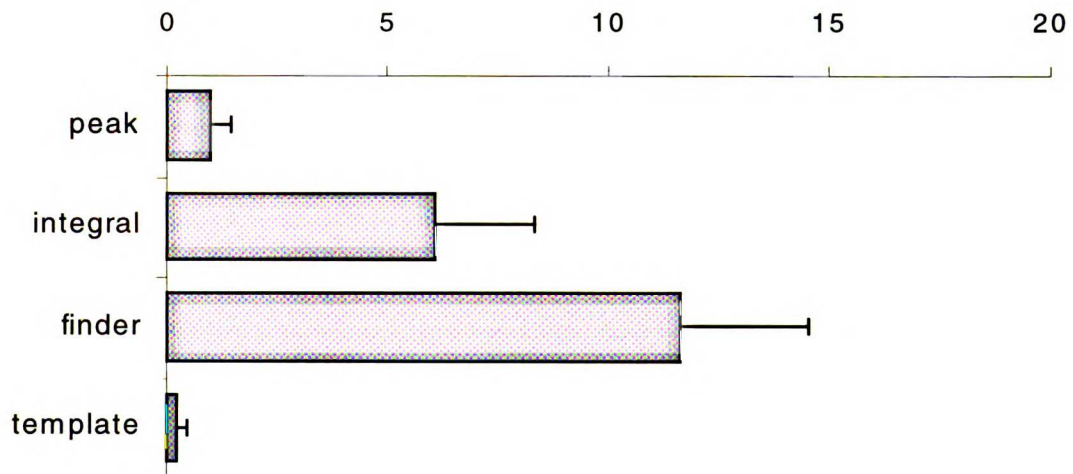
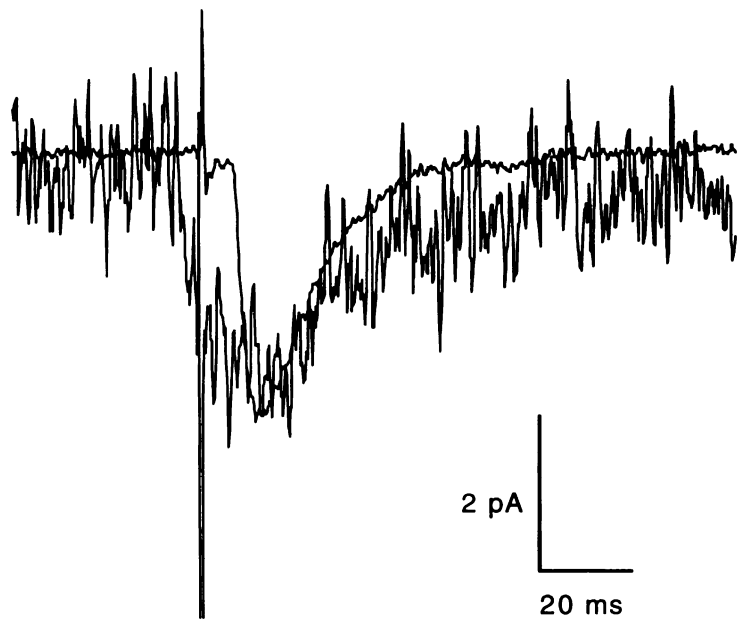


Figure 5. Effects of spontaneous noise on measurements.

A spontaneous event that occurred prior to the stimulus would be classified a success by an amplitude measure, but a failure by a template measure. Superimposing the raw data trace with the template (average of all traces) shows that the response occurred prior to the stimulus artifact.

UCSF LIBRARY



UCSF LIBRARY

CHAPTER THREE

**INDEPENDENT MECHANISMS FOR LONG-TERM DEPRESSION
OF AMPA AND NMDA RESPONSES**

UCSF LIBRARY

Summary

While the mechanisms responsible for long-term potentiation (LTP) and long-term depression (LTD) of excitatory synaptic responses mediated by AMPA (α -amino-3-hydroxy-5-methyl-4-isoxazolepropionic acid) receptors (AMPA receptors) have been extensively characterized, much less is known about the regulation of NMDA (N-methyl-D-aspartate) receptors (NMDARs) by synaptic activity. In hippocampal CA1 cells, prolonged low frequency afferent stimulation depresses synaptic responses mediated by either NMDARs or AMPARs. However, this apparently similar LTD is accompanied by a change in the coefficient of variation (CV) of only the AMPAR mediated synaptic responses; the CV of the NMDAR mediated synaptic responses is unaffected. Moreover, by varying the pattern of synaptic stimulation the responses mediated by one receptor subtype can be modified without affecting the responses mediated by the other. These results indicate that the mechanisms underlying activity-dependent plasticity of NMDAR mediated synaptic responses are different from those responsible for plasticity of AMPAR mediated synaptic responses.

Introduction

Long-term potentiation (LTP) and long-term depression (LTD) of excitatory synaptic transmission in the mammalian brain are long lasting, activity-dependent changes in synaptic efficacy thought to be important for learning, memory, and neural development. At most excitatory synapses that exhibit LTP and LTD, synaptic responses are mediated by two distinct subtypes of ionotropic glutamate receptors, termed AMPA

(α -amino-3-hydroxy-5-methyl-4-isoxazolepropionic acid) and NMDA (N-methyl-D-aspartate) receptors (AMPA and NMDARs) after their specific exogenous ligands. The changes in synaptic efficacy that define LTP and LTD are routinely measured by examining basal synaptic responses, which are predominantly mediated by AMPARs. In contrast, NMDARs, because of their strong voltage-dependence, contribute minimally to basal synaptic responses at the resting membrane potential but nevertheless serve an essential role in triggering LTP and LTD (Malenka and Nicoll, 1993). Moreover, NMDARs are important contributors to the neuronal injury and death seen in many neurologic disorders, presumably due to their ability to raise intracellular Ca^{2+} (Lipton and Rosenberg, 1994).

Despite these well-established roles for NMDARs, relatively little is known about their regulation by synaptic activity. For example, the factors that determine whether or not NMDAR mediated synaptic responses in CA1 pyramidal cells undergo LTP have not been well defined (Asztely et al., 1992; Clark and Collingridge, 1995; Kauer et al., 1988; Muller and Lynch, 1988; O'Connor et al., 1995; Perkel and Nicoll, 1993). Here we present evidence that NMDAR mediated synaptic responses can be depressed by specific patterns of afferent activity and that this plasticity has a mechanism distinct from that underlying plasticity of AMPAR mediated synaptic responses.

Methods

Hippocampal slices were prepared from 2-6 week old Sprague-Dawley rats. All experiments were conducted at 23-28°C. Pharmacologically isolated NMDAR EPSPs/EPSCs were recorded by lowering $MgSO_4$ to 0.1 mM and adding 0.1-.2 mM

microtoxin and 10 μ M CNQX or DNQX. For the experiments shown in Figure 4 the superfusing solution contained: 119 mM NaCl, 4 mM KCl, 4 mM CaCl₂, 4 mM MgSO₄, 1 mM NaH₂PO₄, 26.2 mM NaHCO₃, 11 mM glucose, and 0.1 mM microtoxin. For the experiments in Figures 7 and 10, the whole cell pipette solution contained 117.5 mM cesium gluconate, 17.5 mM CsCl, 8 mM NaCl, 10 mM HEPES, 0.2 mM EGTA, 4 mM Mg-ATP, and 0.3 mM GTP (pH=7.2, 280-290 mOsm). For the experiments in Figure 11, the pipette solution also contained tetraethyl-ammoniumchloride (10 mM) and QX314 (5 mM) and CsCl replaced Cs gluconate. Data in the text and in the figures are presented as mean percent of control (set to 100%) \pm SEM. The change in EPSP/EPSC magnitude was calculated by averaging over a 10 min window taken 20-30 min after the LTD/LTP induction protocol and comparing this value to the control input in the same slice or to the 10 min baseline period.

For the experiments in Figures 8 and 9, 50 μ M D-APV was applied at the end of each experiment to isolate the fiber volley and stimulus artifact. This was subsequently subtracted from all sweeps to prevent any contamination of the slope measurements. The NMDAR EPSPs were normalized with respect to the baseline AMPAR EPSPs and the two inputs were then directly compared by setting the control NMDAR EPSPs to 100% and scaling the test NMDAR EPSPs accordingly.

$1/CV^2$ was calculated as μ^2/σ^2 where μ is the mean and σ is the standard deviation of the EPSC amplitude and was determined for successive epochs of 10-30 EPSCs throughout each experiment. $1/CV^2$ of each input was then normalized with respect to the average value taken over the initial 10 min baseline. EPSC amplitudes were measured using a window at the peak of the event (1-3 ms for AMPAR- and 4-10 ms for NMDAR-

mediated events) measured relative to the baseline taken immediately before the stimulus artifact. For the experiments in Figure 10, $1/CV^2$ of the AMPAR EPSCs or NMDAR EPSCs in the test input was then directly compared to that in the control input by setting the average normalized value for $1/CV^2$ of the control input over the 10 minutes following the LTD/LTP induction protocol to 100%. For the experiments in Figure 11, $1/CV^2$ for each input was calculated after the experimental manipulation (20-30 min after LFS or 10-20 min after adenosine application) and compared directly to $1/CV^2$ of the baseline EPSCs in that input.

Results

Before presenting our results, it is important to discuss briefly why the examination of changes in NMDAR-mediated synaptic responses in brain slice preparations is subject to much greater experimental error than examination of AMPAR-mediated synaptic responses. The foremost difficulty is caused by the strong voltage dependence of the NMDAR-mediated response. NMDAR-mediated currents are minimal at membrane potentials more negative than -70 mV and exhibit a region of negative slope conductance from approximately -70 mV to -40 mV (Hestrin et al., 1990). Thus, to record NMDAR-mediated responses the cell is often depolarized to a level at which small changes in membrane potential, either due to changes in the recording conditions or due to changes in the AMPAR-mediated synaptic responses, can strongly influence the magnitude of the response. In theory, voltage-clamp recording eliminates this problem but because of the extensive dendritic arborization, it is doubtful that perfect voltage control of synapses is achieved when recording from pyramidal cells in slice preparations

(Spruston et al., 1993). One method that helps to minimize this problem is to record NMDAR-mediated currents at positive holding potentials where the current-voltage (IV) relationship is linear and voltage-dependent conductances are largely inactivated (Perkel and Nicoll, 1993). Alternatively, extracellular magnesium (Mg^{2+}) can be removed substantially reducing the voltage dependence of the NMDAR-mediated response. The NMDAR channel is also highly permeable to Ca^{2+} and thus a second problem is that any repeated measurement of NMDAR-mediated synaptic currents is accompanied by a change in intracellular Ca^{2+} that may itself cause gradual modifications of the synaptic responses (Rosenmund and Westbrook, 1993a; Tong and Jahr, 1994).

Because of these significant technical difficulties, we have taken several different but complementary experimental approaches to examine whether NMDAR-mediated synaptic responses change during LTD. In an initial set of experiments, we recorded extracellular field potentials from hippocampal slices to examine whether synaptic activity could depress pharmacologically isolated NMDAR-mediated synaptic responses (NMDAR EPSPs) recorded in reduced extracellular Mg^{2+} (0.1 mM) from CA1 pyramidal cells. Prolonged low-frequency afferent stimulation (LFS; 1 Hz for 5-7 min), which elicits homosynaptic LTD of AMPAR-mediated synaptic responses (AMPA EPSPs) caused a depression of the NMDAR EPSP ($77 \pm 4\%$ of control; $n=8$) that, like LTD of AMPAR EPSPs, was input specific (Figure 6) (Dudek and Bear, 1992; Mulkey and Malenka, 1992).

To determine whether the depression of NMDAR EPSPs required a rise in postsynaptic Ca^{2+} , again like LTD of AMPAR EPSPs (Mulkey and Malenka, 1992) we loaded cells with the Ca^{2+} chelator BAPTA (10 mM) using standard whole-cell recording

techniques. While control cells showed robust LTD of NMDAR EPSPs (Figure 7A; $60\pm 7\%$, $n=9$), LFS did not elicit LTD of NMDAR EPSPs in cells filled with BAPTA (Figure 7B; $120\pm 7\%$, $n=7$) even though surrounding cells in the same slices exhibited LTD as assayed by the simultaneously recorded field NMDAR EPSPs.

Although these experiments demonstrate that LFS elicits LTD of NMDAR EPSPs in pharmacologically altered conditions, an important issue is whether such changes occur following the generation of LTD of AMPAR EPSPs under more physiological conditions, since NMDAR currents are altered by lowering extracellular Mg^{2+} . To address this question, we compared the magnitude of the NMDAR EPSP in two independent inputs in the same slice after inducing LTD of AMPAR EPSPs in one of the two inputs. This technique has the advantage that any change in NMDAR function due to the measurements themselves should affect both inputs equally as will any non-specific change in the preparation during the course of the experiment. An important requirement for this approach is that within a slice the pharmacologically isolated NMDAR EPSP is similarly proportioned to the AMPAR EPSP in both inputs. Figure 8A shows a summary of experiments in which, after first recording stable AMPAR EPSPs in standard solution, we isolated NMDAR EPSPs by changing the perfusing solution to one in which $MgSO_4$ was reduced to 0.1 mM and CNQX (10 μ M) and picrotoxin (100 μ M) were added. When normalized to the baseline AMPAR EPSPs, the NMDAR EPSPs in the two inputs were virtually identical. This is more easily seen in Figure 8B where we have scaled the NMDAR EPSPs in the test input by the size of the NMDAR EPSPs in the control input.

Confirmation of the assumption that two independent and random inputs in a slice activate the same proportion of NMDARs and AMPARs permitted the generation of LTD

of the AMPAR EPSP in one path and subsequent comparison of the NMDAR EPSPs between the two paths to determine whether LTD of NMDAR EPSPs had occurred. Figure 9A demonstrates that generation of homosynaptic LTD with LFS causes a decrease in both the NMDAR EPSPs and AMPAR EPSPs (59 ± 5 and $72\pm 4\%$ respectively, $n=8$). When the NMDAR antagonist D-APV ($50\ \mu\text{M}$) was present during the induction protocol, LTD of both the NMDAR and AMPAR EPSPs was blocked ($n=4$, data not shown).

Using the same experimental design, we also examined LTP and found that unlike LTD, LTP did not result in a similar change in the AMPAR EPSP and NMDAR EPSP. A high frequency tetanus (100 Hz, 1 sec given twice) caused an increase in the AMPAR EPSP that was larger than that of the NMDAR EPSP (195 ± 8 and $122\pm 8\%$ respectively, $n=7$, $p<0.002$) (Figure 9B). Interestingly, this same tetanus administered following LTD appeared to potentiate the NMDAR EPSP (Figure 9C, $n=6$) to a greater extent than when applied to a naive input (Figure 9B). Since in this experiment we were unable to measure directly the NMDAR EPSPs immediately following the LFS, to test this impression we compared the NMDAR EPSPs following the repotentiating tetanus (Figure 9C) to the interaction of the LFS alone (Figure 9A) and the tetanus alone (Figure 9B). If there were no interaction between the two stimuli, we would have expected that the input which was depressed by 41% to be potentiated by 22% giving a value of 72% ($(100-41)\cdot 1.22$) compared to the actual NMDAR EPSP value of $110\pm 21\%$. This interaction was tested statistically using a two-factor ANOVA and found to be significant ($p<0.05$) suggesting that the tetanus was capable of reversing the LTD of the NMDAR EPSP.

What mechanisms might account for the differential modulation of NMDAR EPSPs and AMPAR EPSPs by synaptic activity? One method that can be used to address this question relies upon the coefficient of variation (CV), an index of the trial-to-trial variability in synaptic responses. Manipulations that change synaptic efficacy with parallel changes in $1/CV^2$, a measure derived from CV, are customarily attributed to presynaptic changes in quantal content. On the other hand, manipulations that change synaptic efficacy without affecting $1/CV^2$ are assumed to occur via a postsynaptic change in the sensitivity to released neurotransmitter (del Castillo and Katz, 1954a; Bekkers and Stevens, 1990; Kamiya et al., 1991; Malinow and Tsien, 1990; Manabe et al., 1993; but see Faber and Korn, 1991). To determine whether $1/CV^2$ of AMPAR and NMDAR mediated synaptic currents (AMPA EPSCs and NMDAR EPSCs) changes during LTD, we used standard whole-cell voltage-clamp recording techniques and an experimental design similar to that just used for the experiments presented above. Generation of LTD (Figure 10A) in the test input ($61 \pm 9\%$, $n=8$) caused a significant decrease in $1/CV^2$ of AMPAR EPSCs ($72 \pm 8\%$) (Figure 10B). NMDAR EPSCs were then isolated in the same control and test inputs by applying CNQX to the slice and depolarizing the cell to positive potentials (+40 mV). In agreement with the field experiments (Fig 9A), the NMDAR EPSCs in the test inputs were smaller than those in the control inputs ($71 \pm 8\%$; $n=8$) (Figure 10A₃). However, $1/CV^2$ of the NMDAR EPSCs did not change ($96 \pm 16\%$) (Figure 10B).

We also examined $1/CV^2$ following the generation of LTP by pairing depolarization with LFS (1 Hz, 5 min) (Figures 10C and D) and in agreement with previous results found that $1/CV^2$ of the AMPAR EPSCs increases following LTP

($198 \pm 30\%$; $n=8$) (Bekkers and Stevens, 1990; Malinow and Tsien, 1990; Kamiya et al., 1991; Manabe et al., 1993; Kullmann, 1994). Despite the large increase in the AMPAR EPSC in the test input ($231 \pm 23\%$), the NMDAR EPSCs in the two inputs were identical (Figure 10C). Furthermore, as recently reported (Kullmann, 1994), $1/CV^2$ of the NMDAR EPSCs was unchanged by LTP ($112 \pm 20\%$) (Figure 10D).

To ensure that under these experimental conditions, we could in fact detect a change in $1/CV^2$ of NMDAR EPSCs when a change in transmitter release occurred, we examined paired-pulse facilitation (PPF) which is due to a presynaptic increase in quantal content (Katz and Miledi, 1968; Zucker, 1989). PPF caused a parallel increase in $1/CV^2$ of both the NMDAR EPSCs ($187 \pm 17\%$; $n=6$) and AMPAR EPSCs ($214 \pm 41\%$) when $1/CV^2$ of the responses to the second stimulus was compared to $1/CV^2$ of the responses to the first stimulus (Figure 10E). Thus, the lack of change of $1/CV^2$ of NMDAR EPSCs during LTD and LTP is unlikely to be the result of an inability to detect such a change. We also observed that, in the same input, $1/CV^2$ of NMDAR EPSCs (118 ± 14 ; $n=27$) was considerably larger than $1/CV^2$ of AMPAR EPSCs (38 ± 4) (Figure 10F), confirming previous observations (Kullmann, 1994).

These findings—that LTD of NMDAR EPSCs was not associated with any decrease in $1/CV^2$, while a clear decrease in $1/CV^2$ did occur at the same synapses with LTD of AMPAR EPSCs—were surprising and suggest distinct mechanisms of expression for LTD of each component. Because of the novelty and potential importance of this conclusion, we performed further experiments that allowed direct comparison of $1/CV^2$ of NMDAR EPSCs in a single input both before and after generation of LTD. Figure 11A-C shows that LFS elicited robust LTD of pharmacologically isolated NMDAR EPSCs

(66±5%; n=8) that were recorded in perfusing solution containing low Mg²⁺ (0.1 mM). However, as in the previous experiments, LTD did not cause any change in 1/CV² (Figure 11C). Subsequent application of adenosine (0.5 μM), which presynaptically inhibits transmitter release (Dunwiddie and Haas, 1985; Prince and Stevens, 1992), caused both a comparable depression of the NMDAR EPSC in the control input (64±4%) relative to that of the test input in these same cells and, importantly, a proportional decrease in 1/CV² (68±7%). Thus, in these cells the measure was sufficiently sensitive to detect changes in neurotransmitter release. These results provide additional evidence that activity-dependent modulation of NMDAR EPSCs occurs in the absence of detectable changes in 1/CV².

Using a variety of experimental approaches, we have demonstrated that LTD of NMDAR mediated synaptic responses is generated by LFS. An interesting and important related question concerns the possible functional significance of LTD of NMDAR responses. Previous work has demonstrated that modest activation of NMDARs by synaptic activity (Fujii et al., 1991; Huang et al., 1992) or via pharmacological manipulations (Coan et al., 1989; Izumi et al., 1992) in older slices increases the threshold for induction of LTP. To test whether this might be due to a depression of NMDAR EPSPs, we performed experiments to measure changes in the NMDAR EPSP caused by patterns of synaptic activity similar to those reported to increase the LTP induction threshold (Fujii et al., 1991; Huang et al., 1992) and delivered under similar experimental conditions. We found that such manipulations clearly decreased NMDAR EPSPs (Figure 12A) (70±9%; n=7). Like the increase in LTP induction threshold (Huang et al., 1992), the depression of NMDAR EPSPs was blocked when D-APV (50 μM) was

present during the conditioning stimulus (Figure 12B) ($93\pm 13\%$; $n=6$), occurred in the absence of any change in the AMPAR EPSP (Figure 12C, left side) and showed partial recovery over the course of an hour (Figure 12C, right side) ($86\pm 5\%$; $n=7$). A second stimulation protocol that increases LTP induction threshold (Fujii et al., 1991) was also found to depress NMDAR EPSPs ($74\pm 9\%$; $n=7$) in the absence of any long-lasting change in AMPAR EPSPs (Figure 12D).

Discussion

We have demonstrated that different patterns of synaptic activity can depress NMDAR-mediated responses. Although superficially these changes resemble LTD of AMPAR-mediated responses, two lines of evidence strongly suggest that the underlying mechanisms are fundamentally different. First, synaptic activity can selectively affect one response without affecting the other. The AMPAR EPSP/EPSC can be potentiated with little or no change (Figures 9B and 10C) in the NMDAR EPSP/EPSC (Kauer et al., 1988; Muller et al., 1988; Asztely et al., 1992; Perkel and Nicoll, 1993; Kullmann, 1994) and the NMDAR EPSP can be depressed in the absence of any change in the AMPAR EPSP (Figure 12). Differential regulation of NMDAR and AMPAR EPSPs/EPSCs by synaptic activity has also been observed in the nucleus accumbens (Kombian and Malenka, 1994).

Second, even when synaptic activity causes similar decreases in NMDAR and AMPAR EPSCs, $1/CV^2$ of the AMPAR EPSCs decreases while that of NMDAR EPSCs remains unchanged. Classically, changes in $1/CV^2$ are attributed to a change in p_r , the probability of transmitter release and/or a change in n , the number of transmitter release sites. Thus, in the absence of information about $1/CV^2$ of NMDAR responses, it was

reasonable to propose that a change in $1/CV^2$ of AMPAR responses during LTP (Bekkers and Stevens, 1990; Malinow and Tsien, 1990; Kamiya et al., 1991) or LTD (Bolshakov and Siegelbaum, 1994) indicated that a change in quantal content had occurred.

However, assuming NMDARs and AMPARs are co-localized at synapses (Bekkers and Stevens, 1989; McBain and Dingledine, 1992; Stern et al., 1992; Burgard and Hablitz, 1993), the differential change in $1/CV^2$ of AMPAR- and NMDAR-mediated responses during LTP and LTD forces an alternative explanation. A prominent possibility is that some synapses may contain NMDARs but not functional AMPARs (Kullmann, 1994). This would result in release of transmitter at these sites going undetected under normal recording conditions when only AMPAR-mediated responses are monitored. Moreover, any change in the number of synapses containing functional AMPARs would be accompanied by a change in $1/CV^2$ even though this would be due to a postsynaptic, not a presynaptic, change in n . According to this model, LTP and LTD would be caused, at least in part, by the up- or down-regulation of functional AMPAR clusters at some of the activated synapses (Edwards, 1991; Kullmann and Nicoll, 1992; Lisman and Harris, 1993; Manabe et al., 1993; Kullmann, 1994). In contrast, the lack of change in $1/CV^2$ of NMDAR EPSCs during LTP or LTD is difficult to explain by a similar mechanism and instead suggests that synaptic activity modifies NMDAR EPSCs uniformly across activated synapses.

It is important to note that the CV of synaptic responses may be influenced by factors in addition to the classic trial-to-trial variations in quantal content (Faber and Korn, 1991; Kullmann, 1994). These include trial-to-trial fluctuations in quantal amplitude at individual synapses (due to presynaptic and/or postsynaptic factors) and

variability in quantal amplitude between different release sites. For the main conclusions of this work, it is unclear how these additional sources of variance might account for the observed lack of change in $1/CV^2$ of NMDAR EPSCs during LTD and LTP.

Several other laboratories have reported that NMDAR EPSPs can be depressed by synaptic activity using various protocols and recording conditions different than those used in these experiments (Gean and Lin, 1993; Xiao et al., 1994; Xie et al., 1992). We have confirmed that NMDAR responses can be depressed but, importantly, have also demonstrated that this occurs when LTD of AMPAR EPSPs is generated under normal recording conditions. Moreover, we have provided evidence (see Figure 12) suggesting that the depression of NMDAR responses may cause or at least contribute to the increase in the threshold for LTP caused by certain patterns of synaptic stimulation (Fujii et al., 1991; Huang et al., 1992). The exact mechanisms by which NMDAR responses are depressed are unknown but candidate processes include modulation of Ca^{2+} -dependent protein kinases and phosphatases (Chen and Huang, 1992; Kelso et al., 1992; Markram and Segal, 1992; Urushihara et al., 1992; Lieberman and Mody, 1994; Wang and Salter, 1994; Tong et al., 1995) as well as changes in the cytoskeleton (Rosenmund and Westbrook, 1993b).

In contrast to the current data on LTD, whether NMDAR responses are potentiated to the same degree as AMPAR responses by manipulations that elicit LTP remains the subject of active debate (Kauer et al., 1988; Muller and Lynch, 1988; Asztely et al., 1992; Perkel and Nicoll, 1993; Kullmann, 1994; Clark and Collingridge, 1995; O'Connor et al., 1995). Although the reasons for the differences in experimental results between laboratories remain unclear, the results presented in Figure 9 provide additional

complexity in that they suggest that the prior history of activity at synapses may influence the extent to which NMDAR responses are modified by subsequent synaptic activity.

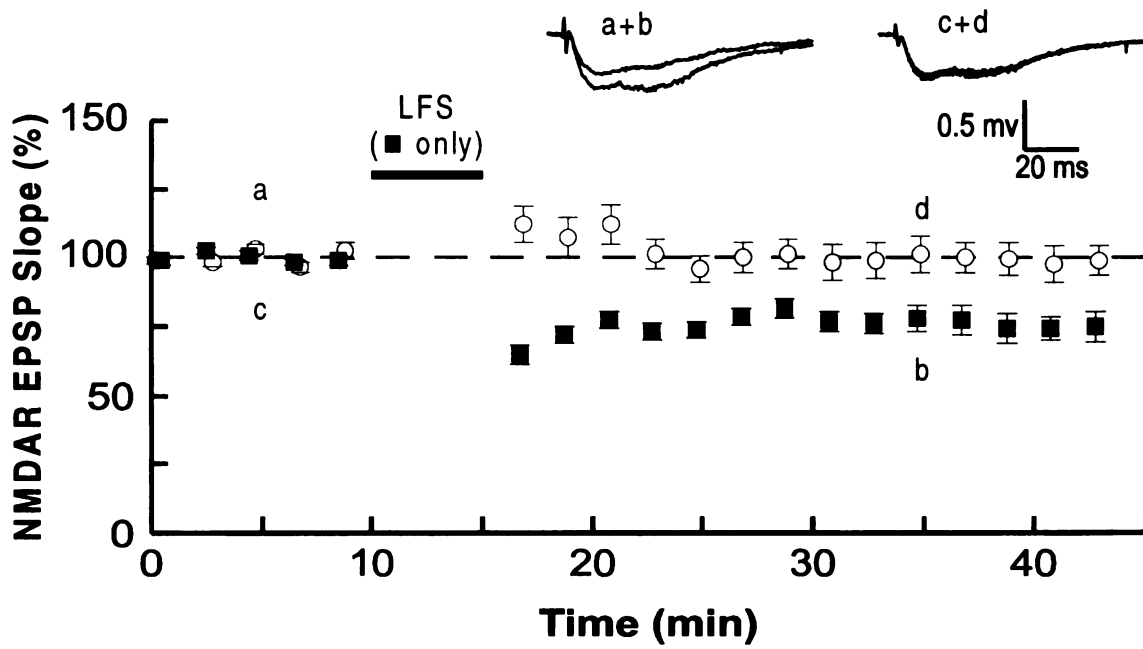
Similar observations have been made for plasticity of AMPAR responses (Christie and Abraham, 1992; Fujii et al., 1991; Huang et al., 1992; Wexler and Stanton, 1993) as well as for synapses on goldfish Mauthner cells (Yang and Faber, 1991).

Independent of the underlying mechanisms, the ability of synaptic activity to modify NMDAR responses has additional functional implications. For example, the modification of NMDARs, and thus the relative contribution of AMPARs and NMDARs at specific synapses, may be important for normal information processing, since NMDARs play important roles in the transfer of sensory information and in the generation of motor rhythms (Daw et al., 1993; Grillner et al., 1991). Additionally, changes in NMDAR function would be expected to influence not only the magnitude, but also both the direction and time course of synaptic weight changes elicited by a given pattern of synaptic activity (Malenka and Nicoll, 1993; Malenka, 1994). Such changes may be particularly important during development (Carmignoto and Vicini, 1992; Hestrin, 1992; Crair and Malenka, 1995) and, as suggested above, may contribute to adjustments in the threshold for synaptic modification that have been incorporated into some biologically based neural network models (Bienenstock et al., 1982; Bear et al., 1987).

UCSF LIBRARY

Figure 6. LTD of the isolated NMDAR EPSP can be induced by low-frequency stimulation and is input specific.

Graph illustrates the effect of prolonged low-frequency stimulation (LFS; 1 Hz for 5-7 min) on pharmacologically isolated NMDAR EPSPs (n=8). LTD occurred only in the input receiving the LFS. The sample traces are averages of 6 consecutive responses taken at the times indicated.



UCSF LIBRARY

Figure 7. LTD of the isolated NMDAR EPSP requires a rise in postsynaptic Ca^{2+}

A. LFS elicits LTD of the NMDAR EPSP in both the cell and the simultaneously recorded field EPSP (n=9).

B. Loading cells with BAPTA (10 mM) blocks the generation of LTD by LFS, although LTD was generated in the simultaneously recorded field EPSP (n=7).

UCSF LIBRARY

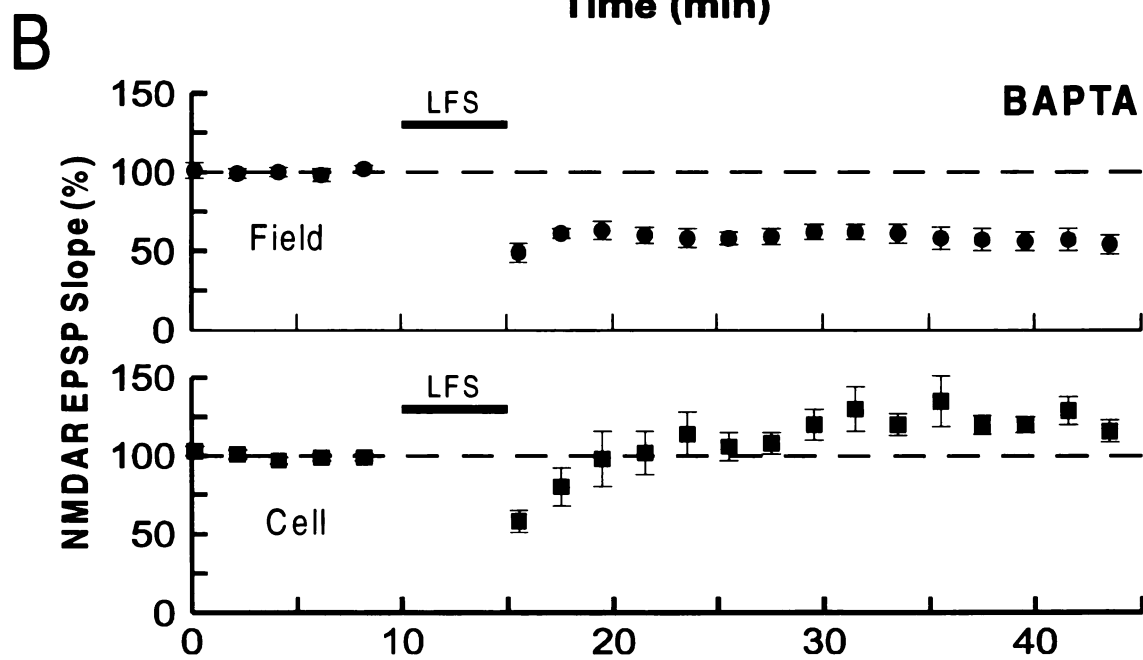
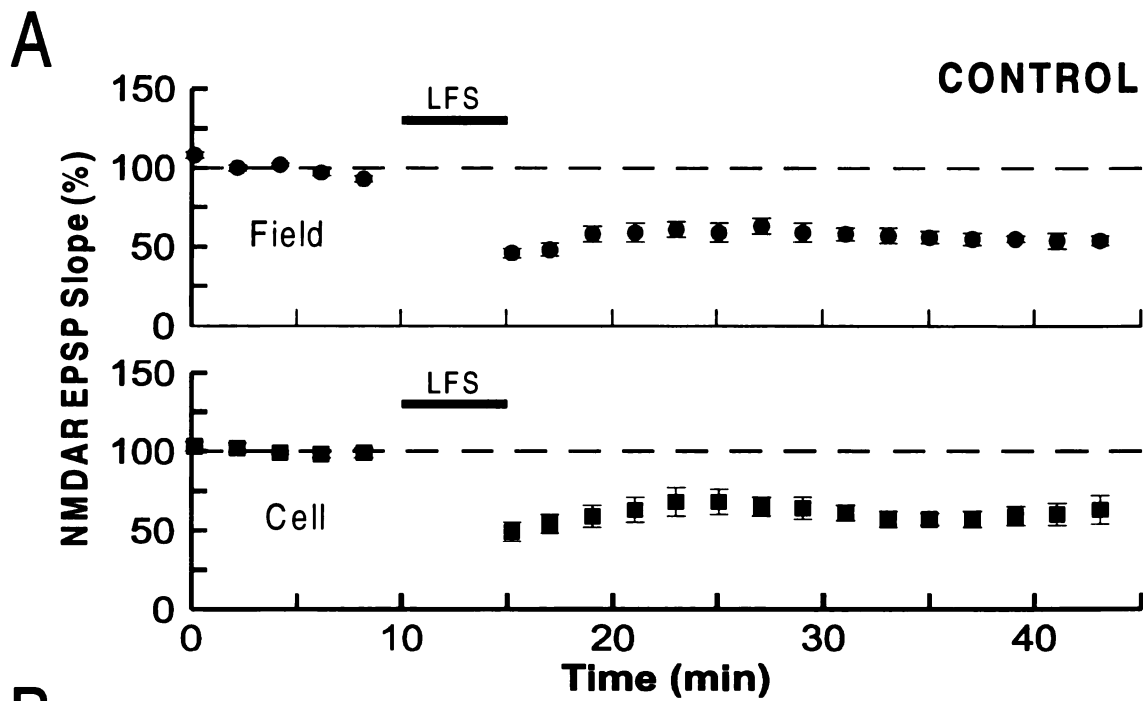


Figure 8. The NMDAR EPSP is on average the same between two inputs.

A. The magnitude of the NMDAR EPSP is on average the same when compared between two inputs (■ and ○) in the same slice. After obtaining stable AMPAR EPSPs in the two inputs (n=7), a superfusing solution containing CNQX (10 μ M), picrotoxin (100 μ M) and lowered Mg (0.1 mM) was applied and the initial slope measurement advanced and widened to measure the slower, pharmacologically isolated NMDAR EPSP.

B. The NMDAR EPSPs are scaled to the control input and plotted on the same graph as the AMPAR EPSPs in the same inputs (same data as in A).

UCSF LIBRARY

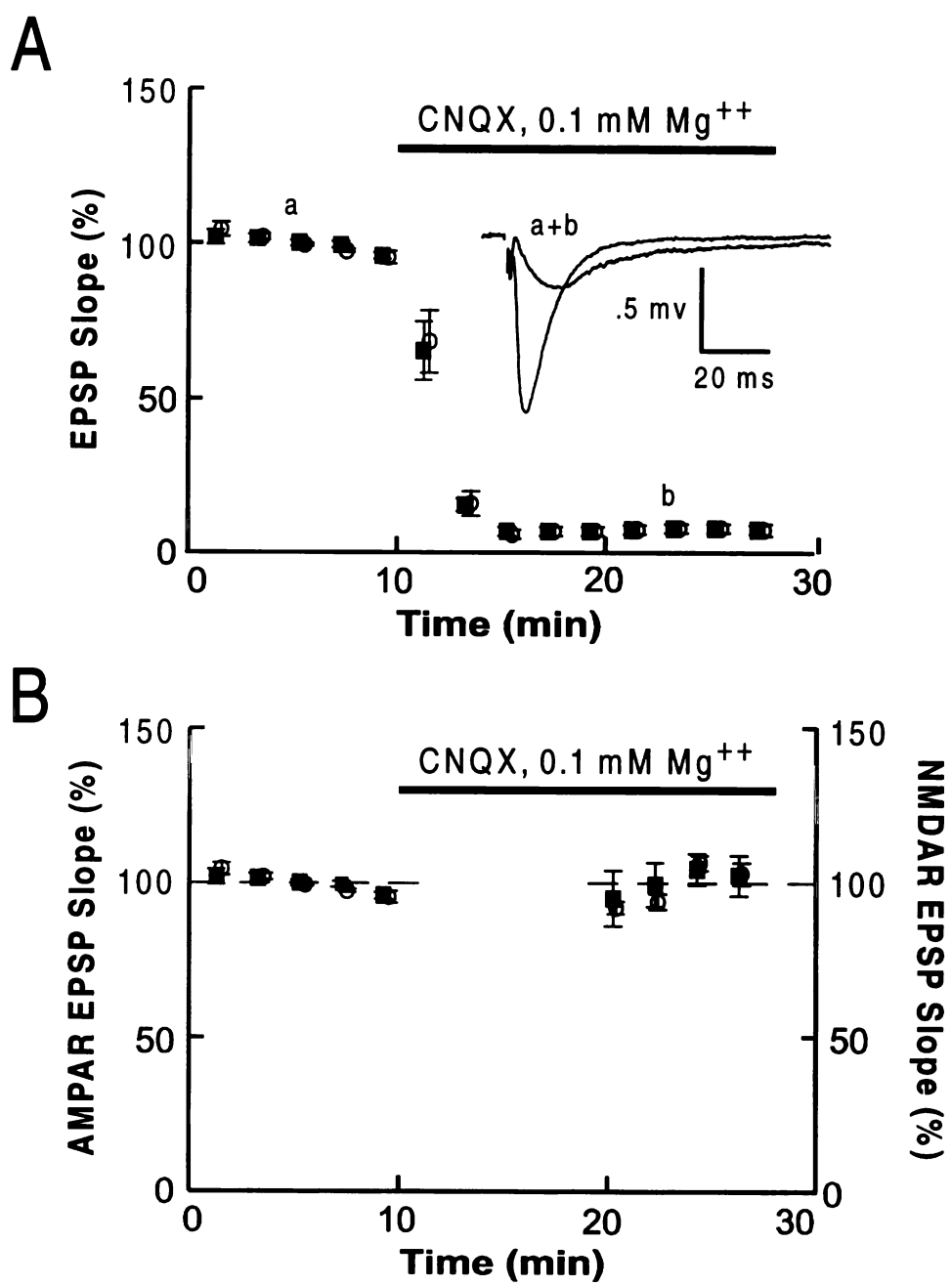


Figure 9. Changes in the NMDAR EPSP following generation of LTD and LTP under normal conditions.

A. LTD of AMPAR EPSPs (elicited by 1 Hz stimulation for 10 min, given twice separated by 10 min) is accompanied by a decrease in NMDAR EPSPs (n=8).

B. LTP of AMPAR EPSPs (elicited by a tetanus of 100 Hz, 1 sec given twice) is not accompanied by a significant change in NMDAR EPSPs (n=7).

C. Following the generation of LTD using LFS, both AMPAR and NMDAR EPSPs are repotentiated by tetanic stimulation (n=6).

UCSF LIBRARY

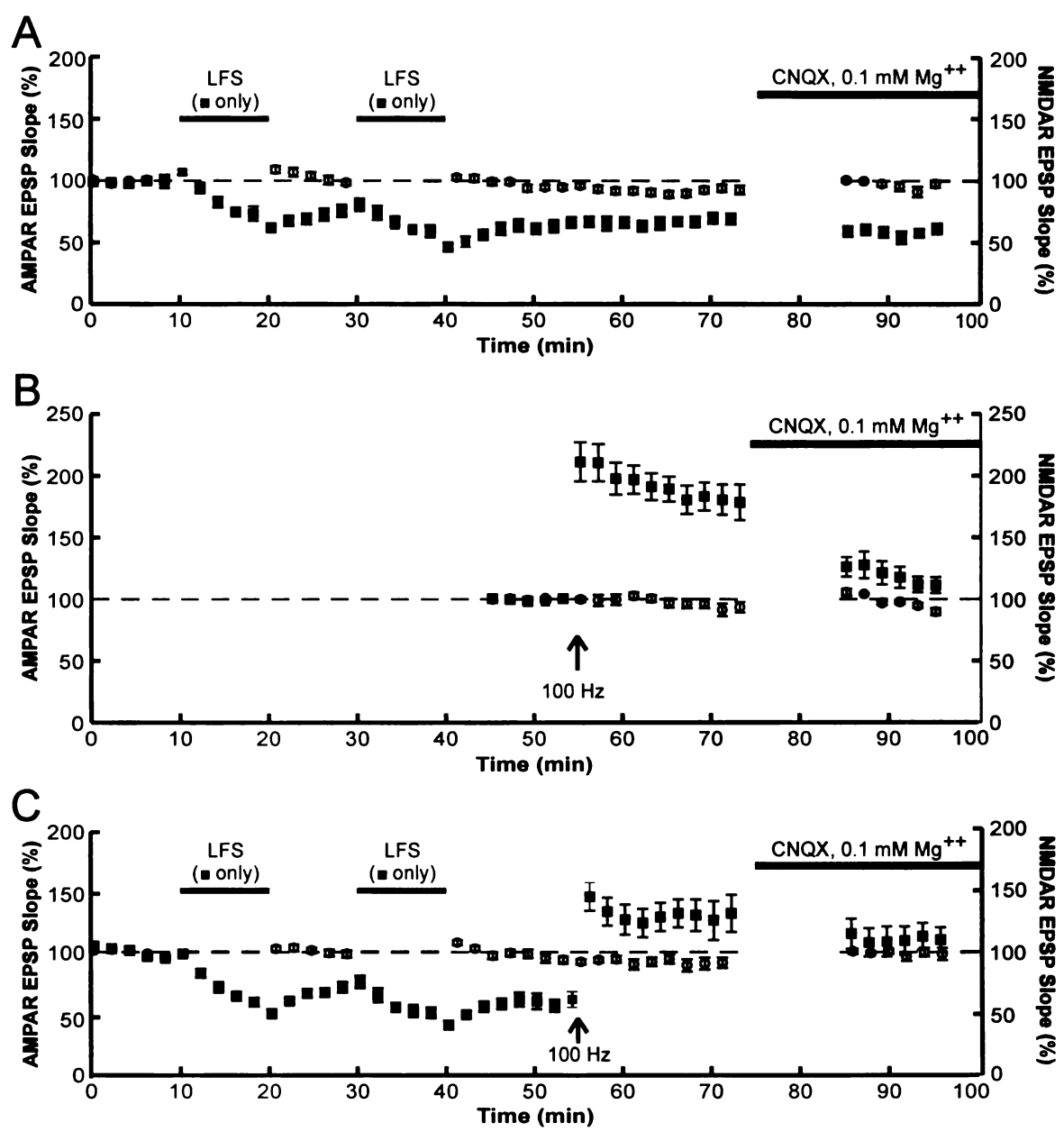


Figure 10. $1/CV^2$ of AMPAR EPSCs but not NMDAR EPSCs changes during LTD and LTP.

A. LFS causes LTD of both AMPAR and NMDAR EPSCs. An example (A_1 and A_2) and summary ($n=8$) (A_3) of experiments in which LFS (1 Hz for 5 min at -40 mV) was applied to one input while holding the cell at -90 mV. 15-20 minutes after LFS, CNQX (10 μ M) was applied and the cell was depolarized to +40 mV to record NMDAR EPSCs. Sample traces (A_1) (20 consecutive responses) were taken at the times indicated.

B. Changes in $1/CV^2$ of the AMPAR and NMDAR EPSCs following the generation of LTD. Only $1/CV^2$ of the AMPAR EPSCs in the test input changed with LTD (* indicates $p<0.02$).

C. LTP of AMPAR EPSCs occurs without a change in the NMDAR EPSCs. An example (C_1 and C_2) and summary ($n=8$) (C_3) of experiments in which LTP of AMPAR EPSCs was generated in one input by a pairing protocol (1 Hz for 5 min at 0 mV). 15-30 minutes after pairing, NMDAR EPSCs were isolated as in A. Sample traces (C_1) were taken at the times indicated.

D. Changes in $1/CV^2$ of the AMPAR and NMDAR EPSCs following LTP. Only $1/CV^2$ of AMPAR EPSCs in the test input was changed by LTP (* indicates $p<0.005$).

E. Paired-pulse facilitation (interstimulus interval=50 ms) causes an increase in $1/CV^2$ of both AMPAR and NMDAR EPSCs ($n=6$). (* indicates $p<0.05$, AMPA; $p<0.005$, NMDA)

F. $1/CV^2$ of AMPAR EPSCs is much less than that of NMDA EPSCs recorded in the same input ($n=27$). (* indicates $p<0.0001$)

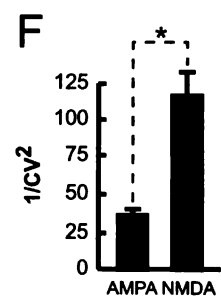
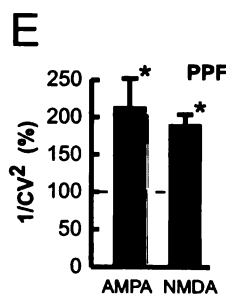
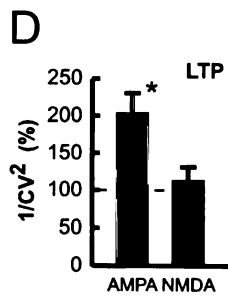
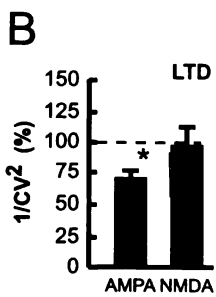
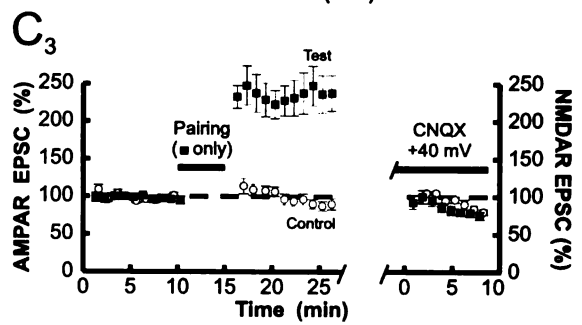
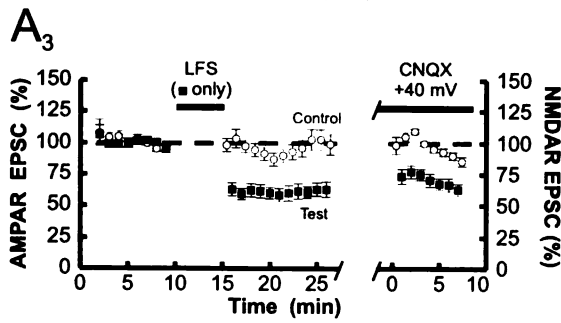
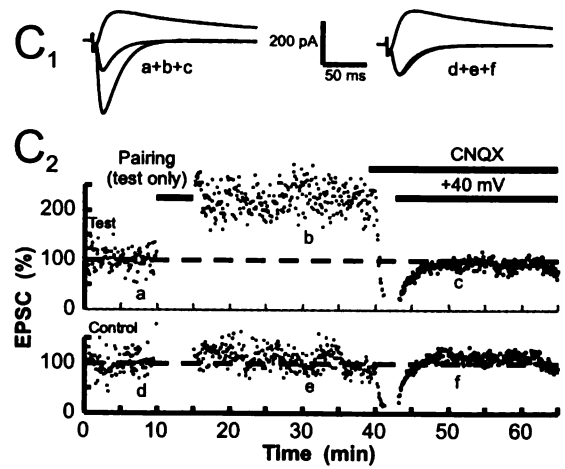
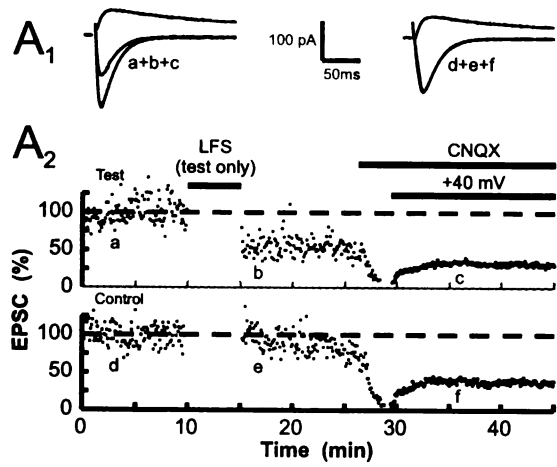


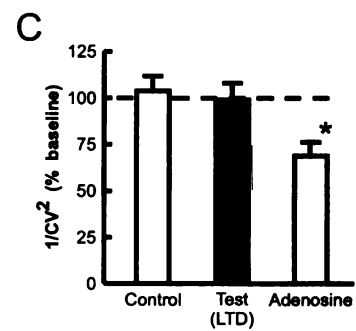
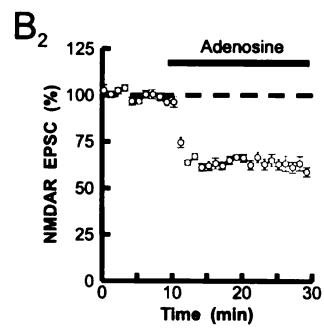
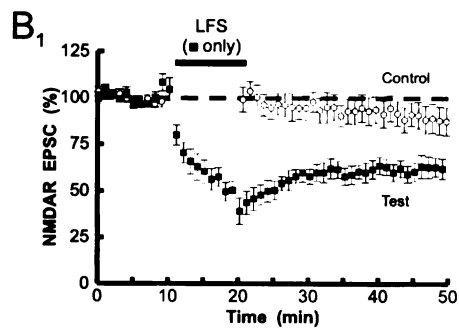
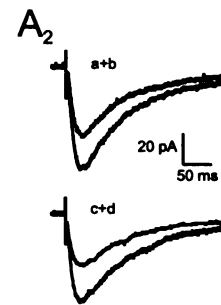
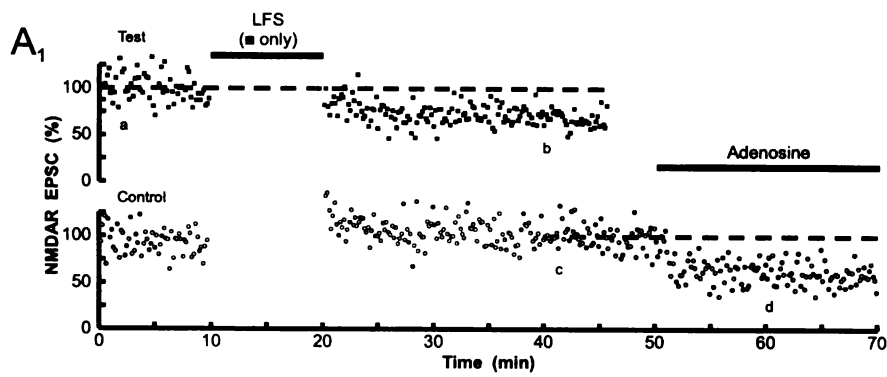
Figure 11. $1/CV^2$ of pharmacologically isolated NMDAR EPSCs is unaffected following generation of LTD.

A. An example (A_1) of an experiment in which LFS (1 Hz, 10 min holding cell at -40 mV) was applied to one of two inputs. Thirty minutes following LFS, adenosine (0.5 μ M) was applied. Sample traces (A_2) were taken at the times indicated.

B. Summary ($n=8$) of experiments like that in A. B_1 shows the effects of LFS applied to the test input. B_2 shows the effects of adenosine (0.5 μ M applied 30-45 minutes after the LFS) on the control input.

C. Changes in $1/CV^2$ of NMDAR EPSCs in the control and test inputs following generation of LTD and following application of adenosine. (* indicates $p<0.002$)

UCSF LIBRARY



UCSF

Figure 12. Synaptic activity can depress the NMDAR EPSP without affecting the AMPAR EPSP.

Brief bursts of stimulation (10 Hz for 10 sec applied 6 times) depress the NMDAR EPSP (n=7; A), an effect that is blocked when D-APV (50 μ M) is present during the 10 Hz stimulation (n=6; B) and which causes no significant or long-lasting changes in the AMPAR EPSP (n=7; C).

Repetitive periods of LFS (2 Hz, for 5 min) can also depress the NMDAR EPSP without inducing any long lasting change in the AMPAR EPSP (n=7; D). All experiments were performed and analyzed as described for the experiments in Figure 8.

UCSF
SFMRI

CHAPTER FOUR

CAM-KINASE II AND LTP ENHANCE SYNAPTIC TRANSMISSION BY THE SAME MECHANISM

Summary

Calcium-sensitive kinases are thought to play a role in long-term potentiation (LTP). To test the involvement of calcium/calmodulin-dependent kinase II (CaM-kinase II), a truncated, constitutively active form of this kinase was directly injected into CA1 hippocampal pyramidal cells. Inclusion of CaM-kinase II in the recording pipette resulted in a gradual increase in the size of excitatory postsynaptic currents (EPSCs). No change in evoked responses occurred when the pipette contained heat-inactivated kinase. The effects of CaM-kinase II mimicked several features of LTP in that it caused a decreased incidence of synaptic failures, an increase in the size of spontaneous EPSCs, and an increase in the amplitude of responses to iontophoretically applied AMPA. To determine if the CaM-kinase II-induced enhancement and LTP share a common mechanism, occlusion experiments were carried out. The enhancing action of CaM-kinase II was greatly diminished by prior induction of LTP. In addition, following the increase in synaptic strength by CaM-kinase II, tetanic stimulation failed to evoke LTP. These findings indicate that CaM-kinase II alone is sufficient to augment synaptic strength and that this enhancement shares the same underlying mechanism as the enhancement observed with LTP.

Introduction

Repetitive activation of excitatory glutamatergic synapses results in a long-lasting enhancement in synaptic strength, referred to as long-term potentiation (LTP). The most widespread form of LTP requires the activation of postsynaptic N-methyl-D-aspartate receptors (NMDARs) and a rise in postsynaptic Ca^{2+} . Considerable evidence suggests

U.S.N.

that the rise in Ca^{2+} activates Ca^{2+} -dependent kinases (Bliss and Collingridge, 1993; Lisman, 1994; Larkman et al., 1995; Nicoll and Malenka, 1995) . In particular the Ca^{2+} /calmodulin-dependent kinase II (CaM-kinase II), which is present at extremely high concentrations in the postsynaptic density (Kennedy et al., 1983; Kelly et al., 1984), is an attractive candidate for mediating the effects of Ca^{2+} . Many lines of indirect evidence support a role for this kinase in mediating the effects of Ca^{2+} on synaptic strength (Lisman, 1994; Nicoll and Malenka, 1995) . A direct approach to investigating a role for CaM-kinase II in LTP is to determine its effects on synaptic strength and LTP when the concentration of activated kinase is elevated in postsynaptic cells. Recently two groups, one using vaccinia virus in acute hippocampal slices (Pettit et al., 1994) and one using mouse genetics (Mayford et al., 1995), have expressed constitutively active forms of this enzyme. In the vaccinia virus experiments (Pettit et al., 1994) evidence consistent with an enhancement in synaptic transmission was presented, and LTP induction was impaired. In contrast, in the transgenic mouse experiments (Mayford et al., 1995) no change in synaptic transmission or in the ability to generate LTP was found. Aside from the apparent discrepancies in these reports, it is difficult in these experiments to entirely exclude indirect effects associated with the use of expression systems. In the present experiments we have examined the effects of CaM-kinase II by directly injecting a constitutively active form of this enzyme into the postsynaptic cell.

Methods

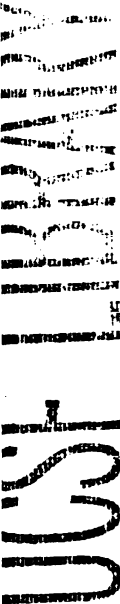
Hippocampal slices prepared from 3- to 5-week-old male Hartley guinea pigs or 2- to 3-week-old Sprague Dawley rats. All bathing solutions contained picrotoxin

WISCONSIN

(100 μ M). Field electrodes contained 1 M NaCl and intracellular electrodes contained 2 M potassium-acetate with either 1 μ M activated CaM-kinase II or heat-inactivated CaM-kinase II as control. The tips of whole-cell pipettes were filled with a solution containing (in mM): 123 Cs-gluconate, 15.5 CsCl, 10 HEPES, 10 Cs-EGTA, 8 NaCl, 1 CaCl₂, 2 Mg-ATP, 0.3 Na₃-GTP, 0.2 cAMP, 10 D-glucose and 10 μ M microcystin-LR (pH 7.3 with CsOH, 280-290 mosM). These patch electrodes were then backfilled with the same solution containing either 200 nM activated CaM-kinase II or heat-inactivated CaM-kinase II. Cells were maintained at a membrane potential between -70 and -85 mV.

To evoke synaptic responses, stimuli (100 μ s duration at a frequency of 0.05-0.1 Hz) were delivered through fine bipolar stainless steel electrodes placed in stratum radiatum. For two pathway experiments, two stimulating electrodes were placed on either side of the recording electrodes. To elicit LTP tetani (4 trains of 100 pulses [100 Hz] at 20 sec intervals) were delivered at test stimulus intensity. AMPA responses were evoked by iontophoretically applying AMPA (negative 75-150 nA, 1 s) every 120 s with an electrode containing 10 mM AMPA (pH 8) placed close to the cell body layer. For the first 2-3 min after break-in, AMPA pulses were applied more frequently and the iontophoretic current adjusted to obtain 100-200 pA responses.

Minimal stimulation recordings were stimulated at a frequency of 1 Hz. No attempts were made to obtain recordings from only a single site. Instead, a stimulus level was chosen which resulted in synaptic failures on 50% or more of the responses. Failure rates were estimated by the method described in Chapter Two for successive epochs of 180 stimuli. Pipette solutions were exchanged using a 2PK+ perfusion kit (Adams & List Assoc.). Fast green (1%) was included in the solution to verify diffusion into the



cell, which took approximately 8-10 minutes (Figure 13). Unless otherwise stated, values given in the text are means \pm s.e.m and significance was assessed using either a paired or unpaired Student's *t* test.

Baseline values of EPSPs, EPSCs and iontophoretic responses were obtained from averages of responses during the first two to three minutes (time 0 on each graph) or for the perfusion experiments the 6 min prior to the time of perfusion and defined as 100% for subsequent analyses. For all experiments neurons injected with activated or heat inactivated CaM-kinase II were interleaved during daily sessions. The CaM-kinase II (α subunit) was truncated at residue 316 to give a monomeric (30-40 kDa) enzyme, expressed in baculovirus/Sf9 cells, and purified as described (Mikherji et al., 1994). The kinase (2 μ M) was converted to its constitutively active form (30-40% of Ca²⁺-independent) by autothiophosphorylation as described (McGlade-McCulloh et al., 1993). Inactivated kinase was heated for 10 min at 100° C prior to addition to the autothiophosphorylation reaction. All kinase samples were diluted 2-fold (intracellular recording) or 10-fold (whole-cell recording) in pipette solution just before use and were maintained on ice. Aliquots were renewed within two hours after their preparation. After some experiments, kinase activity of the internal solution containing the diluted activated CaM-kinase II was measured and found to retain 80% of its original activity.

Results

We first tested the effects of the activated CaM-kinase II enzyme by adding it to the whole-cell pipette solution (200 nM) and measuring the amplitude of excitatory postsynaptic currents (EPSCs) over time. While a clear growth in the size of the EPSC

U.S.T.S.N

was seen in some cells, the effect was variable and could not be systematically studied. In an attempt to increase the reliability of this effect we included the phosphatase inhibitor microcystin-LR (10 μ M) in the pipette solution. Under these conditions a very consistent growth in the size of the EPSC was observed (Figure 14). The size began to increase significantly within 6-8 min after establishing the whole-cell recording, and the maximum effect occurred at approximately 15-30 min (Figure 14B, filled circles). The average size of the EPSC reached $164 \pm 16\%$ ($n=8$) of the initially recorded EPSC. CaM-kinase II had no effect on the cells' passive membrane properties. To ensure that the enhancement resulted from the CaM-kinase II and not from nonspecific effects or from the microcystin-LR, interleaved recordings were made with the identical internal recording solution, except that heat-inactivated kinase (200 nM) was used instead of the active kinase. Under these recording conditions, no enhancement was observed ($105 \pm 6\%$, $n=15$) (Figure 14B, open circles).

To gain more insight into the mechanisms involved in the CaM-kinase II-induced enhancement, we carried out experiments using minimal stimulation so that we could record failures of evoked responses (Kullmann and Nicoll, 1992; Liao et al., 1992; Isaac et al., 1995). In these experiments, the pipette was internally perfused under visual control to deliver the CaM-kinase II in a temporally controlled manner (see Methods). In the example shown in Figure 15, the stimulus intensity was initially adjusted so that it produced mostly failures. After a stable baseline was established, perfusion of the pipette with CaM-kinase II was initiated and about 10 min later the failure rate began to decrease accompanied by an increase in the mean size of the response (Figure 15B). A summary of 5 experiments with the active kinase (Figure 16A; closed circles) demonstrates that the

USM

failure rate on average decreased by $27 \pm 10\%$ ($P < 0.02$), while the heat-inactivated kinase had no significant effect on either the failure rate (Figure 16A; open circles) or on the mean size of the EPSC (Figure 16B) ($n=5$). Consistent with the decrease in failure rate we also found that, associated with the increase in the evoked response, the frequency of spontaneous EPSCs increased $32 \pm 6\%$ ($n=4$) (compared to $6 \pm 4\%$ [$n=3$]) for the heat-inactivate CaM-kinase II ($P < 0.02$) (data not shown).

The results presented thus far can be explained by either an increase in the probability of transmitter release (Stevens and Wang, 1994) and/or an all-or-none upregulation of clusters of AMPA receptors (AMPA receptors) (Liao et al., 1995; Isaac et al., 1995). Indeed, we also found that CaM-kinase II increased the size of the spontaneous EPSCs (Figure 17A) (active = $36 \pm 3\%$, $n=4$; inactive = $6 \pm 4\%$, $n=3$ [$P < 0.002$]). This observation suggested that CaM-kinase II might be enhancing the EPSCs, at least in part, by increasing the sensitivity of AMPARs to synaptically released glutamate. This possibility was tested directly by monitoring the responses of CA1 cells to iontophoretically applied AMPA. The response to AMPA slowly increased when the recording pipette contained CaM-kinase II ($151 \pm 10\%$ measured at 40-50 min, $n=8$) (Figures 17B₁ and C, filled circles), but not when it contained the inactive form ($101 \pm 14\%$, $n=8$) (Figures 17B₂ and C, open circles) ($P < 0.02$). These results indicate that CaM-kinase II, applied directly into the cell, can increase the sensitivity of AMPARs, an effect that likely contributes to the enhancement of the EPSC.

Are the effects of CaM-kinase II related to LTP? To address this question we designed occlusion experiments in which the effects of CaM-kinase II on control synapses were compared to its effect on synapses expressing LTP. In these experiments,

two independent inputs onto the same population of pyramidal cells were monitored with field electrode recordings (Figure 18A). A saturating level of LTP was induced in one of the pathways (S1), while the other pathway (S2) served as a control (Figure 18A). Once LTP was observed to be stable (typically within 60 min), a whole-cell recording was made from a cell within the population sampled by the field electrode (Figure 18B). The effect of CaM-kinase II on the LTP expressing pathway was then compared to the effect on the control pathway (Figures 18B₁ and B₂), while continuing to monitor the field EPSPs from both pathways (Figure 18B₃). Figures 18B₁ and B₂ demonstrate that CaM-kinase II had its normal enhancing effect on the control pathway, but was without effect on the pathway expressing LTP. A summary graph of all the experiments (Figure 19) clearly demonstrates that the enhancing action of CaM-kinase II was markedly attenuated on synapses expressing LTP (an increase of $17\pm 9\%$, $n=6$ versus $67\pm 16\%$, $n=6$, measured at 40-55 min from tetanized and untetanized pathways, respectively, $P<0.0001$) (Figure 19B₁). The average amplitude of the CaM-kinase II-induced potentiation was less than that for saturated LTP (compare Figures 19A₁ and B₁). This most likely is due to the variable loading of the cells with the kinase, as suggested by the fact that the potentiation observed in some of the loaded cells was equivalent to that observed with saturated LTP (data not shown). To verify that this selective effect was, in fact, due to the CaM-kinase II, a series of control experiments, in which heat-inactivated enzyme was used, were interleaved with the above experiments (Figure 19B₂) ($n=6$) and no change in the EPSCs in either pathway occurred. The simultaneously recorded extracellular responses to both the control and LTP expressing pathways remained constant in all of these experiments (Figure 19A₂).

In a final set of experiments we performed the reverse occlusion experiment in which we first potentiated the synapses with CaM-kinase II and then asked if this potentiation affected the ability to induce LTP. Whole-cell recording techniques could not be used for this experiment, because the ability to induce LTP washes out over the 10-30 min period required for the CaM-kinase II effect to stabilize. We therefore loaded sharp microelectrodes with the enzyme (1 μ M). Because this method of loading neurons with CaM-kinase II was less successful than that used with the whole-cell approach, we only examined the ability to generate LTP in those cells in which CaM-kinase II caused an enhancement. Figure 20A₁ shows a summary graph of these cells (n=5). In these experiments we also simultaneously monitored field potentials, so that the magnitude of LTP in the field could be compared to that generated in the cell. While tetanization caused substantial LTP in the field (Figure 20A₂), it produced no LTP in the cells loaded with CaM-kinase II (Figure 20A₁) ($208 \pm 40\%$ vs. $79 \pm 33\%$ of baseline, $P < 0.0001$ for field potential and intracellular recordings, respectively). In a series of control experiments with the heat-inactivated enzyme, the magnitude of the LTP in the cells (Figure 6B₁) was similar to that recorded in the field (Figure 20B₂) (n=5). These findings provide further evidence that LTP and CaM kinase II enhance EPSCs by the same underlying mechanisms.

Discussion

The hypothesis that CaM-kinase II mediates the effects of the NMDAR-dependent rise in postsynaptic Ca²⁺ that triggers LTP is attractive and is based on a variety of experimental approaches. First, biochemical studies have shown that the kinase can act

as a molecular switch, conferring properties that are advantageous for long-lasting storage of changes initiated by brief Ca^{2+} signals (Lisman, 1985; Miller and Kennedy, 1986; Lisman, 1994). Second, manipulations that interfere with CaM-kinase II function interfere with LTP. These experiments include the use of inhibitors (Malenka et al., 1989; Malinow et al., 1989; Ito et al., 1991; Wyllie and Nicoll, 1994) and the knockout of the α subunit of CaM-kinase II in mice (Silva et al., 1992). Third, LTP is associated with an increase in the activity of the Ca^{2+} independent form of CaM-kinase II (Fukunaga et al., 1993). Fourth, recent experiments established that one of the targets for CaM-kinase II is the AMPAR itself. Thus, activated CaM-kinase II can phosphorylate AMPARs in the postsynaptic density, and can enhance responses to AMPAR agonists in cultured hippocampal neurons (McGlade-McCulloh et al., 1993) and acutely isolated dorsal root ganglion neurons (Kolaj et al.,1994). Responses evoked by activating GluR 1 receptors expressed in oocytes are also enhanced by CaM-kinase II (Yakel et al., 1995).

The present results demonstrate that in hippocampal pyramidal cells *in situ* CaM-kinase II enhances EPSCs and that this enhancement is due, at least in part, to an enhancement of AMPAR sensitivity, thus extending previous results in cultured neurons (McGlade-McCulloh et al., 1993) and spinal cord neurons (Kolaj et al.,1994).

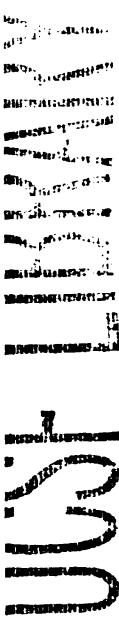
CaM-kinase II also caused an increase in the frequency of spontaneous EPSCs and a reduction in the number of failures of evoked responses. These results can be explained by a presynaptic enhancement in transmitter release (Stevens and Wang, 1994) and/or an all-or-none upregulation of clusters of AMPARs (Isaac et al., 1995; Liao et al., 1995). The finding that the enhancement of responses to exogenously applied AMPA was of similar magnitude to that observed with the evoked EPSC favors the latter hypothesis.

L
I
S
M
A
N

Most importantly, occlusion experiments establish that the synaptic enhancement evoked by CaM-kinase II shares the same underlying mechanism as LTP. Two reports recently appeared that examined the effects of over expression of constitutively active CaM-kinase II on LTP. One study found that over expression with vaccinia virus in the hippocampal slice impaired the ability to induce LTP (Pettit et al., 1994) , while the other study using transgenic mice found no impairment in LTP (Mayford et al., 1995) , even though significant effects on LTD were observed. The results of our acute experiments are more consistent with the former study.

Based on the use of inhibitors it has been proposed that protein kinase C activity (PKC) (Linden and Routtenberg, 1989; Malinow et al., 1989; Wang and Feng, 1992; Hvalby et al., 1994) and tyrosine kinase activity (O'Dell et al., 1991) are also required for LTP. Since our results indicate that CaM-kinase II alone mimics LTP, either CaM-kinase II can, in some unknown manner, activate these enzymes, or certain levels of basal PKC and tyrosine kinase activity are required in order for CaM-kinase II to cause a synaptic enhancement.

In summary, the present results indicate that the enhancement of synaptic strength caused by postsynaptic injection of activated CaM kinase II shares the same underlying mechanism(s) as LTP. It would appear that elucidating the substrates targeted by CaM-kinase II should shed considerable light on the molecular mechanisms underlying LTP. A likely target is the AMPAR itself, which is colocalized in the PSD with CaM-kinase II. Therefore, defining the mechanism by which CaM-kinase II increases AMPAR function should be particularly informative.

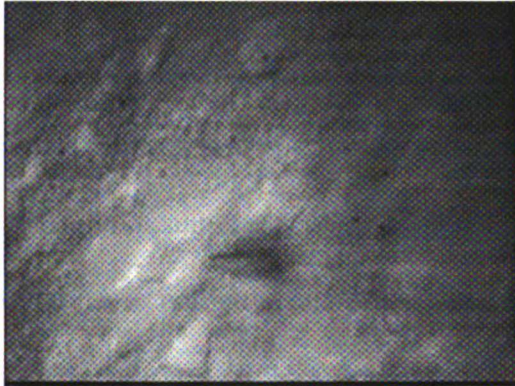


USP

Figure 13. Perfusion of the Dye Fast Green occurs in 8-10 Minutes

IR images of hippocampal slice at specified times following introduction of the dye Fast Green into the patch pipette (time=0) using a patch perfusion system.

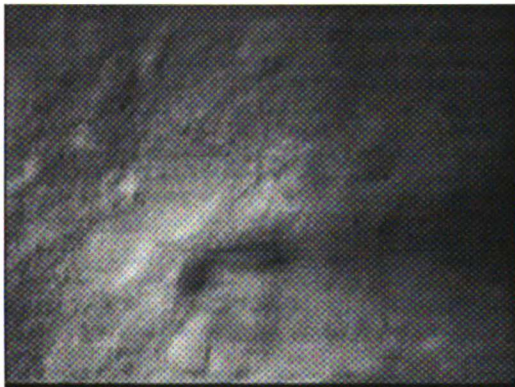
WEST



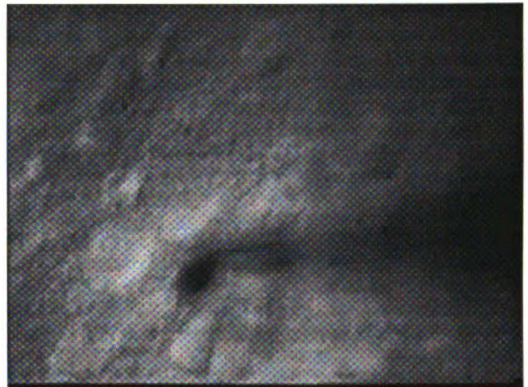
0 minutes



5 minutes



10 minutes



15 minutes

Figure 14. The Activated Form of CaM-kinase II Potentiates Evoked EPSCs Recorded in Hippocampal CA1 Neurons.

A. The average of 6 consecutive EPSCs obtained during whole-cell recordings at the indicated times following break-in are shown. Recordings were made with pipette solutions containing activated (upper traces) or heat-inactivated CaM-kinase II (lower traces). EPSCs are superimposed to the right.

B. Graph of summarized data illustrating the time course of EPSC amplitudes (see Methods for normalization procedure), in the presence of activated (filled circles) or heat-inactivated (open circles) CaM-kinase II.

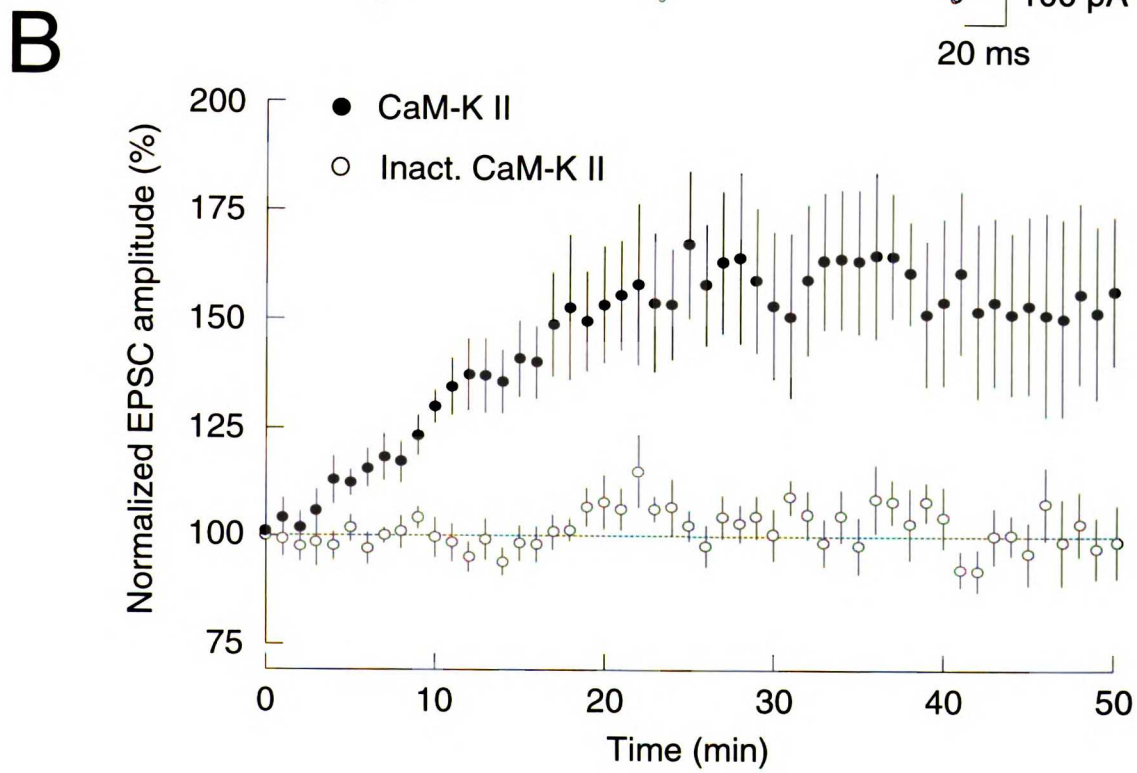
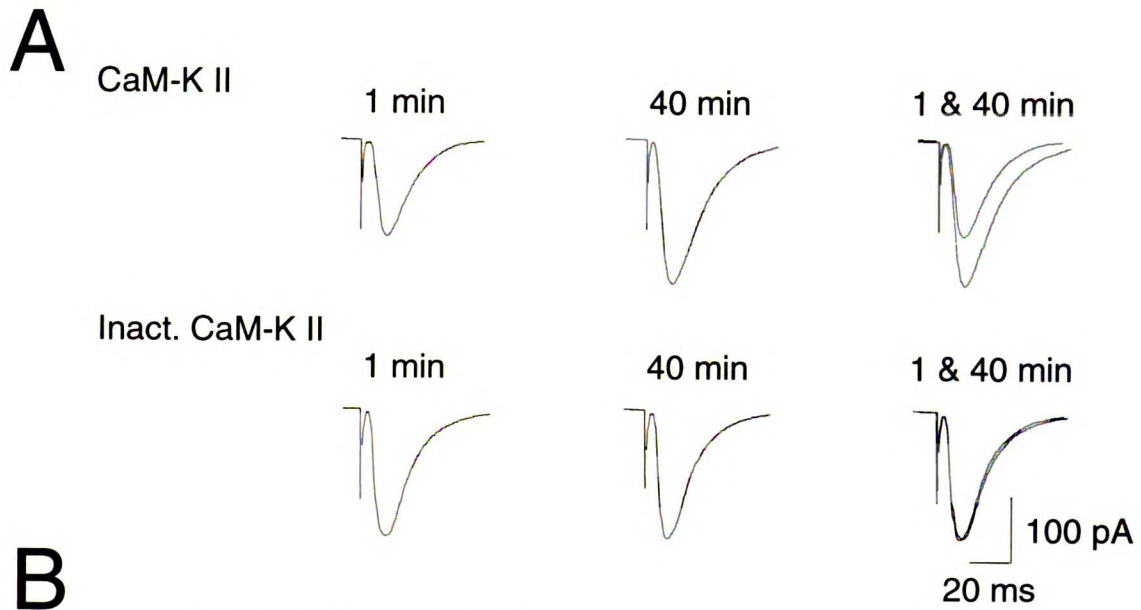
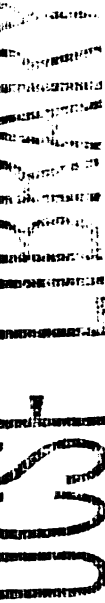


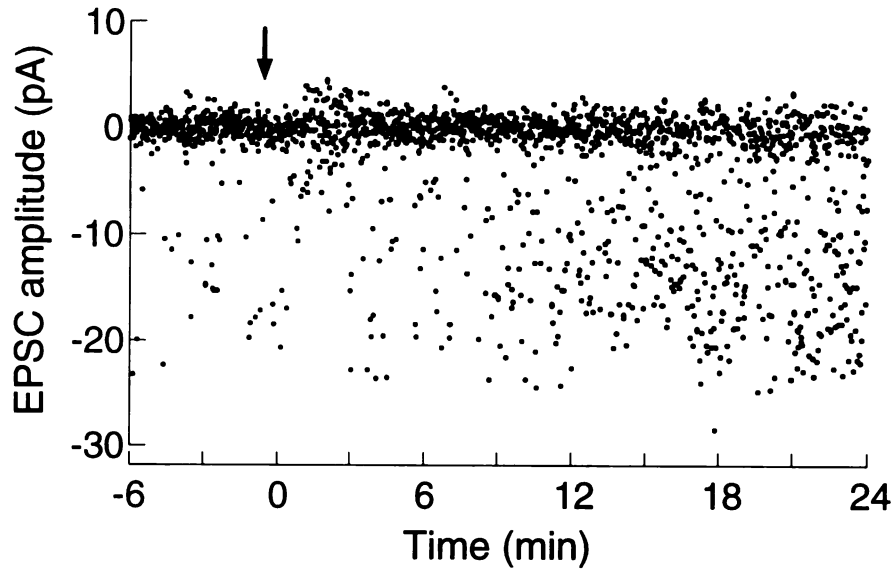
Figure 15. Individual Example showing the effects of CaM-kinase II perfusion on EPSCs evoked with minimal stimulation .

A. Individual example shows the decrease in failure rate following exchange of the pipette solution with one containing activated CaM-kinase II. Time 0 is defined as when the solution reaches the tip of the electrode.

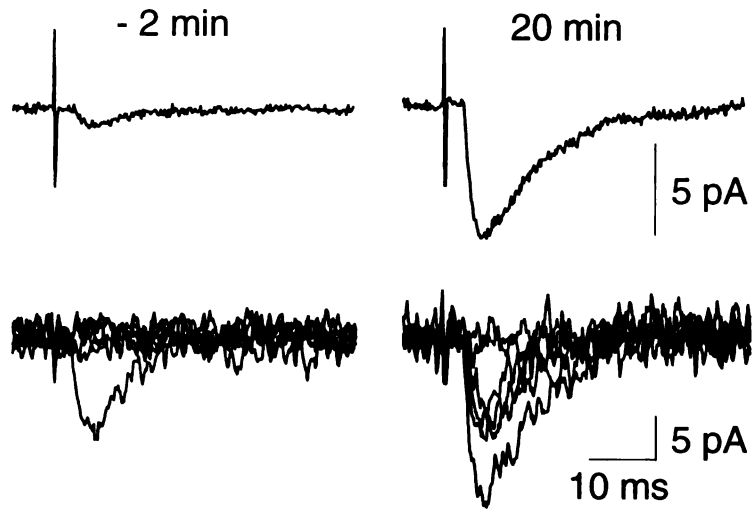
B. Average of 100 (top) or composite of 6 consecutive traces (bottom) at times indicated.



A



B



U.S. J. S. N.

Figure 16. CaM-kinase II induced potentiation is associated with a change in the number of synaptic failures

A. Summary of failures for experiments using activated (filled circles) or heat-inactivated CaM-kinase II (open circles).

B. Average amplitude of all events (including failures) for the same set of experiments.

UNIVERSITY OF
SOUTH ALABAMA

Figure 17. Postsynaptic sensitivity to AMPA is increased by CaM-kinase II.

A. Amplitude of spontaneous events increases with CaM-kinase II potentiation.

Cumulative amplitude distributions (A_1) comparing events collected 2-10 min (open circles) and 40-48 min (filled circles) after break-in with a CaM-kinase II containing pipette. Averages of events shown in panel A_1 are shown in A_2 superimposed (upper traces) and scaled (lower traces).

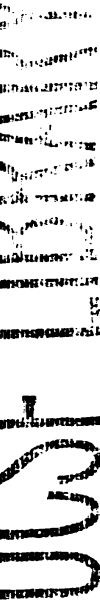
B. Chart records of membrane current from voltage-clamped CA1 pyramidal cells held at -75 mV show responses to brief iontophoretic pulses of AMPA. The presence of activated but not heat-inactivated CaM-kinase II potentiated AMPA responses 45 min after recordings were initiated.

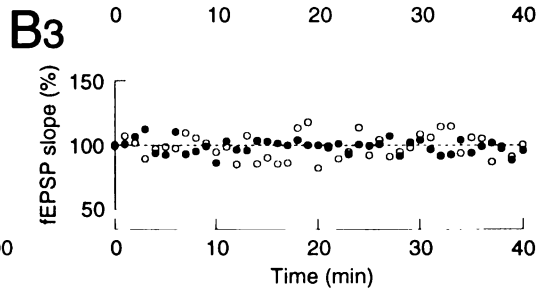
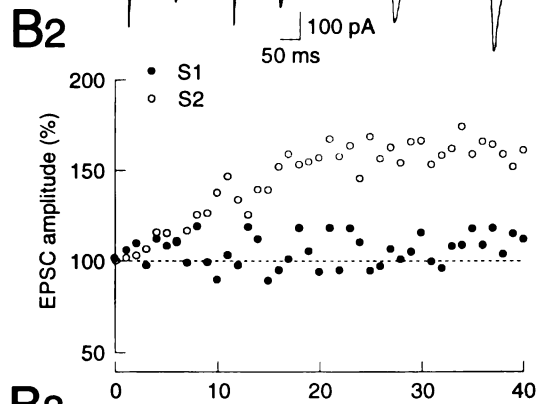
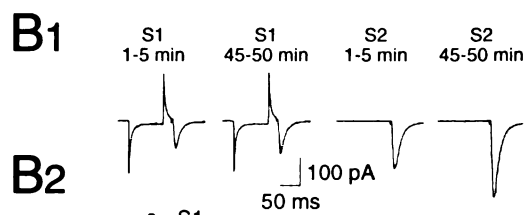
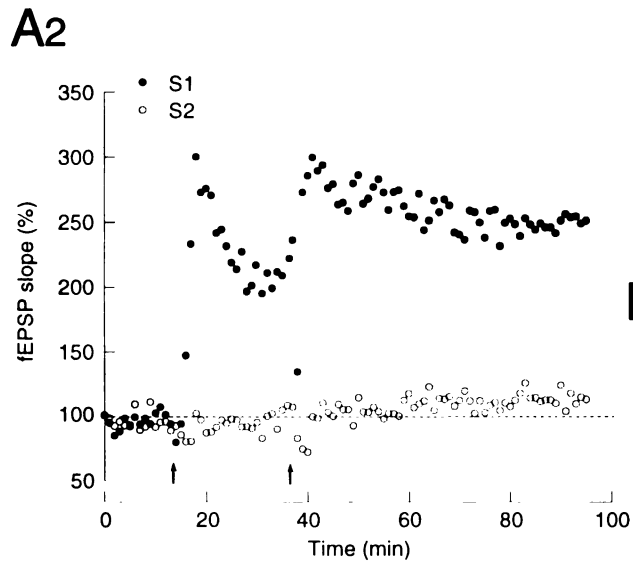
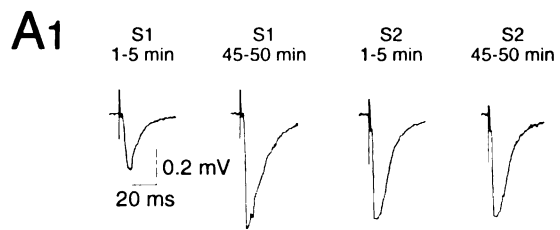
C. Plots of summarized data illustrating the time courses of the mean amplitude of AMPA-induced current expressed as percentage of the mean control amplitude, in the presence of either activated (filled circles) or heat-inactivated CaM-kinase II (open circles).

Figure 18. CaM-kinase II-induced potentiation of evoked EPSCs is occluded at synapses expressing saturated LTP.

A. Two independent inputs (S1 and S2) onto the same population of CA1 neurons were alternatively stimulated. LTP was induced by tetanic stimulation of S1; S2 served as the control input. Average of 15 consecutive traces (A_1) from a representative experiment were taken at the indicated times. (A_2) Normalized field EPSP slopes evoked in the tetanized pathway (S1; filled circles) and in the untetanized control pathway (S2; open circles). Two tetanizations were given in this experiment (see arrows).

B. Simultaneous recordings of whole-cell EPSCs obtained with a pipette containing CaM-kinase II (B_1 and B_2) and field potentials (B_3) performed 80 min after having induced LTP (A_2). EPSCs and field EPSPs were normalized to the initial responses at the beginning of the whole-cell experiment (dotted baseline). Panel B_1 shows representative EPSCs recorded at the indicated times from the two independent pathways.





100
 200
 300
 400
 500
 600
 700
 800
 900
 1000

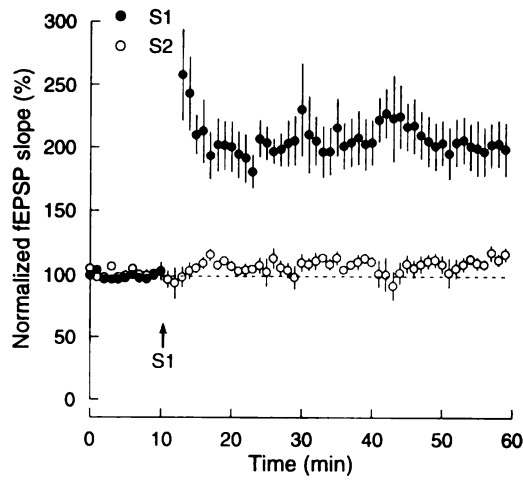
Figure 19. Summary data showing occlusion of LTP by the CaM-kinase II-induced potentiation.

A. The time course of changes in extracellular field EPSPs. A₁ illustrates LTP was induced in S1, but not S2, prior to whole-cell recordings; and A₂ the stability of field EPSPs during the whole-cell recordings (normalized to the initial recordings at the beginning of whole-cell experiments). Arrow indicates the time of the first tetanus given to S1.

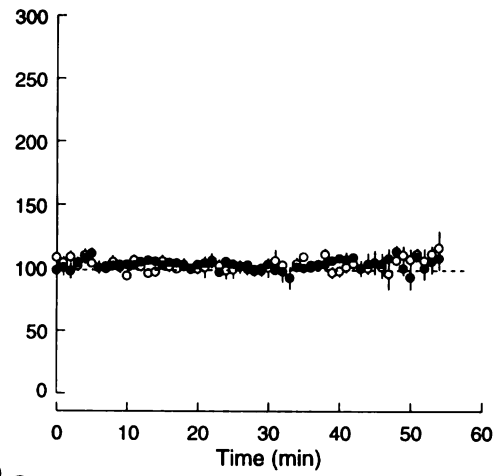
B. Graph illustrating potentiation of EPSC amplitudes by CaM-kinase II only in the untetanzed control pathway (S2; open circles) (panel B₁). EPSCs did not change when the pipette solution contained heat-inactivated CaM-kinase II (B₂). Because there was no difference in the magnitude of LTP induced in the two sets of experiments (active kinase = $117 \pm 11\%$ [n=6]; inactive kinase = $102 \pm 10\%$ increase [n=6]), the data from these experiments were combined in A.

1
2
3
4
5
6
7
8
9
10
11
12
13
14
15
16
17
18
19
20
21
22
23
24
25
26
27
28
29
30
31
32
33
34
35
36
37
38
39
40
41
42
43
44
45
46
47
48
49
50
51
52
53
54
55
56
57
58
59
60
61
62
63
64
65
66
67
68
69
70
71
72
73
74
75
76
77
78
79
80
81
82
83
84
85
86
87
88
89
90
91
92
93
94
95
96
97
98
99
100

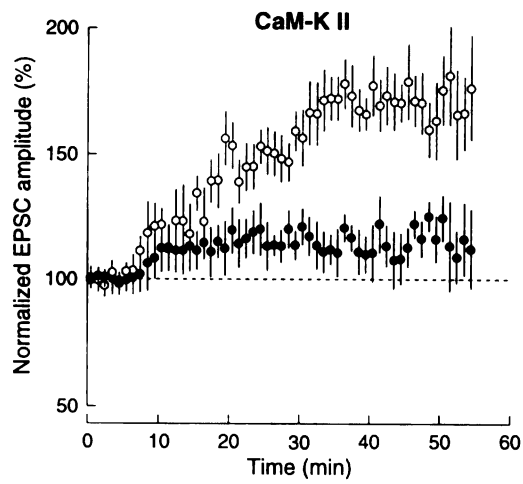
A1 Extracellular



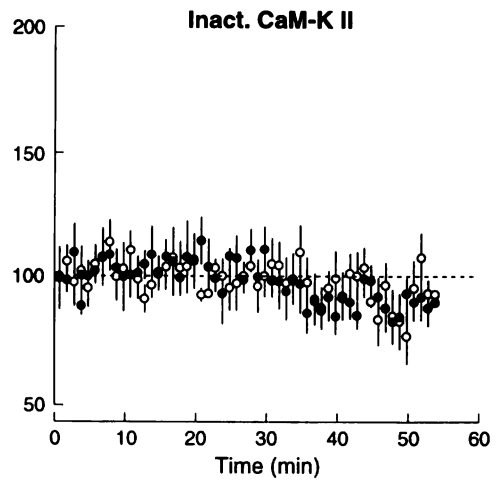
A2



B1 Whole-cell



B2



100
150
200
250
300

100
150
200

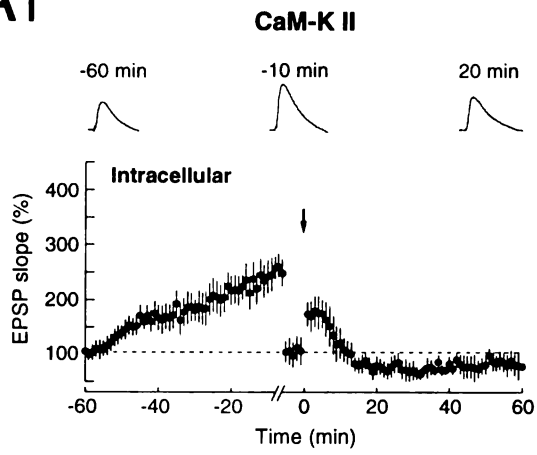
Figure 20. Summary data from occlusion experiments examining LTP at synapses already potentiated by activated CaM-kinase II.

A. Time course of EPSP changes recorded with intracellular electrodes containing CaM-Kinase II (A_1) with simultaneous recordings of field potentials (A_2).

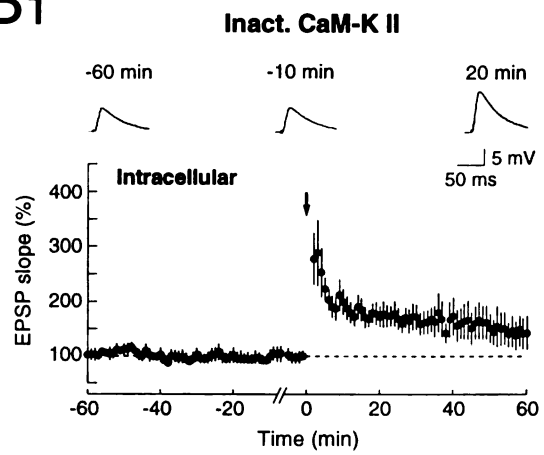
B. Similar experiments using heat-inactivated CaM-Kinase II as a control. Arrow indicates the tetanus given at time 0 min. Slopes of EPSPs in LTP were then re-normalized 5 min before the tetanus (dotted baseline). Insets show averaged EPSPs taken at indicated time.

85

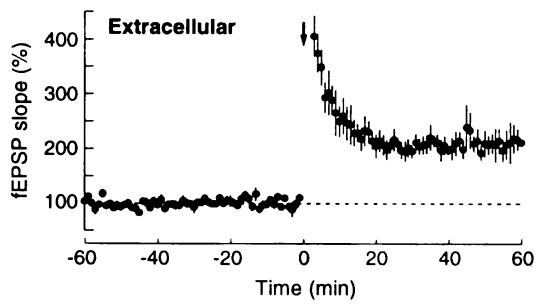
A1



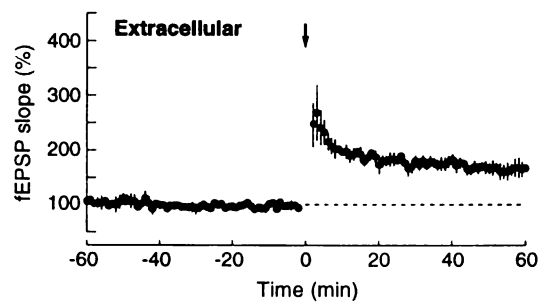
B1



A2



B2



Journal Pre-proof

CHAPTER FIVE

**LONG-TERM POTENTIATION AT SINGLE FIBER INPUTS TO
HIPPOCAMPAL CA1 PYRAMIDAL CELLS**

1
2
3
4
5
6
7
8
9
10
11
12
13
14
15
16
17
18
19
20
21
22
23
24
25
26
27
28
29
30
31
32
33
34
35
36
37
38
39
40
41
42
43
44
45
46
47
48
49
50
51
52
53
54
55
56
57
58
59
60
61
62
63
64
65
66
67
68
69
70
71
72
73
74
75
76
77
78
79
80
81
82
83
84
85
86
87
88
89
90
91
92
93
94
95
96
97
98
99
100

Summary

Despite extensive investigation, it remains unclear whether presynaptic and/or postsynaptic modifications are primarily responsible for the expression of long-term potentiation (LTP) in the CA1 region of the hippocampus. Here we address this issue by using techniques that maximize the likelihood of stimulating a single axon and thereby presumably a single synapse before and after the induction of LTP. Several basic properties of synaptic transmission were examined including the probability of neurotransmitter release (p_r), the quantal amplitude (q), and the potency, which is defined as the average size of the postsynaptic response when release of transmitter does occur. LTP was routinely associated with an increase in potency, whereas increases in p_r alone were not observed. LTP was also reliably induced when baseline p_r was high indicating that synapses with high p_r can express LTP. These results suggest that the mechanism for the expression of LTP involves an increase in q and is difficult to explain by an increase in p_r alone.

Introduction

Long-term potentiation (LTP), an activity-dependent, long-lasting increase in synaptic strength, has received considerable attention because of its potential role in learning and memory. However, confusion exists concerning whether the locus of expression of LTP in hippocampal CA1 pyramidal cells is primarily presynaptic or postsynaptic (Kullmann and Siegelbaum, 1995). One approach that has been used by several laboratories involves the technique of minimal stimulation in the CA1 region in which the stimulus is reduced to a level so that only a single or a few fibers are activated.

In most of these studies (Malinow and Tsien, 1990; Kullmann and Nicoll, 1992; Larkman et al., 1992; Liao et al., 1992; Stevens and Wang, 1994; Bolshakov and Siegelbaum, 1995; Stricker et al., 1996b) LTP was associated with a decrease in the incidence of synaptic failures, a result that has been attributed to an increase in the probability of transmitter release (p_r). Evidence was also presented that an increase in quantal amplitude (q) accompanied LTP (Foster and McNaughton, 1991; Kullmann and Nicoll, 1992; Larkman et al., 1992; Liao et al., 1992), a result that, in contrast, is consistent with a postsynaptic modification.

Recently, an alternative explanation has been offered for the change in failures associated with LTP (Isaac et al., 1995; Liao et al., 1995): silent synapses that lack functional AMPA receptors may exist and be converted to functional synapses following the induction of LTP. Such a scenario provides a postsynaptic mechanism that can explain almost all of the electrophysiological changes observed during LTP. However, results from two recent reports, based primarily on minimal stimulation in either the CA1 region (Stevens and Wang, 1994) or in the CA3 pyramidal cell layer (Bolshakov and Siegelbaum, 1995) appear to be incompatible with a significant postsynaptic contribution to LTP since no change in q was observed. Instead it was proposed that LTP must be due solely to a robust increase in p_r .

One possible explanation for the discrepancy between the results obtained with minimal stimulation is that in those studies suggesting a change in q , more than one fiber was stimulated whereas in the studies reporting only changes in p_r , multiple fibers were never inadvertently activated. Since several other lines of evidence suggest that LTP is associated with postsynaptic changes (Davies et al., 1989; Manabe et al., 1992; Oliet et

al., 1996), we have reinvestigated the quantal changes that occur during LTP when every effort is made to activate only a single fiber, and presumably a single synapse. In contrast to some recent results (Stevens and Wang, 1994; Bolshakov and Siegelbaum, 1995), we find that when LTP is examined with single fiber stimulation, it is routinely associated with a significant increase in q and cannot be explained by an increase in p_r alone.

Methods

Transverse hippocampal slices were prepared from 12-18 day-old Sprague-Dawley rats. 100 μ M picrotoxin was included in the external solutions during all experiments. The composition of the whole-cell solution was 107.5 mM cesium gluconate, 20 mM Hepes, 0.2 mM EGTA, 5 mM QX-314-bromide, 8 mM NaCl, 10 mM tetraethylammonium chloride, 4 mM MgATP, and 0.3 mM GTP (pH 7.2). For both whole-cell and perforated patch-clamp recordings only cells with initial seal resistances greater than 10 $G\Omega$ were used. Cells were held at -60 mV unless otherwise stated and series resistance was monitored continuously during recordings as described in Chapter Two. For perforated patch-clamp recordings data collection commenced only when the series resistance had stabilized, typically 20-40 minutes after seal formation. The mean series resistance values were: whole-cell = $13.2 \pm 2.6 M\Omega$, $n = 8$; perforated patch-clamp = $33.0 \pm 2.0 M\Omega$, $n = 13$. EPSCs were evoked at 0.67 Hz (whole-cell) or 0.33-0.5 Hz (perforated patch) using a patch electrode filled with external solution as a stimulating electrode. It was placed in stratum radiatum as far away as possible (1-3 mm) from the recording site. During perforated patch recording experiments, it was difficult to find a response that met criteria for a single fiber response and it was often necessary to change

stimulation position while recording in order to do so (success rate was 13 of 24 stimulus positions tested). Once afferent stimulation was commenced, it was maintained at the same frequency without interruption for the entire experiment. LTP was induced by depolarizing the cell to -10 mV (whole cell) or +10 mV (perforated patch) for 100 consecutive stimuli.

At the end of the majority of experiments (18 of 21 cells), CNQX (10 μ M) was applied and the contribution of the stimulus artifact to evoked EPSCs subtracted. The magnitude of LTP was calculated by averaging all of the responses (successes and failures; 400-1000 total) beginning 5 min after the LTP induction protocol and comparing this to the average of all the responses collected during the baseline period (150-200 events). Potency (Stevens and Wang, 1994) was defined as the mean amplitude of the EPSC (calculated by averaging all trials together) divided by the number of trials classified as successes (i.e. 1 - failure rate). If only a single release site is being activated, potency will be the same as quantal size (q). For all data analysis and data presentation in figures, the events collected for the 5 minutes following the pairing protocol were not used. For calculation of the paired pulse potency and for failure rates during single axon tests, both visual classification of failures (Stevens and Wang, 1994) and the method described above (Liao et al., 1995) were used. In the cells in which paired pulse data was collected, an epoch of 100 paired pulse stimuli (inter-pulse interval 40-70 msec) was delivered either immediately prior to, or during the baseline period and was then discontinued. Another epoch of 100 paired pulse sweeps was also collected following pairing. Data are expressed as mean \pm S.E.M. Simple binomial and Poisson distributions were used to model the data.

Results

We first investigated the properties of LTP with putative single fiber activation using standard whole-cell recording and minimal stimulation. By reducing the stimulation intensity until no response was detected on approximately 50% of the trials, we assumed, as previously reported, that we were predominantly recording EPSCs from one fiber and perhaps even a single release site (Stevens and Wang, 1994; Allen and Stevens, 1994; Stevens and Wang, 1995). In the example shown in Figure 21, the initial failure rate was 0.73 and the calculated potency was 4.5 pA. LTP was induced (Figure 21A, Pairing) by holding the cell at -10 mV for 100 stimuli while stimulation was maintained at baseline frequency. This method avoids any possible frequency-dependent changes in axon excitability or stimulation electrode properties. As illustrated in Figure 21B₁ and 21B₂, robust LTP was elicited (312%) which was accompanied by a marked increase in potency (to 8.7 pA, 195% of baseline, Figure 1B₃) but only a modest decrease in the failure rate (to 0.58; 79% of baseline failure rate). Figure 21C shows amplitude histograms of the events recorded prior to (thin line) and following (thick line) LTP induction. The most salient feature of this graph is that the small events (~2-5 pA) which make up the majority of the successes during the baseline period have largely disappeared and have shifted to larger amplitudes (~7-25 pA). This shift in the amplitude distribution, which indicates an increase in potency (Figure 21B₃), is consistent with an increase in q during LTP. The “peakiness” in the distribution of the small events seen in this and subsequent histograms is, most likely, a sampling artifact due to the relatively small number of events in each bin rather than reflecting quantal peaks due to stimulation of

multiple synapses (Magleby and Miller, 1981; Walmsley, 1995; Frerking and Wilson, 1996). Even if we assume that a large number of release sites were activated during the baseline, for a uniform increase in p_r to account for the observed shift in the amplitude distribution, the failure rate would have had to decrease to less than 0.1 during LTP rather than the observed rate of 0.58.

Similar results were observed in a total of 8 cells in which LTP ($258 \pm 30\%$) was evoked. LTP was accompanied by a significant increase in potency in all cells ($194 \pm 22\%$) and a modest reduction in the failure rate in some cells ($0.60 \pm .04$ during baseline, $0.47 \pm .04$ during LTP). Figure 22A shows the ratio of potencies before and after LTP induction (Potency Ratio) plotted as a function of the magnitude of LTP. The horizontal line represents the expected relationship for a change in p_r alone at a single release site, the upper diagonal line represents a change in q alone, and the lower diagonal line a change in p_r alone for a Poisson distribution (a worst case scenario in which the assumption is that a large number of low p_r sites were being activated). Figure 22A shows the ratio of success rates before and after LTP induction (SR Ratio) plotted as a function of the magnitude of LTP. In this graph, the diagonal straight line represents the expected relationship for a change in p_r alone at a single release site, the curved line the expected relationship for a change in p_r alone for a Poisson distribution, and the horizontal line the expected relationship for a change in q alone. Whether or not a single or multiple release sites were activated in each of these experiments, these data indicate that LTP was unlikely to have been generated by a change in p_r alone but instead must have involved changes in q and possibly n .

Since the whole-cell experiments produced results different from those previously reported using similar techniques (Stevens and Wang, 1994; Bolshakov and Siegelbaum, 1995), we decided to take the additional steps of using stimulus intensity ramps (Raastad, 1995) and paired pulse analysis (Stevens and Wang, 1995) to maximize the likelihood of stimulating a single axon and most likely a single synapse (Sorra and Harris, 1993). With standard whole-cell recordings the ability to induce LTP “washes out” within 10-15 minutes (Malinow and Tsien, 1990), and there was insufficient time to perform these single fiber/single synapse tests satisfactorily and still be able to induce LTP. We therefore used amphotericin-B perforated patch-clamp recording techniques (Rae et al., 1991) that allowed us to generate LTP more than an hour after the start of an experiment. Figure 23 shows the data from the beginning of a typical experiment in which the stimulus intensity was increased in a stepwise manner by about 7% (.02 V) every 25 stimuli. The EPSC amplitudes and failure rates show a threshold at a stimulation intensity of 0.30 V, and the next two successive increases in intensity did not produce any further increase in mean EPSC amplitude or a reduction in failure rate. This plateau in the response despite continued increases in stimulus intensity strongly implies that a single axon contacting the recorded cell was being activated reliably (Raastad, 1995; Raastad et al., 1992). It is possible that with this technique, we are stimulating additional fibers that either do not contact the recorded cell or make synapses that are pre- or postsynaptically silent.

Similar single axon tests were performed in 16 cells using perforated patch recording. Because the interpretation of the data from these experiments is critically dependent on the reliable activation of a single axon contacting the recorded cell, every

effort was taken to ensure that this occurred in all cells used for data analysis. To minimize any possible time dependent effects on axon excitability, the order in which the stimulus intensities were changed while performing the single axon test was varied between cells (see Raastad, 1995): seven were performed in successive stimulus intensity increments, four in successive decrements, and five in random order. The stimulus intensity at the middle of the plateau was selected for data collection. In three of the cells, the stimulating patch electrode was pressed onto the CA3 cell body layer as previously described (Bolshakov and Siegelbaum, 1995). In addition, in a subset of cells (n=8) paired pulse stimulation was used to address whether a single release site was being activated (Stevens and Wang, 1995). The reasoning behind this approach is that paired pulse stimulation presumably only affects p_r : if two release sites are being activated, the potency of the responses to the second stimulus will be greater than the potency of the first because the increase in p_r on the second response will increase the likelihood that both sites will release simultaneously. This manipulation also permitted us to determine whether we were activating the fiber reliably. If a significant fraction of the observed failures was due to axon excitation failures, the potency of the second response would be smaller for trials in which the first response was a failure versus trials in which the first response was a success (Stevens and Wang, 1995). By taking these precautions and performing these analyses, we have maximized the likelihood that only a single axon contacting the recorded cell is being stimulated reliably. If a cell failed either the single axon test or the paired pulse test it was not used for further data analysis.

Figure 24 shows one example of the changes that occurred at a putative single site following the induction of LTP. Both the individual data points (Figure 24A) and the

amplitude histogram (Figure 24C) show that there was a clear increase in potency (Figure 24B₃: 8.1 pA to 17.1 pA) and that virtually all of the small (<10 pA) events disappeared following LTP induction and were replaced by larger events. Despite this dramatic increase in potency, the failure rate (the area under the peak centered at 0 pA) did not decrease following LTP. Thus, in this cell, all of the LTP can be attributed to an increase in potency, which is equivalent to q if only a single site is involved, with no apparent change in p_r . Similar results were observed in four of the eight cells in which LTP was generated (see summary in Figure 27).

An example that is typical of the changes that occurred in the remaining four cells is shown in Figure 25. After performing the single axon test a baseline of 200 responses was obtained. Following the induction of LTP there was an increase in the potency (Figure 25C₃, 2.0 pA to 9.5 pA) and a shift to the left in the amplitude distribution (Figure 25D). There was also a decrease in the failure rate (from 0.78 to 0.55), which could be attributed to an increase in p_r and/or an increase in n . Examination of the paired pulse data can help distinguish between these possibilities. Figure 26A shows that during the baseline, paired pulse facilitation was elicited by the two stimuli but that the potency remained the same (paired pulse potency ratio=0.95) suggesting that a single, functional release site was being activated (Stevens and Wang, 1995). However, after LTP induction the paired pulse potency ratio increased to 1.27 (Figure 26B). This could not have been caused by a change in p_r at a single release site and suggests that in this cell LTP may have been associated with an increase in n in addition to an increase in q . Very similar results were also obtained in a second cell in which paired pulses were given for a period during the baseline and following the induction of LTP: the baseline paired pulse

potency ratio was 1.00 and increased to 1.21 during LTP again suggesting that an increase in n had occurred (data not shown).

Figure 27 shows a summary of the eight cells which met criteria for reliable stimulation of a single axon. In four of these cells, paired pulses were applied during the baseline period and the paired pulse potency ratio was not greater than 1, implying that a single, functional synapse was being stimulated. In panel A, the change in potency following LTP is plotted as a function of the magnitude of LTP. The diagonal line is the expected relationship for a change in q only, the horizontal line for a change in p_r only at a single release site, and the curved line for a change in p_r only for a Poisson distribution. It can be seen that LTP was accompanied by an increase in potency in all eight cells (i.e. all points are above the horizontal line). In panel B, the change in the rate of successes following LTP is plotted as a function of the magnitude of LTP. In this graph, the horizontal line is the expected relationship for a change in q only, the diagonal line for a change in p_r only at a single release site, and the curved line for a change in p_r only for a Poisson distribution. This graph illustrates that in four of the cells there was no significant increase in the success rate. In the other four cells the success rate did increase. While in these cases it is impossible to rule out that an increase in p_r contributed to the LTP, even assuming a Poisson distribution, an increase in p_r alone cannot account for the results.

It has been reported that synapses with a $p_r > \sim 0.8$ cannot express LTP, a finding that has been used as evidence that an increase in p_r alone is responsible for LTP (Bolshakov and Siegelbaum, 1995). To test this hypothesis directly in a final set of perforated patch experiments, we increased the concentration of Ca^{2+} in the external

medium to 5 mM (Mg^{2+} was unchanged) to raise p_r and attempted to elicit LTP. Under these conditions, the success rate was increased dramatically to 0.84 ± 0.05 ($n=5$) yet LTP was induced in all 5 cells ($247 \pm 58\%$). Figure 28 shows the results from one of these cells. Consistent with a high success rate at this site, paired stimuli elicited a paired pulse depression (Figure 28D₁) but no change in potency (Figure 28D₂). Following the pairing protocol during which the cell was depolarized to +10 mV, stable LTP was induced (figure 28A, B₁ and B₂). This was accompanied by a large increase in potency (Figure 28B₃: potency increased by > 4 fold), a dramatic shift in the amplitude distribution to larger events (Figure 28C) and no significant decrease in the failure rate. Thus, as in several of the cells recorded in 2.5 mM external Ca^{2+} , there was a dramatic increase in potency and no apparent change in p_r . A summary of these experiments (Figure 29) emphasizes that, despite the very high baseline Pr, LTP could be reliably induced and was not dependent on the initial p_r .

Discussion

The ability to examine LTP at a single synapse would be an extremely powerful approach for determining its mechanism of expression because theoretically it allows the three classic parameters of synaptic transmission, p_r , n , and q , to be determined directly. Recent studies (Stevens and Wang, 1994; Bolshakov and Siegelbaum, 1995) have provided evidence that such an approach is possible and that with this approach increases in p_r alone are responsible for LTP. These results, however, have been difficult to reconcile with a number of other studies suggesting that changes in q and n occur during LTP (Davies et al., 1989; Foster and McNaughton, 1991; Kullmann and Nicoll, 1992;

Larkman et al., 1992; Liao et al., 1992; Manabe et al., 1992; Isaac et al., 1995; Liao et al., 1995; Oliet et al., 1996; Stricker et al., 1996b). We have therefore re-examined LTP at putative single synapses primarily using perforated patch-clamp recording techniques that allowed sufficient time to carry out various tests that maximized the likelihood that we were stimulating a single fiber prior to inducing LTP. We found that in all 13 of the cells that met our criteria for single axon stimulation, LTP was accompanied by an increase in potency and that a change in p_r alone could not account for the results. Identical results were obtained in an additional eight cells in which standard whole-cell recording was used but for which time did not permit rigorous tests for single axon stimulation.

Anatomical data suggest that most (>70%) individual axons in the CA1 region make a single contact with the dendritic tree of an individual CA1 pyramidal cell (Sorra, and Harris, 1993). Thus, stimulation of a single fiber, in most instances, should activate a single synapse on the cell being examined. An important unresolved issue is whether at a single release site, the quantal variability is large or small. The large variability in response size typically observed with minimal stimulation has been interpreted as reflecting the release of multiple quanta (Kullmann, and Nicoll, 1992; Liao et al., 1992; Stricker et al., 1996a). However several recent studies, including the present one, in which particular attention has been paid to maximizing the stimulation of a single fiber, favor the conclusion that considerable quantal variability exists at a single release site (Stevens and Wang, 1994; Raastad, 1995; but see Bolshakov and Siegelbaum, 1995).

If a single synapse is being examined, potency, defined as the mean amplitude of responses when transmitter release occurs (Stevens and Wang, 1994), is equivalent to q . However if multiple synapses are being sampled, an increase in potency could be due in

part to an increase in p_r at a number of these sites. Several lines of evidence argue against this scenario explaining our results. First, in all cells in which paired pulse facilitation was elicited prior to LTP, the potency ratio was not greater than 1. If multiple release sites were being activated, the potency in response to the second stimulus should be larger than that in response to the first (Stevens and Wang, 1995). It is important to acknowledge, however, that this paired pulse test has limitations in terms of its sensitivity such that activation of additional sites with small quantal sizes or low p_r conceivably could be missed (Stevens and Wang, 1995; Malinow and Mainen, 1996). Second, assuming a Poisson distribution as a worst case scenario, the changes observed during LTP cannot be accounted for by an increase in p_r alone. Third, the magnitude of the decrease in the failure rate, when this occurred, was never sufficient to account for the shift in the amplitude distributions from small to larger events.

The change in failure rate, however, could be explained by an increase in the number of functional synapses (n). Indeed, the changes in the paired pulse potency ratio observed in two cells following LTP induction are consistent with this possibility. Such a mechanism could account for all the data sets in which the number of failures decreased, and agrees with recent reports of changes in n contributing to LTP (Kullmann, 1994; Isaac et al., 1995; Liao et al., 1995; Stricker et al., 1996b).

None of our results, however, definitively rules out a contribution of an increase in p_r to LTP. Formally, it is still possible that changes in p_r alone could account for the results. In one scenario a selective increase in the p_r at a synapse with a large quantal size and a p_r that was close to zero prior to LTP would have to be coupled with a dramatic decrease in p_r at a synapse with a much smaller quantal size and high p_r during the

baseline period. A second possible explanation is that a large component of the failures are actually failures to excite the axon and that a large number of synapses are being inconsistently activated. However, this seems very unlikely because, as previously mentioned, an analysis of the paired pulse data revealed that there was no correlation between release occurring in response to the first and second stimuli of the pair.

Perhaps the strongest evidence indicating that an increase in p_r alone cannot account for LTP is the finding that LTP can still be elicited at synapses which at baseline exhibit very high success rates (Figure 5). One reason this may not have been observed in a previous study of high p_r synapses (Bolshakov and Siegelbaum, 1995) could be that perforated patch recording techniques were not used and “wash-out” occurred (Malinow and Tsien, 1990).

However, wash-out cannot explain the discrepancy between this study and two previous studies which report no change in potency during LTP was observed (Stevens and Wang, 1994; Bolshakov and Siegelbaum, 1995). It is not clear what accounts for this difference. The non-linear effects of series resistance on small EPSCs are not well understood, but very high (>80 M Ω) can produce histograms with discrete peaks between successes and failures (Lüthi, A., personal communication). Furthermore, it is unclear what effect series resistance may play on potency measures. Neither of the previous studies report values for series resistance. Alternatively, some systematic bias, on the part of either group, may underlie this discrepancy. Resolution of this issue may provide important insights into the underlying mechanisms responsible for the expression of NMDA receptor-dependent LTP in the hippocampus.

Figure 21. LTP monitored with whole-cell recording and minimal stimulation is associated with an increase in potency.

A. Individual response amplitudes during the course of an experiment (A-C from one experiment). Time 0 (not shown) is the time at which the whole cell recording configuration was established.

B. Traces from the experiment in A: (B₁, left panel) Average (n=100) of responses during baseline. (B₁, right panel) 9 superimposed consecutive responses from the baseline. (B₂, left panel) Average of responses during LTP (10 min. after pairing to the end of the recording). (B₂, right panel) 9 superimposed consecutive responses during LTP. (B₃) superimposed averages of successes only during baseline (smaller trace) and LTP (larger trace; same epochs as used for averages in B₁ and B₂).

C. Amplitude histograms (bin width = 0.5 pA) of all baseline data (thin line), and all data from 5 mins after the end of pairing (thick line).

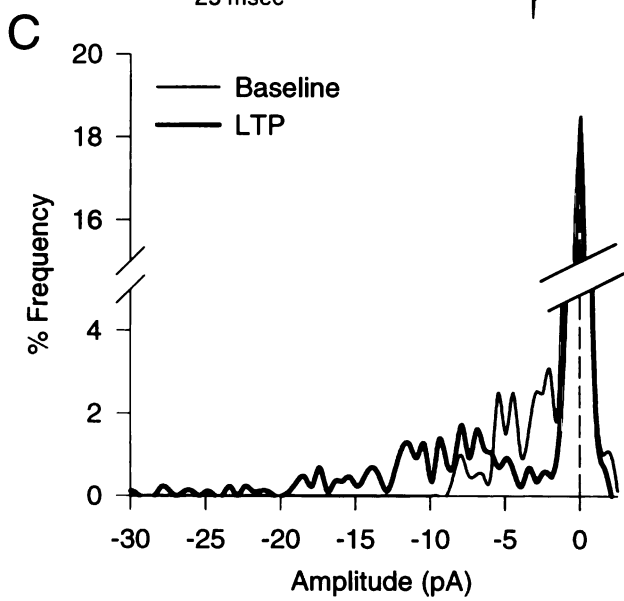
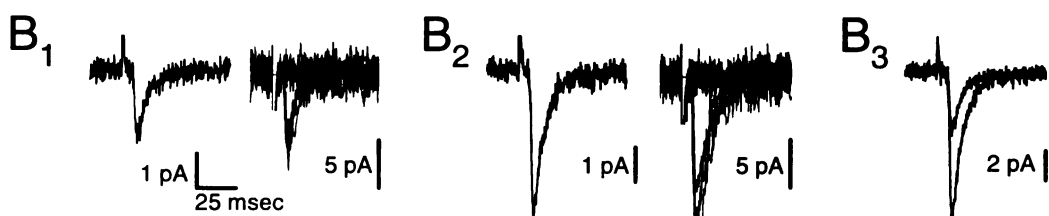
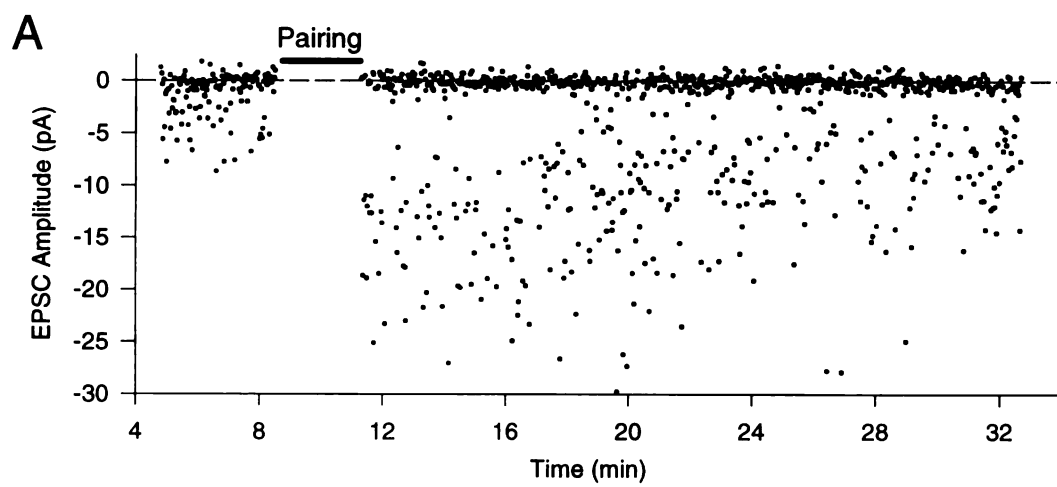


Figure 22. Summary data for eight whole-cell experiments (each coded with a symbol that is consistent for both graphs)

A. Potency ratio plotted as a function of LTP magnitude. Horizontal line is the expected relationship for a change in p_r only at a single site, upper diagonal line for a change in q only, and lower diagonal line for a change in p_r only for a Poisson distribution. The extent of the solid portion of the lower diagonal line represents the largest amount of LTP that can be generated using this model for the greatest experimentally observed change in failures. The shaded areas indicate the portions of the graph in which an increase in p_r alone could account for LTP.

B. Success rate (SR) ratio (LTP/baseline) plotted as a function of LTP magnitude. Horizontal line represents the expected relationship for a change in q only, diagonal line for a change in p_r only at a single release site, and curved line for a change in p_r only for a Poisson distribution.

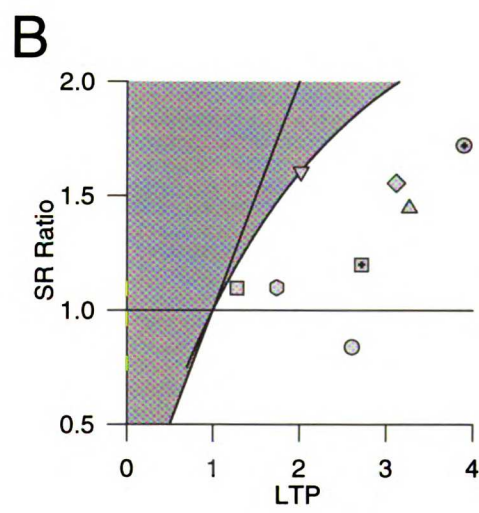
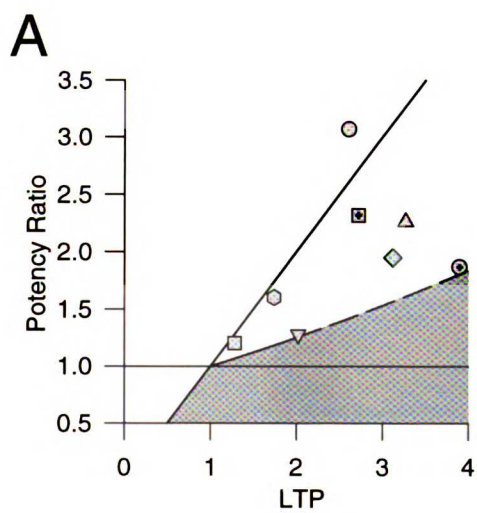


Figure 23. Example of a single axon stimulation test monitored with perforated patch recording.

A. Individual (●) and mean (; 17 responses) EPSC amplitudes for each stimulus intensity during stepwise decreases in stimulus intensity (solid line).

B. Success rate as a function of the stimulus intensity.

C. Averaged EPSCs (25 responses) for each stimulus intensity.

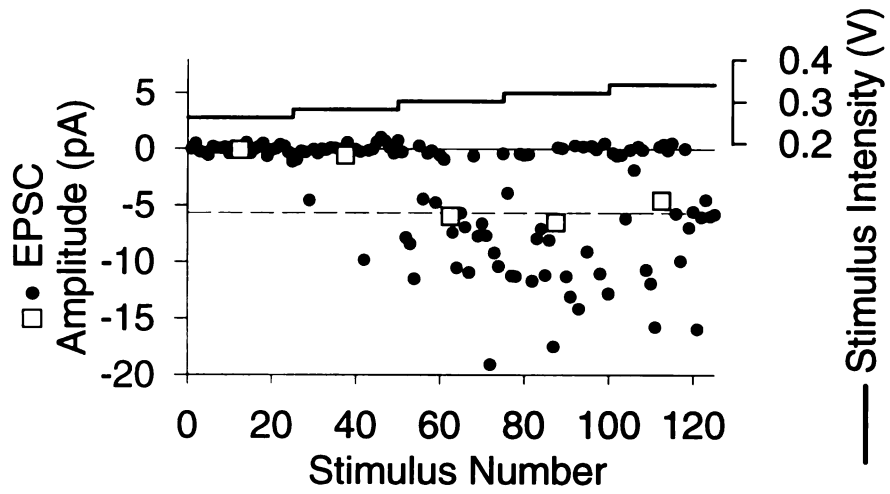
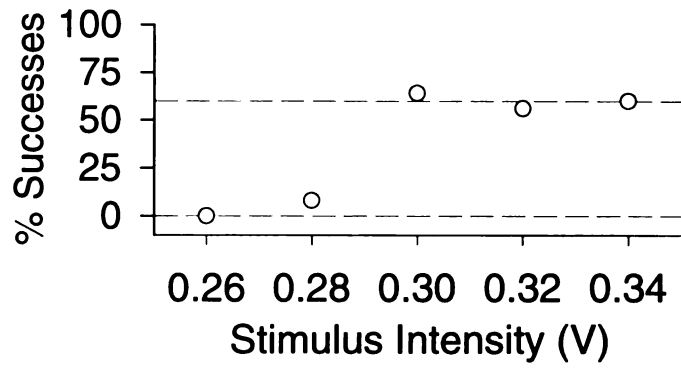
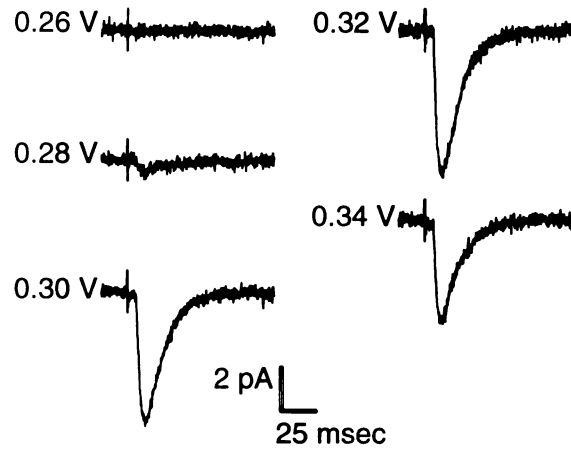
A**B****C**

Figure 24. Example of LTP monitored with perforated patch recording and single axon stimulation that was associated with an increase in potency and no decrease in failure rate

A. Individual response amplitudes during the course of an experiment. Time 0 (not shown) was the time at which a 10 G Ω seal was established.

B. Traces for the above experiment: (B₁, left panel) Average of responses (n=100) during the baseline. (B₁, right panel) 9 superimposed consecutive traces from the baseline. (B₂, left panel) Average of responses (n=100) during LTP (10 min after pairing). (B₂, right panel) 9 superimposed consecutive responses during LTP. (B₃) Superimposed averages of successes only during baseline (smaller trace) and LTP (larger trace; same epochs as used for averages in B₁ and B₂).

C. Amplitude histograms (bin width = 0.5 pA) of all baseline data (thin line) and all LTP data from 5 min after the end of pairing (thick line).

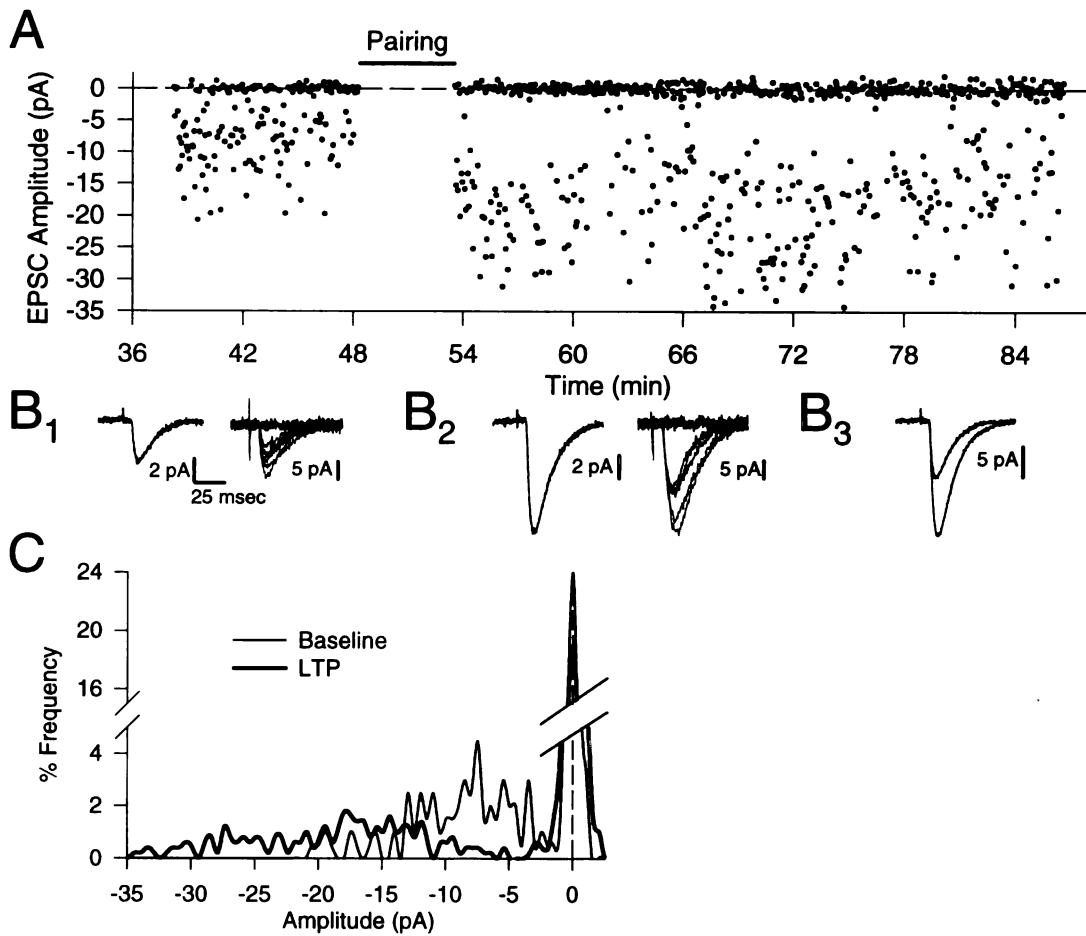


Figure 25. Example of LTP monitored with perforated patch recording and single axon stimulation that was associated with an increase in potency and a decrease in failure rate

A. Individual response amplitudes during the course of the experiment. Time 0 was the time at which a 10 G Ω seal was established.

B. Traces for the above experiment: (B₁, left panel) Average of responses (n=100) during the baseline, (B₁, right panel) 9 superimposed consecutive traces from the baseline. (B₂, left panel) Average of responses (n=100) during LTP (10 min after pairing). (B₂, right panel) 9 superimposed consecutive responses during LTP. (B₃) Superimposed averages of successes only during baseline (smaller trace) and LTP (larger trace; same epochs as used for averages in B₁ and B₂).

C. Amplitude histograms (bin width = 0.3 pA) of all baseline data (thin line), and all LTP data from 5 min after the end of pairing (thick line).

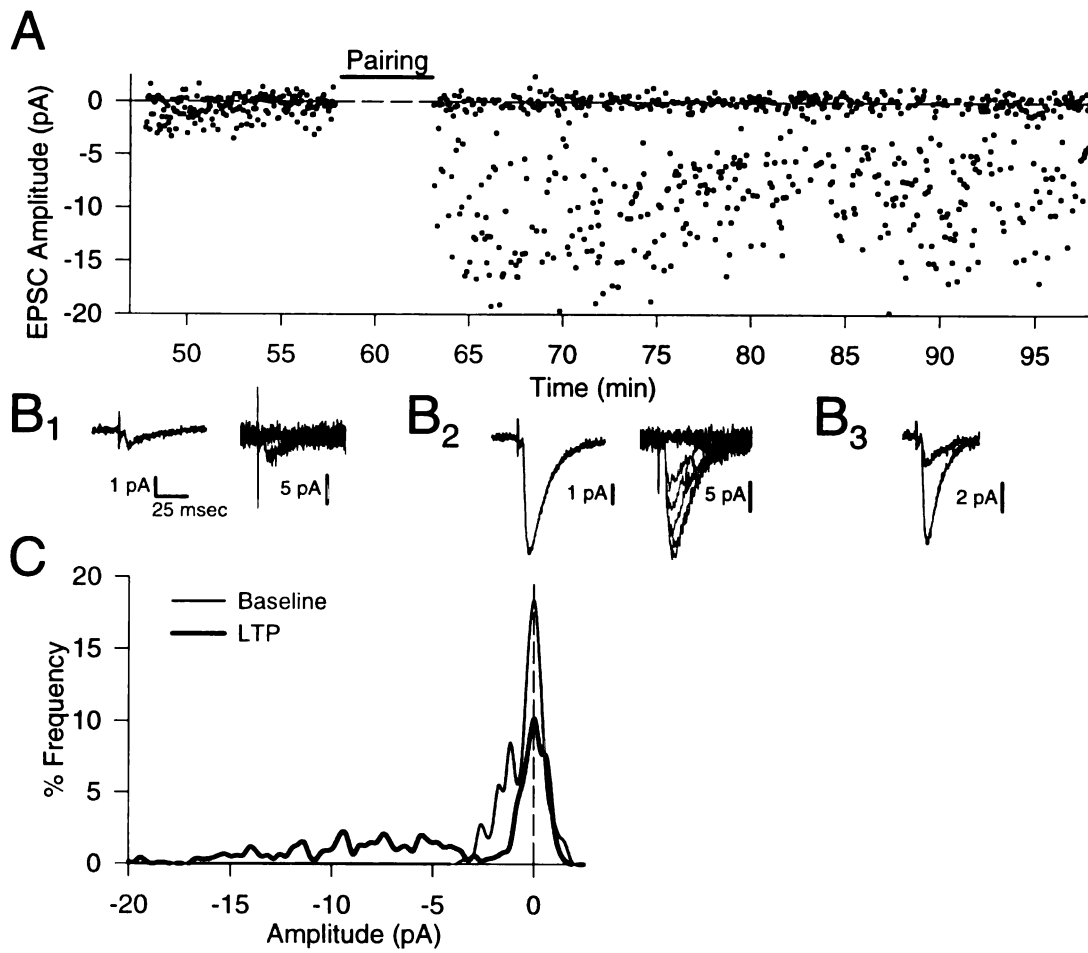
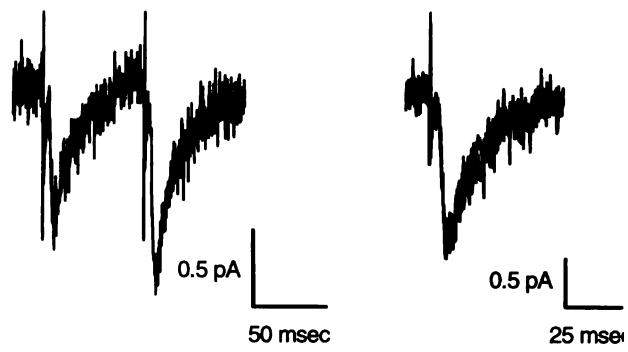


Figure 26. Paired pulse stimulation indicates an increase in n during LTP.

A. Paired pulse stimulation data during baseline. (Left panel) Average ($n=100$) of responses to paired pulse stimuli (70 ms interval) collected during the baseline. (Right panel) Superimposed averages of successes only to the first stimulus and second stimulus during baseline paired pulse stimulation.

B. Paired pulse stimulation data during LTP. (Left panel) Average ($n=100$) of responses to paired pulse stimuli collected during LTP (30 min after pairing) (Right panel) Superimposed average of successes only to the first stimulus and second stimulus when paired pulse stimulation was applied during LTP.

A



B

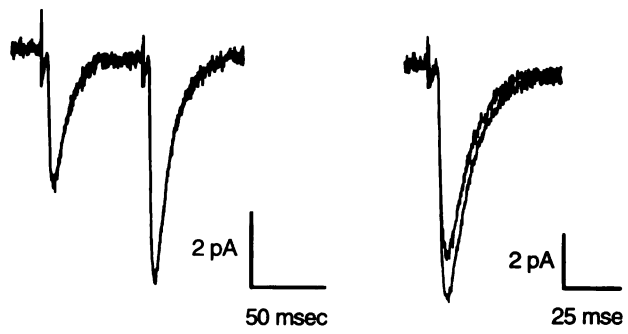


Figure 27. Summary data for all eight perforated patch LTP experiments in 2.5 mM Ca^{2+} (each data set is coded with a symbol which is consistent for both graphs).

A. Potency ratio plotted as a function of the LTP magnitude. Horizontal line is the expected relationship for a change in p_r only at a single site, diagonal line for a change in q only, and curved line for a change in p_r only for a Poisson distribution. The solid portion of the curved line represents the greatest LTP that could be generated using the largest experimentally observed change in failure rate.

B. Success rate (SR) ratio plotted as a function of LTP magnitude. Horizontal line represents the expected relationship for a change in q only, diagonal line for a change in p_r only at a single release site, and curved line for a change in p_r only for a Poisson distribution. The shaded areas indicate the portions of the graph in which an increase in p_r alone could account for LTP. The symbols containing a plus sign represent experiments in which the stimulation electrode was placed on the CA3 cell body layer.

Figure 28. LTP can be induced even when p_r is high.

A. Individual response amplitudes during the course of the experiment. Time 0 was the time at which a 10 G Ω seal was established.

B. Traces for the above experiment: (B₁, left panel) Average of responses (n=100) during the baseline, (B₁, right panel) 9 superimposed consecutive traces from the baseline. (B₂, left panel) Average of responses (n=100) during LTP (10 min after pairing). (B₂, right panel) 9 superimposed consecutive responses during LTP. (B₃) Superimposed averages of successes only during baseline (smaller trace) and LTP (larger trace; same epochs as used for averages in B₁ and B₂).

C. Amplitude histograms (bin width = 1.0 pA) of all baseline data (thin line), and all LTP data from 5 min after the end of pairing (thick line).

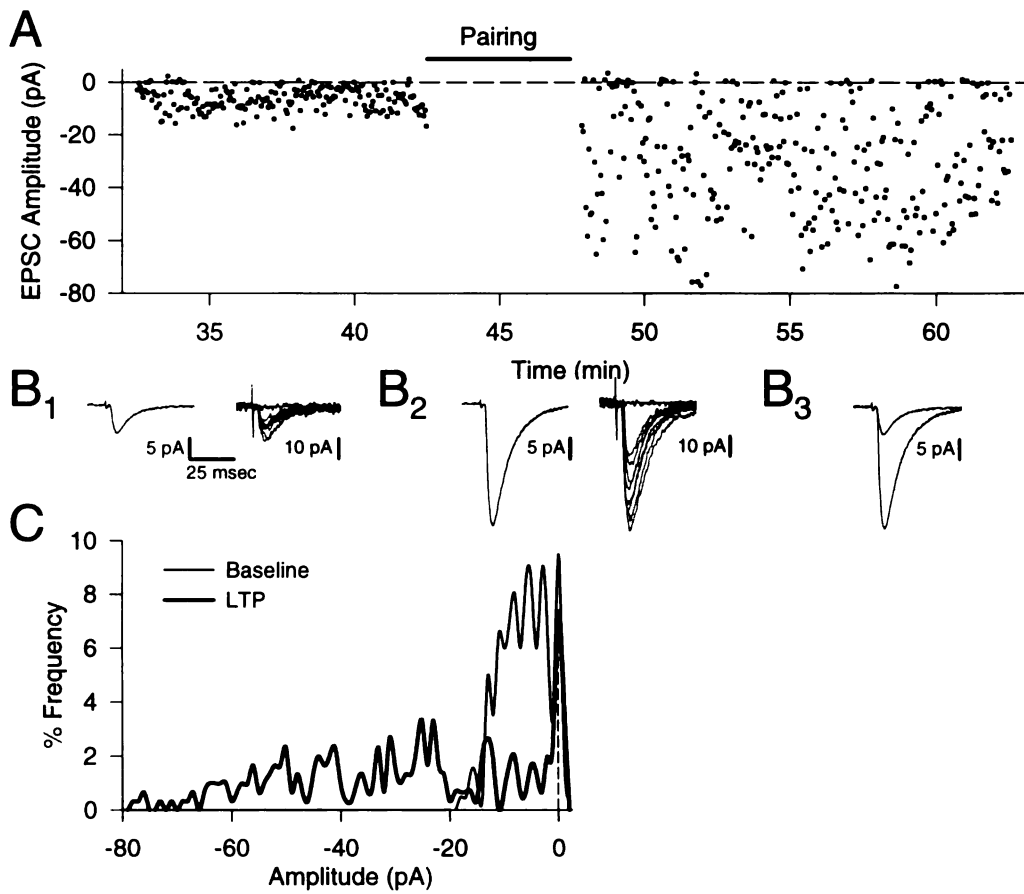
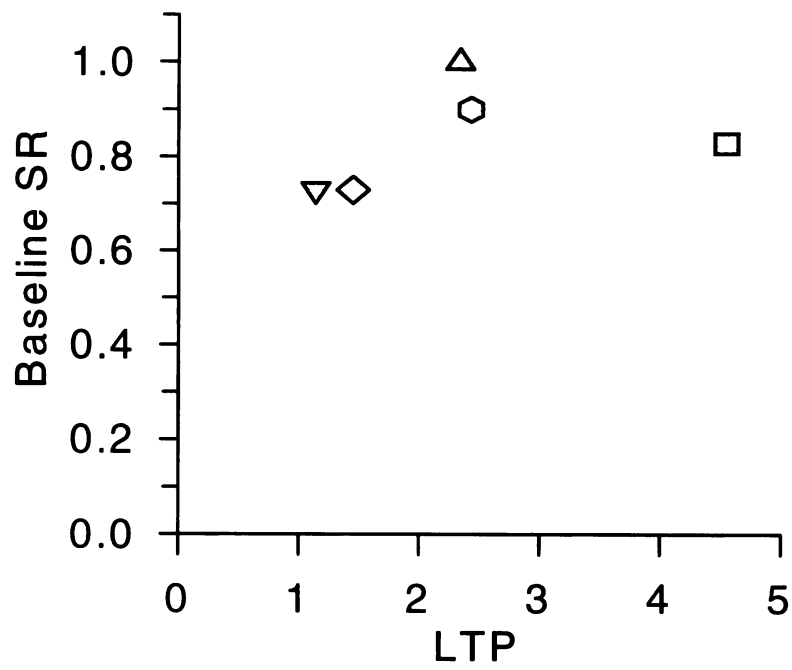


Figure 29. Summary graph of five perforated patch experiments in 5 mM Ca^{2+} in which baseline success rate is plotted as a function of LTP magnitude.



CHAPTER SIX

**SYNAPTIC REFRACTORY PERIOD PROVIDES A MEASURE OF
PROBABILITY OF RELEASE IN THE HIPPOCAMPUS**

Summary

Despite extensive research, much controversy remains regarding the locus of expression of long-term potentiation (LTP) in area CA1 of the hippocampus, specifically, whether LTP is accompanied by an increase in the probability of release (p_r) of synaptic vesicles. We have developed a novel method for assaying p_r , which utilizes the synaptic refractory period—a brief 5-6 ms period following release where the synapse is incapable of transmission (Stevens and Wang, 1995). We show that this assay is sensitive to a battery of manipulations that affect p_r , but find no change following either NMDA receptor-dependent LTP or long-term depression (LTD).

Introduction

Long-term potentiation is a use-dependent increase in synaptic efficacy that may play an important mechanistic role in learning and memory. For pyramidal cells in area CA1 of hippocampus, the essential induction mechanisms underlying LTP have largely been determined and involve calcium entry through NMDA receptors on the postsynaptic cell (Bliss and Collingridge, 1993; Nicoll and Malenka, 1995). The site of expression for LTP, however, has remained controversial and it is still unclear whether LTP is due to an increase in the postsynaptic responsiveness to a quantum of released glutamate (q), to an increase in the presynaptic probability of release (p_r) to an increase in the number of active synapses (n), or some combination of these (Nicoll and Malenka, 1995; Kullmann and Siegelbaum, 1995).

A number of approaches have been utilized specifically to determine whether or not LTP is accompanied by an increase in p_r . Paired-pulse facilitation (PPF), a

phenomenon which is sensitive to changes in the presynaptic probability of release (Manabe et al., 1993; Dobrunz and Stevens, 1997) does not appear to change with LTP (Manabe et al., 1993; Asztely et al., 1996; but see Schultz et al., 1994). It has been argued, however, that LTP might alter probability of release in a novel way that does not interact with PPF. A second method for determining a change in p_r has looked at the relative change in the AMPA receptor versus the NMDA receptor-mediated components of synaptic responses following LTP. While an increase in p_r should affect both components equally, many reports show little or no change in the NMDA component following LTP (Kauer et al., 1988; Muller and Lynch, 1988; Asztely et al., 1992; Perkel and Nicoll, 1993; Kullmann, 1994; Selig et al., 1995; but see Clark and Collingridge, 1995; O'Conner et al., 1995) arguing against an increase in p_r alone accounting for LTP. However, it has been proposed that the spillover of glutamate from one synapse to another could, in part, be responsible for this observation (Kullmann et al., 1996).

A third method for examining changes in p_r during LTP utilizes the NMDA receptor open channel blocker, MK-801. MK-801 causes a use-dependent decrease in the NMDA receptor-mediated EPSC, the rate of this decrease being proportional to p_r (Rosenmund et al. 1993, Hessler et al., 1993). In theory, this assay is a fairly direct measure of p_r but whether there is a change in the rate of decline of the NMDA receptor-mediated EPSC in the presence of MK-801 following LTP is controversial (Manabe and Nicoll, 1994, Kullmann et al., 1996). Furthermore, changes in NMDA receptor properties could cause a change in the MK-801-induced decay rate and therefore be mistaken for a change in p_r . Finally, several groups have attempted to look directly at quantal parameters by recording from only one or a few release sites. Conclusions from

these experiments have varied ranging from LTP being due solely to a change in p_r (Stevens and Wang, 1994, Bolshakov and Siegelbaum, 1995) to LTP being due to a change in q and n (Chapter 5). Analysis of these data are confounded by the inherent difficulty in ensuring that one has a stable recording from only a single release site.

Because of this continuing debate and the limitations inherent in each of the approaches described above, we have continued to work on developing new methods that allow estimates of p_r . In this paper, we describe a novel method of estimating p_r which is based on the finding that individual synapses exhibit a short absolute refractory period following transmitter release during which the synapse is incapable of transmission (Stevens and Wang, 1995). This method, based on comparing the size of EPSCs in response to paired pulse stimulation at different intervals, is independent of PPF, does not rely on a measurement of the NMDA receptor-mediated EPSC, and also is independent of the number of synapses being sampled (i.e. does not require that one is recording from only one release site). To test the usefulness of this novel assay of p_r we first performed a series of manipulations that change p_r in a predictable fashion. We then used this method to study changes in p_r during NMDA receptor-dependent LTP and its counterpart, LTD.

Methods

Hippocampal slices were prepared from 2-4 week-old Sprague-Dawley rats, 0.1 mM Picrotoxin was included in the external solution during all experiments. For the experiments illustrated in figures 2-7, 1 μ M CNQX was included to reduce EPSC variance. Whole-cell recording pipettes (2-4 M Ω) were filled with a solution containing: 107.5 mM Cs-gluconate, 20 mM HEPES, 0.2 mM EGTA, 8 mM NaCl, 10 mM TEA-Cl,

4 mM Mg-ATP and 0.3 mM GTP (pH 7.2 with CsOH, osmolarity adjusted to 270-280). Cells were held at -65 to -75 mV during the recordings. Series resistance was monitored online throughout the experiment. Stimulation of Schaffer collateral/commissural afferents (.25 Hz, whole cell, .033 Hz, field, perforated patch) was performed using either a stainless steel or Platinum-Iridium bipolar electrode.

Minimal stimulation recordings were performed by reducing stimulus strength until most stimuli resulted in synaptic failures. Single sites were determined on the basis of having a uniform onset latency and waveform and by comparing the potency of single responses to the potency of paired responses at 30 ms (Stevens and Wang, 1995). Successes and failures to both initial and paired pulses were assayed visually. A scaled average EPSC to single stimuli was subtracted from the responses elicited by paired stimuli at short (5-10 ms) intervals to determine whether any detectable response occurred in response to the second stimulus.

Results

We began by investigating the properties of synaptic transmission at short paired-pulse intervals while recording EPSCs from putative single release sites. Consistent with published results (Stevens and Wang, 1995), at longer intervals (>20 ms) the potency, defined as the amplitude of the responses when they occur, were equal for the first and second stimulus, indicating that we were recording from a single site. Additionally, there was no difference in p_r following a success or a failure on the first stimulus (Fig. 30A)—in either case, the subsequent response was facilitated (p_r'), presumably due to residual calcium in the terminal (Zucker, 1989). At short (5 msec) paired pulse intervals we

observed that when release of neurotransmitter occurred in response to the first stimulus, no response was elicited by the second stimulus; that is the synapse exhibited an absolute refractory period lasting several milliseconds (Fig 30A and B). When a failure occurred in response to the first stimulus, the subsequent EPSC responded with a facilitated probability of release comparable to that seen at longer intervals.

This synaptic refractory period is not due to an inability to identify responses at short intervals. Even at intervals of 5 ms, EPSCs in response to the first pulse could be distinguished from EPSCs in response to the second stimulus by the clear onset of the EPSC (figure 30B₁). At longer intervals where EPSCs occasionally occurred in response to both stimuli, the response to the second could be clearly identified as a deflection on the falling phase of the first EPSC (figure 30B₂). Finally, if these double responses were occurring at shorter intervals but were being misidentified as single responses to the first pulse, we would expect to see some difference in the shape or decay of the EPSC which was not observed (figure 30B₃).

The recovery curve following a response to the first pulse was best fit by an exponential curve with an offset (t_0) of 6.2 ± 0.5 ms and a time constant of 3.4 ± 0.7 ms. These values are consistent with previously reported data (Stevens and Wang, 1995). Figure 30C shows measurements of the potency, defined as the amplitude of the responses when they occur, normalized to the potency of the first response. There was no significant difference (repeated measures ANOVA) in the potency of the second response following a failure or following a success down to 10 ms. This indicates that at least at intervals of 10 ms or longer, AMPA receptor desensitization is not causing a decrease in the EPSC amplitude.

These data are most consistent with a scenario where following a synaptic release there is a 5-6 ms refractory period where the synapse can not transmit. Assuming that this synaptic refractory period is a common feature of all excitatory synapses on CA1 cells, we predicted that if we were recording from a population of synapses, following an EPSC some proportion of the synapses would be in this refractory period and that this fraction should reflect the probability of release. For example, if $p_r = 1.0$, all of the synapses would release and therefore would be refractory at 5 ms. The amplitude of an evoked EPSC at that time would be zero (figure 31A, dashed line). As p_r decreases, fewer synapses would be refractory, leaving more synapses available to release at 5 ms.

Figure 31-32 show a simulation of the expected amplitude of an EPSC generated by 40 release sites (i.e. 40 synapses assuming one release site per synapse) in response to the second of paired stimuli given at various short intervals. Figure 31A shows the simulated curves when p_r ranges from 0.3 to 0.5. When we normalize these curves to the EPSC amplitude at a 30 ms interstimulus interval (figure 31B), it becomes clear that the amplitude at 5 ms is equivalent to $(1 - p_r)$ (a derivation of this is provided in the Appendix). Simulations changing the number of synapses (i.e. release sites) over a similar range, shown in figure 32, did not differ following normalization (figure 32B). Similarly, changing the magnitude of PPF or q had no effect on the normalized curve (not shown).

As a first test of the validity of this approach when simultaneously assaying multiple synapses, we recorded standard EPSCs in response to paired pulse stimulation at variable intervals. As shown in figure 33, the EPSCs (after subtraction of the first response) could be fit quite well ($r^2 = 0.975$, $p < 0.01$) with a curve that used the time

constants measured in figure 30 and which was generated by allowing only p_r and the nq product to vary ($p_r = 0.44$, $nq = -92$ pA).

P_r is unlikely to be uniform at all synapses (Hessler et al., 1993; Isaacson and Hille, 1997; Rosenmund et al., 1993; Murthy et al., 1997), a fact that may have important effects on the interpretation of quantal measurements (Faber and Korn, 1991). The effect that intersite variability in p_r has on our analysis is shown in figure 34. If the amount of PPF is inversely proportional to p_r across all synapses, the variability in p_r will have no effect on our measure (figure 34, horizontal line on X axis). On the other hand, if the facilitation function is less than inverse, we will tend to overestimate the true p_r . The maximal possible error (figure 34, dotted line) is in the unlikely condition that the magnitude of PPF is constant at all synapses despite their initial p_r . A recent estimate for the facilitation function (Dobrunz and Stevens, 1997) results in the dashed line. Even then, when the coefficient of variation of p_r is 50%, our error in calculating p_r is only 15%.

The refractory period for synaptic transmission at a single synapse has been attributed to a refractory period for vesicle exocytosis (Stevens and Wang, 1995). However our data do not allow us to rule out contributions from other mechanisms such as postsynaptic receptor desensitization. Importantly, for the purposes of this study, it is not critical to delineate the mechanism(s) responsible for the refractory period. That is, this method of measuring p_r based on the paired-pulse ratio of EPSCs is only dependent on the existence of a refractory period and should work independent of the underlying mechanisms responsible for it.

To test directly the applicability of using the refractory period to assay p_r , we determined whether this measurement is sensitive to experimental manipulations of p_r . We assayed p_r by interleaving EPSCs evoked with paired pulses separated by 5 ms and 30 ms. P_{calc} , our estimate of p_r , was then determined by

$$P_{\text{calc}} = 1 - \frac{\text{EPSC}(5)}{\text{EPSC}(30)}$$

where EPSC(5) and EPSC(30) are the amplitudes of the paired pulse at 5 and 30 ms respectively after subtracting the EPSC evoked by the first pulse.

Initially, we examined the effects of 4-AP, a drug which enhances transmitter release by blocking presynaptic potassium currents (Heuser et al., 1979; Llinás et al., 1976). At a concentration of 50 μM , 4-AP caused a marked enhancement in the EPSC amplitude (Figure 35A) and similarly, a large increase in p_{calc} . This increase in p_{calc} was seen in 5/5 cells (Figure 35B), and averaged $197.6 \pm 28.6\%$ of baseline. A similar increase in EPSC amplitude and in p_{calc} was observed following application of the A_1 adenosine receptor antagonist, 8-cyclopentyl-1,3-dimethylxanthine (CPT) (10 μM , applied in the presence of a basal level of 0.5 μM adenosine) (figure 36, $n=4$). Cadmium, a non-specific Ca^{2+} channel blocker caused a large decrease in the size of the EPSC and also caused a decrease in our calculation of p_r (Figure 37, $n=4$). In contrast, increasing the stimulus strength, which increases n but should not affect p_r did not cause a change in p_{calc} (figure 38, $n=6$).

We were concerned that perhaps our calculation was simply assaying for changes in PPF, which are known to correlate with changes in p_r (Manabe et al., 1993). To test this, we examined the effects of applying the membrane permeant calcium buffer EGTA-

AM (200 μ M) (figure 39). This caused a decrease in the amplitude of the EPSC and, unlike other pharmacological manipulations that decrease p_r , also decreased (rather than increased) PPF ($1.78 \pm .07$ before, $1.32 \pm .09$ after application, $n=4$). This decrease in both PPF and release probability is consistent with the ability of EGTA-AM to buffer calcium in the presynaptic terminal (Castillo et al., 1996; Borst and Sakmann, 1996). Importantly, p_{calc} also decreased during EGTA-AM application demonstrating that this measure is not simply reflective of changes in PPF.

Having established that our assay is sensitive to changes in p_r , we examined what effects NMDA receptor-dependent LTP and LTD have on p_{calc} . Fig 40A shows a typical example of LTP induced by a pairing protocol. The EPSC amplitude increased by 75% yet there was no change in p_{calc} (0.34 ± 0.04 , baseline; 0.36 ± 0.02 , LTP). A summary of 6 cells is shown in figure 40B. Following LTP, the amplitude increased to 216 ± 30 % of baseline but p_{calc} remained constant ($102 \pm 7\%$ of baseline) as did PPF ($99 \pm 6\%$). In two of these cells, a tetanus (100 Hz for 1 sec given twice) was used to induce LTP with similar results to those obtained when LTP was induced using a pairing protocol.

LTD also had no effect on p_{calc} . ($n=6$) (figure 41). Prolonged low-frequency stimulus paired with depolarization to -40 mV, which elicits an NMDA receptor-dependent LTD, caused a depression in the EPSC amplitude to $72 \pm 4\%$ of baseline. p_{calc} , on the other hand, remained at $100 \pm 5\%$ of baseline (figure 41B).

A summary of all of our experiments is shown in figure 42. All of the experimental manipulations of p_r caused a significant change in p_{calc} . A regression analysis of the individual experiments gave a highly significant correlation ($r^2=0.82$, $p \ll 0.01$, $df=15$). LTP and LTD, on the other hand, had no effect on this assay of p_r . This

suggests that these forms of LTP and LTD are not due to a change in probability of release, but are more likely due to changes in q and/or in n .

It is theoretically possible that if there is a very high variability in p_r across synapses, LTP could be due to a selective increase in p_r only at synapses with low p_r . This would cause a reduction in the variability across synapses, and a concomitant reduction in the error due to that variability. However, to account for our data, it would be necessary to have a CV of p_r of 100% or greater in the baseline and a CV of near 0% following LTP. This would also require that the magnitude of PPF is nearly constant across all synapses, a suggestion that is incompatible with recently published experiments examining PPF at putative single release sites (Dobrunz and Stevens, 1997).

Nevertheless because of the on-going debate concerning the role of increases in p_r during LTP, we performed additional experiments which addressed this issue. We reasoned that if LTP is due primarily to an increase in p_r , then synapses with high p_r should exhibit LTP that is smaller than synapses with lower p_r . This prediction has been tested previously by a number of investigators and the experiments have yielded confusing results. Several groups found that raising extracellular Ca^{2+} had no effect on the magnitude of LTP (Muller and Lynch, 1989; Asztely et al., 1994; Isaac et al., 1996). On the other hand Schulz (1997) reported a significant decrease in the magnitude of LTP when elicited in high extracellular Ca^{2+} . It also has been argued that LTP cannot be elicited in neonatal slices under normal conditions because p_r is close to 1 but can be elicited if p_r is lowered experimentally (Bolshakov and Siegelbaum, 1995). To re-address this issue we raised p_r by first applying 4-AP to the slice. We then performed a pairing protocol to elicit LTP using perforated patch recording techniques. It was necessary to

use perforated patch recording because the ability to induce LTP often washes out when doing standard whole cell recording (Malinow and Tsien, 1990) and a true test of the influence of raising p_r on LTP required that we compare the saturated level of LTP reached under high p_r versus control conditions. Figure 43A shows a comparison of the LTP elicited in cells recorded in our standard experimental conditions and the LTP elicited while perfusing the slice with 4-AP (50 μ M) which increases the mean p_r by 2 fold. It can be seen that the LTP was essentially identical in these two conditions ($377 \pm 47\%$ versus $390 \pm 29\%$ of baseline in control versus 4-AP conditions).

We also performed the converse experiment. That is, if LTP is primarily due to an increase in p_r , experimental manipulations that increase p_r should have less of an effect at synapses that have undergone LTP than control synapses. Indeed, it has been demonstrated that synapses with low p_r are more sensitive to manipulations that increase p_r , such as 4-AP, than high p_r synapses (Hessler et al., 1993). To directly compare the effects of 4-AP on potentiated versus control synapses in the same preparation, we recorded field EPSPs in response to stimulation of two independent pathways. In one pathway, we induced LTP repeatedly (figure 43B, arrows) until the LTP was saturated (i.e. a subsequent tetanus caused no further increase in the EPSP). This protocol induced robust LTP ($257 \pm 23\%$; n=6). After turning the stimulus strength down, so that the potentiated and control field EPSPs were of similar size, we added 4-AP (50 μ M) to the bath. Similar to its effects on whole-cell EPSCs, this concentration of 4-AP caused a more than two-fold increase in the field EPSPs. More importantly, the effect of 4-AP on the two paths was indistinguishable ($285 \pm 26\%$ vs. $293 \pm 47\%$ for LTP and control paths respectively, n.s. paired t-test). This demonstrated lack of an interaction between LTP

and p_r in this and the preceding experiment provides further evidence against a significant role for a change in p_r underlying LTP.

Discussion

We have confirmed (Stevens and Wang, 1995) that following transmitter release at putative single release sites, there is a brief refractory period during which the synapse cannot transmit. Utilizing this observation, we developed a novel measure that assays probability of release from a population of synapses by comparing the change in synaptic strength elicited by paired stimuli given at a short and longer interstimulus interval. This method of calculating p_r was sensitive to an array of manipulations that are known to modify p_r but did not change following the generation of NMDA receptor-dependent LTP or LTD.

The existence of a synaptic refractory period following release has been proposed (Betz, 1970; Korn et al., 1984; Triller and Korn, 1985) and is a necessary correlate of the one-vesicle hypothesis which states that, following an action potential, no more than one vesicle can be released from an individual release site (Korn et al., 1982; Korn et al., 1994). Indeed evidence has been presented (Stevens and Wang, 1995) consistent with a release-dependent process lasting up to 10 ms during which subsequent exocytosis at that release site cannot occur. While our data are consistent with a presynaptic locus for this refractory period, we cannot rule out that the refractoriness may be due to a postsynaptic mechanism resulting in EPSCs that are so small they are classified as failures. For instance, the postsynaptic receptors may still be bound by the glutamate released on the

first pulse. These receptors would have to be in a desensitized state, since the synaptic conductance should be complete within a few milliseconds (Jonas and Spruston, 1994). However, the reported time constants for entry into (~ 10 ms) and recovery from (~ 50 ms) desensitization in hippocampal pyramidal neurons (Colquhoun et al., 1992) are too slow to account for either the decay of a single EPSC or our measured refractory period. Nevertheless, whatever the mechanism(s) responsible for the refractory period, an attractive feature of our method of calculating p_r is that the underlying mechanism is immaterial; only the observation that a synapse does not transmit twice within 5 ms pertains.

Although we have demonstrated that our assay is very sensitive to changes in p_r , the change in p_{calc} with pharmacological manipulations did not correlate perfectly with the change in EPSC amplitude—that is, the slope of the regression line in Figure 42 is less than one. There are a number of possible reasons for this modest discrepancy. First, as has been pointed out, variability in p_r across synapses may cause an overestimate in our measure of p_r if PPF is less than inversely correlated with p_r . Furthermore it is likely that manipulations that increase p_r preferentially act on lower p_r synapses and thus decrease the CV of p_r . This would result in an underestimate of the true change in p_r . How much variability there is between synapses is unclear. Recent studies utilizing FM1-43 in cultured hippocampal cells provide estimates ranging from 33% (see figure 4 in Isaacson and Hille, 1997) to greater than 50% (Murthy et al., 1997). Second, our method assumes that the probability of release following a failure at 5 ms is the same as the probability of release at 30 ms. This may not be the case at all synapses for a number of reasons. For instance, it is possible that facilitation is not a step function, but develops over time or

there may be additional refractory mechanisms involved that are not dependent on the release of a vesicle (e.g. calcium channel inactivation or an extended period of action potential refractoriness in some axons). Third, it is possible that a change in p_r may not account for the entire change in EPSC amplitude although it seems unlikely that this would be true for all of our pharmacological manipulations. Finally, our model assumes independence between release sites, which, if not true, may also cause an underestimation of the true changes in p_r .

Despite these potential sources of error, all of our control pharmacological manipulations showed highly significant changes in p_{calc} whereas LTP and LTD showed no change at all. Furthermore, there was no difference between the initial p_{calc} of the control experiments (0.48 ± 0.05 ; excluding the CPT experiments which were performed in a basal level of adenosine and therefore had a lower p_{calc}) and the LTP/LTD experiments (0.50 ± 0.05) indicating that the degree of error was similar in both groups. Indeed, if the error we observed with known changes in p_r is taken into account, we end up with a corrected p_{calc} of 0.34 ± 0.03 , a value that is quite similar to estimates of p_r in the literature from paired recordings or with minimal stimulation (Malinow, 1991; Allens and Stevens; 1994; Stevens and Wang; 1995; Isaac et al., 1996; Raastad and Lipowski, 1996; Dobrunz and Stevens, 1997).

While the most straightforward explanation of these results is that LTP is not accompanied by an increase in p_r , an alternative explanation can be put forward to account for our results. For instance, a reduction in the error associated with p_{calc} following LTP might counteract an actual change in p_r . However, this scenario seems

improbable. To counteract a change in p_r sufficient to account for LTP, the initial error would have to start at >100% and, following LTP, be reduced to virtually 0%.

Although we were confident that our assay can accurately measure changes in p_r when they occur, we performed additional experiments which directly tested two straightforward predictions of the hypothesis that LTP is due primarily to an increase in p_r . First, we asked whether the magnitude of LTP is less at synapses that have a high p_r . In agreement with our previous work (Chapter 5, Figures 28 and 29) we found that the magnitude of LTP was unaffected by significantly increasing p_r . Second, we asked whether application of 4-AP, a manipulation that increases p_r and has been shown to have less of an effect at high p_r synapses (Hessler et al., 1993), has less of an effect at synapses expressing LTP when compared to control synapses in the same preparation. Consistent with a previous report that examined the effects of increasing extracellular calcium on potentiated versus control synapses (Muller and Lynch, 1989) there was no difference in the effects of 4-AP on the two sets of synapses. These results provide additional evidence that LTP at synapses on CA1 pyramidal cells is not due to significant increases in the probability of transmitter release.

While the present results argue against an important role for changes in p_r contributing to the expression of LTP (and LTD), this set of experiments does not rule out the involvement of other presynaptic mechanisms. For example, LTP could involve the activation of presynaptically silent synapses (Malenka and Nicoll, 1997), a mechanism that would cause an increase in n . Similarly, an increase in quantal size due to modification of postsynaptic receptor number and/or function is not readily distinguishable from an increase in the amount of transmitter in a vesicle at a synapse

whose receptors were not saturated by exocytosis of the contents of a single vesicle.

Currently we favor a model where postsynaptic glutamate receptor function and number is modulated during LTP, perhaps accompanied by structural changes that ultimately could affect both sides of the synapse.

Appendix

Probability of release was estimated by interleaving paired pulses at 5 ms and 30 ms with a single pulse. The ratio of the amplitude at 5 ms to the amplitude at 30 ms (after subtracting the initial response), was subtracted from one to give p_{calc} . This calculation was performed on each series of stimuli and averaged into 2.5-4 minute bins.

The minimal stimulation data in figure 1A was fit with the following functions: $S(t)$, the time-dependent probability of release following a success, and $F(t)$, the time-dependent probability of release following a failure, where t is the interpulse interval. For the time range of 5-30 ms, $F(t) = p_r'$, the maximal facilitated probability of release, and

$$S(t) = (1 - e^{-\frac{t-t_0}{\tau_s}}) \cdot p_r'$$

where t_0 is the absolute refractory period and τ_s the time constant of recovery.

The curve to fit multiple synapses is a simple summation. A synapse that initially fails will add $q \cdot F(t)$. A synapse which releases will add $q \cdot S(t)$. Since the number of synapses which release on a given stimuli is equal to the product of n and p , and the number that fail is the product of n and $(1-p)$, the EPSC amplitude at an interval t is:

$$\text{EPSC}(t) = n \cdot (1 - p_r) \cdot q \cdot F(t) + n \cdot p_r \cdot q \cdot S(t)$$

At very short intervals, all of the synapses that have released are refractory and $S(t) = 0$, so:

$$\text{EPSC}(5) = n \cdot (1 - p_r) \cdot q \cdot p_r'$$

at longer intervals:

$$\text{EPSC}(30) = n \cdot p_r \cdot q \cdot S(30) + n \cdot (1 - p_r) \cdot q \cdot p_r'$$

but at this interval, the synapses that released are no longer refractory and $S(30)=p_r'$.

Therefore,

$$\text{EPSC}(30) = n \cdot q \cdot p_r'$$

Taking the ratio of EPSC(5) to EPSC(30) gives:

$$\frac{\text{EPSC}(5)}{\text{EPSC}(30)} = \frac{(1 - p_r) \cdot n \cdot q \cdot p_r'}{n \cdot q \cdot p_r'} = (1 - p_r)$$

Finally, solving for p_r leaves:

$$p_r = 1 - \frac{\text{EPSC}(5)}{\text{EPSC}(30)}$$

Since probability of release and quantal amplitude are most likely not equal from site to site, a more appropriate equation for the ratio of paired pulse intervals would be:

$$\frac{\text{EPSC}(5)}{\text{EPSC}(30)} = \frac{\sum_i^{(1-p_r)n} p r_i' \cdot q_i}{\sum_i^n p r_i' \cdot q_i}$$

The reducibility of this equation depends on the relationship between p_r and the amount of PPF. If the relationship is less than inverse, an error in p_{calc} will result.

Figure 30. Minimal stimulation of single sites reveals a synaptic refractory period.

A. Probability of release (p_r) of the second of a pair of EPSCs plotted against the paired pulse interval depending on whether the initial stimulus resulted in a success (open diamonds) or a failure (filled circles) ($n=4$). Dashed line is the mean p_r of the initial EPSCs (shaded area provides S.E.M.). Horizontal line (p_r') is the facilitated release probability determined by the data at 15 and 30 ms intervals. The curved line is the average of the best fit from each experiment for data following an initial success.

B. Traces from a single experiment: (B₁) Average of all trials at a 5 ms interpulse interval that responded with an EPSC to the first or to the second stimuli. (B₂) Average of all trials at a 10 ms interpulse interval that responded with an EPSC to the first, second or to both stimuli. (B₃) aligned decay phase of EPSCs in B₁ illustrates that no responses to both stimuli were hidden in the EPSCs.

C. Potency (mean amplitude of successes only) normalized to the initial EPSC potency as a function of the paired pulse interval for the second EPSCs following either a success (open diamonds) or a failure (filled circles). Shaded squares is the potency for the initial EPSCs.

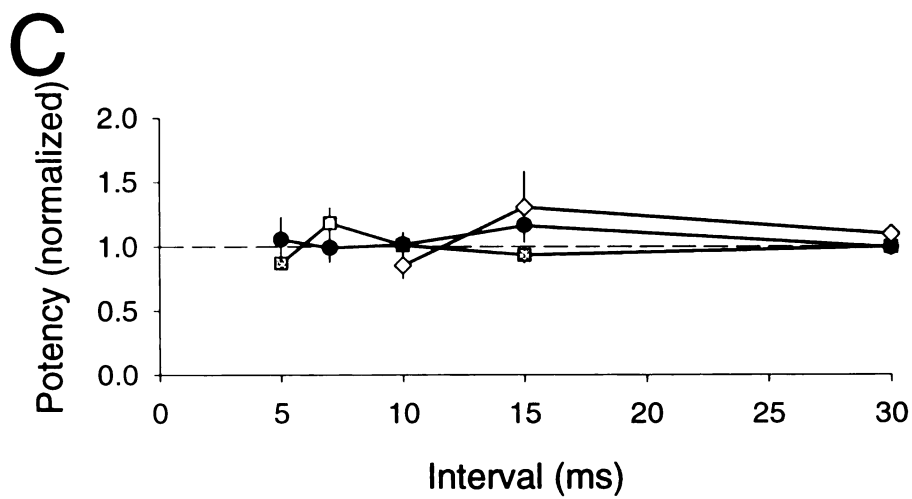
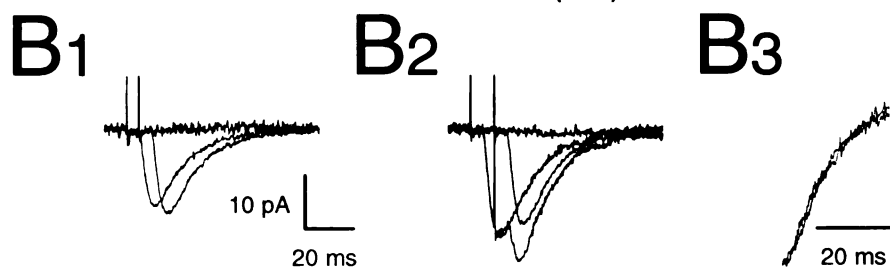
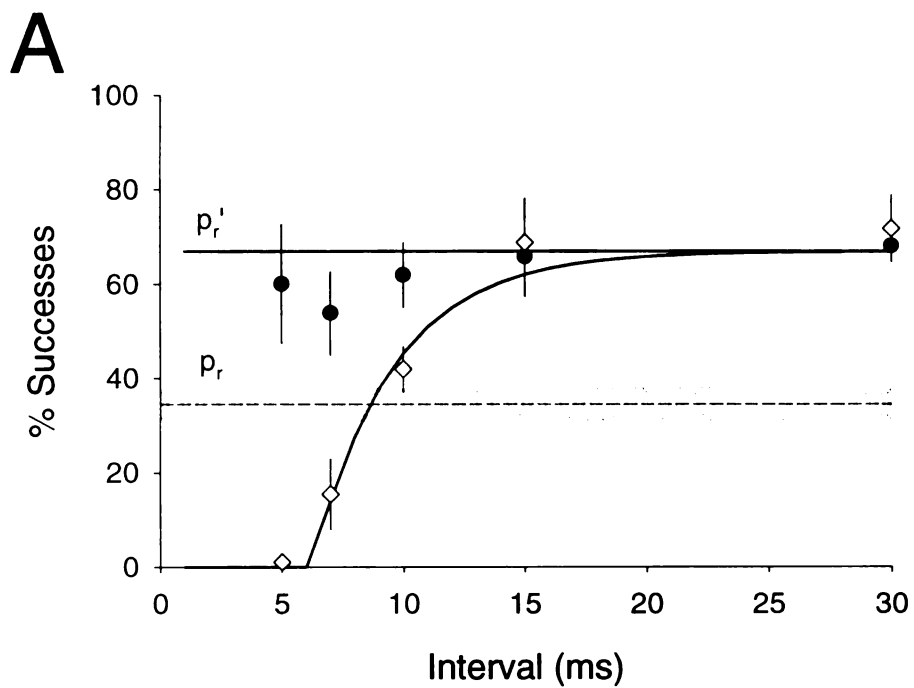


Figure 31. Computer simulations illustrate the sensitivity of paired pulse intervals to changes in p_r for multiple site recordings.

A. Calculated amplitude of a paired EPSC as a function of paired pulse interval for various initial values of p_r with constant values of n (40), q (5 pA) and paired pulse facilitation (1.5). The dashed line is the extreme example where all of the synapses release on the first pulse.

B. Amplitude normalized to the amplitude at 30 ms reveals the relationship between p_r and the normalized amplitude of paired pulses at short intervals.

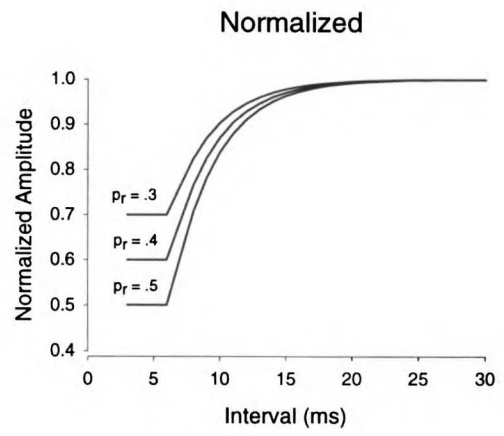
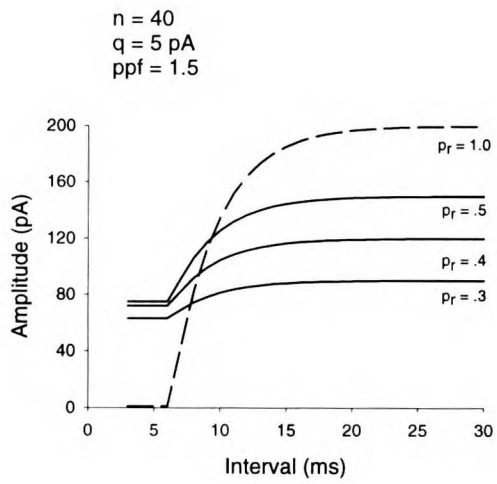
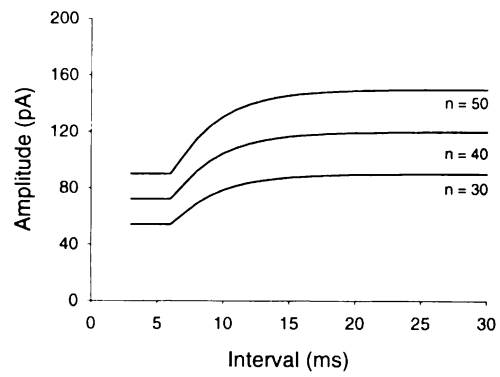


Figure 32. Computer analysis of changes in the number of release sites.

Changes in n affect the amplitude of the second EPSC (A) but do not reveal a similar **r**elationship at short paired pulse intervals when normalized (B).

$p_r = 0.4$
 $q = 5 \text{ pA}$
 $ppf = 1.5$



Normalized

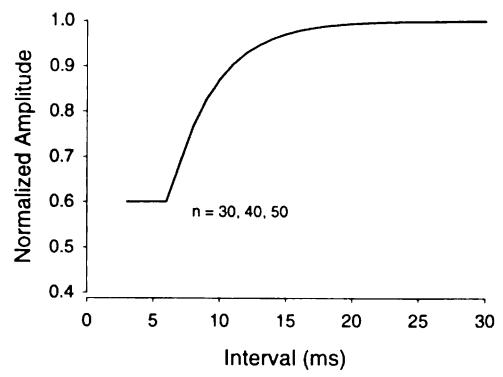


Figure 33 Actual data is fit well by the calculated curve.

Second EPSCs elicited at various intervals are well fit by a curve in which only q and p_r were allowed to vary. The upper panel shows the raw data prior to subtraction of the initial EPSCs. Data is average of 20 trials at each interval.

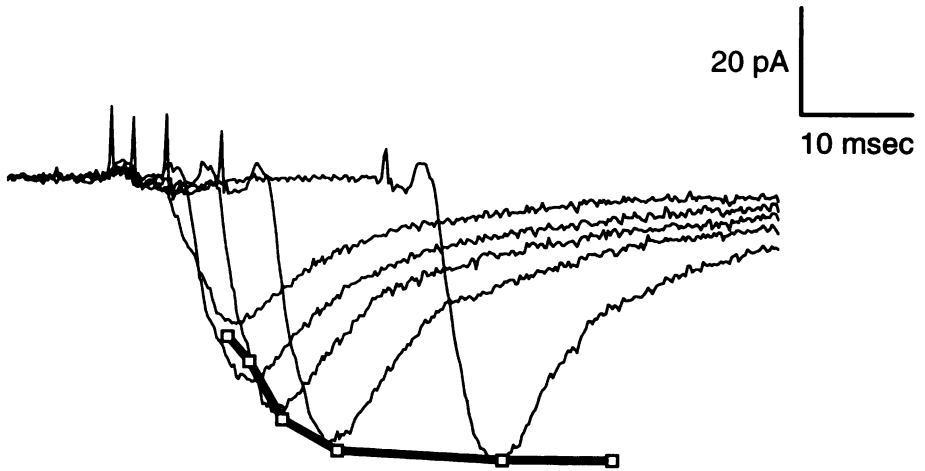
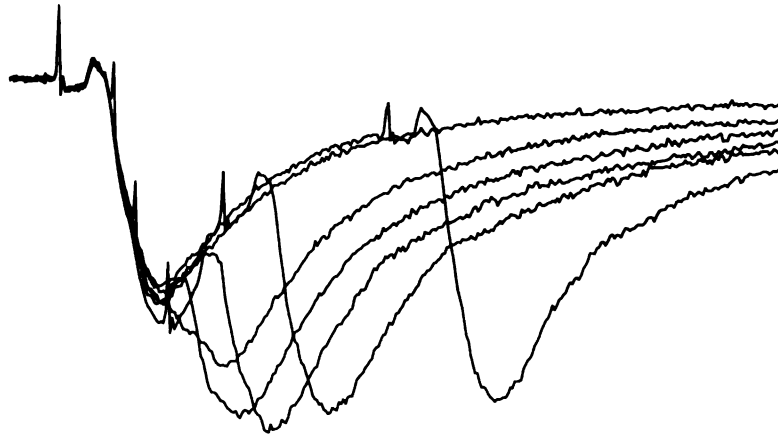


Figure 34. Estimate of a possible error in the calculation of p_r (p_{calc}) due to the variability in p_r from site-to-site.

The variability between synapses will result in a possible overestimation of p_r depending on the relationship between paired pulse facilitation and p_r . This error is bound by the two extreme cases where PPF is constant across all synapses (dotted line) and PPF is inversely proportional to p_r (solid line at zero). The dashed line is the error given a recent estimate for the PPF function (Dobrunz and Stevens, 1997).

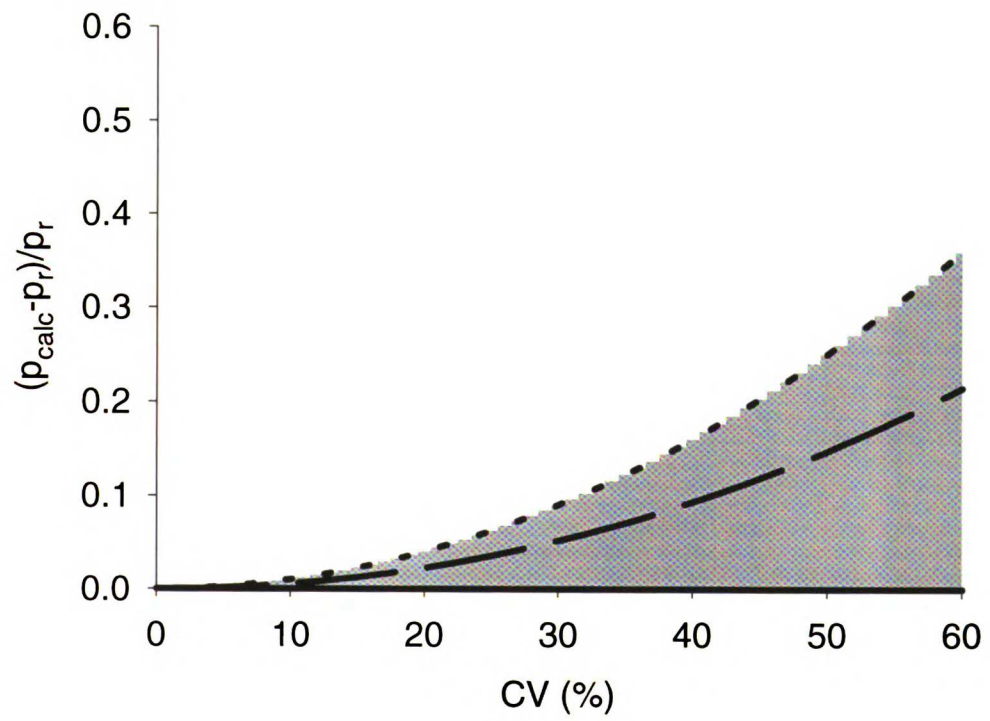


Figure 35. The potassium channel blocker 4-AP causes an increase in the calculated p_r .

A. Individual experiment showing the effects of application of 50 μM 4-AP on the amplitude of the initial EPSCs (upper graph) and on the calculated p_r (lower graph). The dashed lines give the average of all baseline data. Open squares are averages of 15 individual series of trials.

B. Average of five individual experiments showing changes in both amplitude and p_{calc} following 4-AP application.

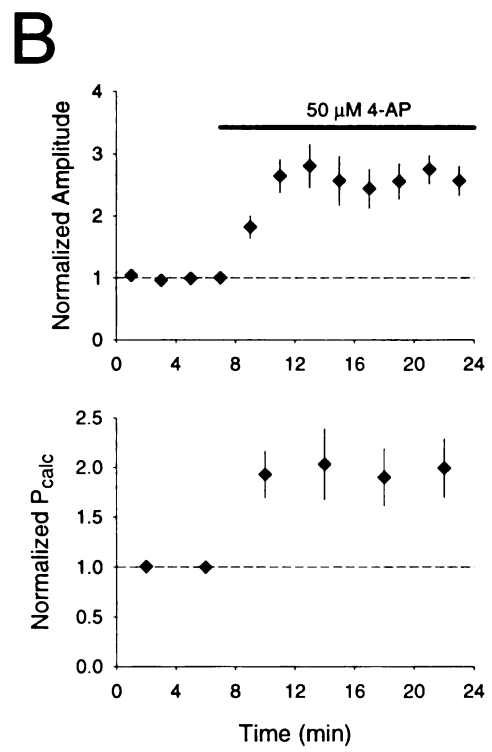
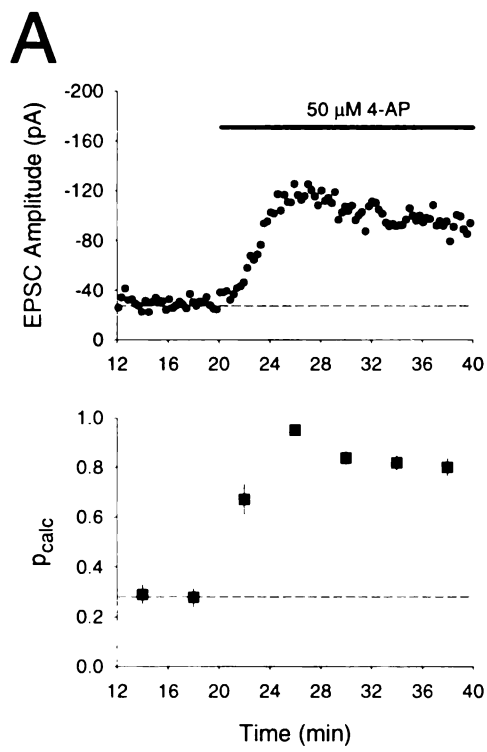


Figure 36. P_{calc} changes following application of 10 μM CPT in the presence of a basal level of 0.5 μM adenosine increases both the EPSC amplitude and p_{calc} (n=4)

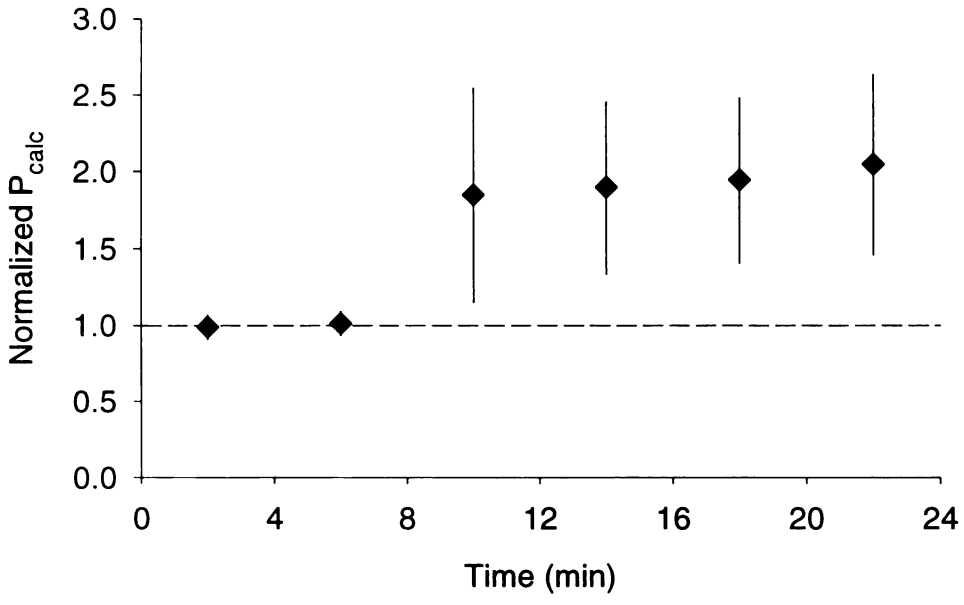
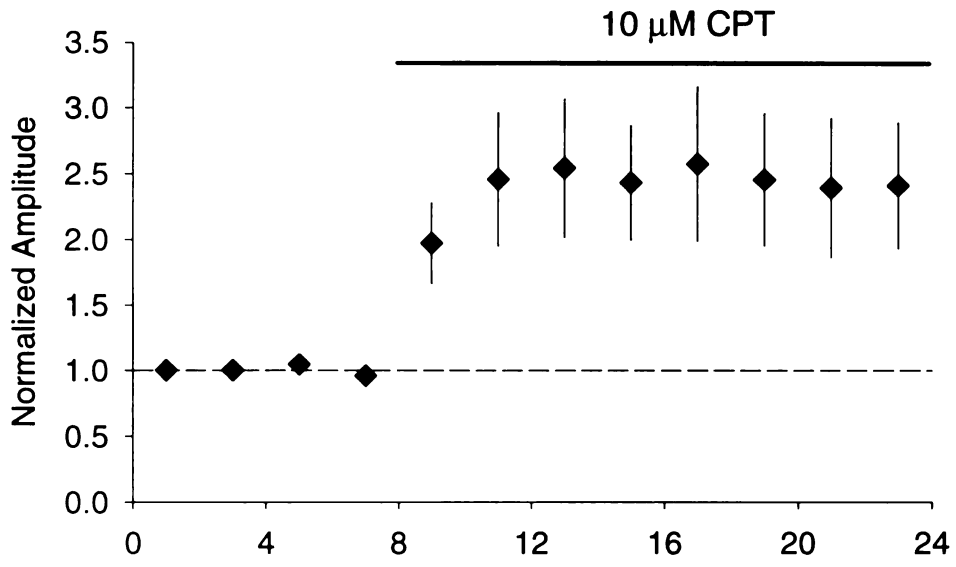
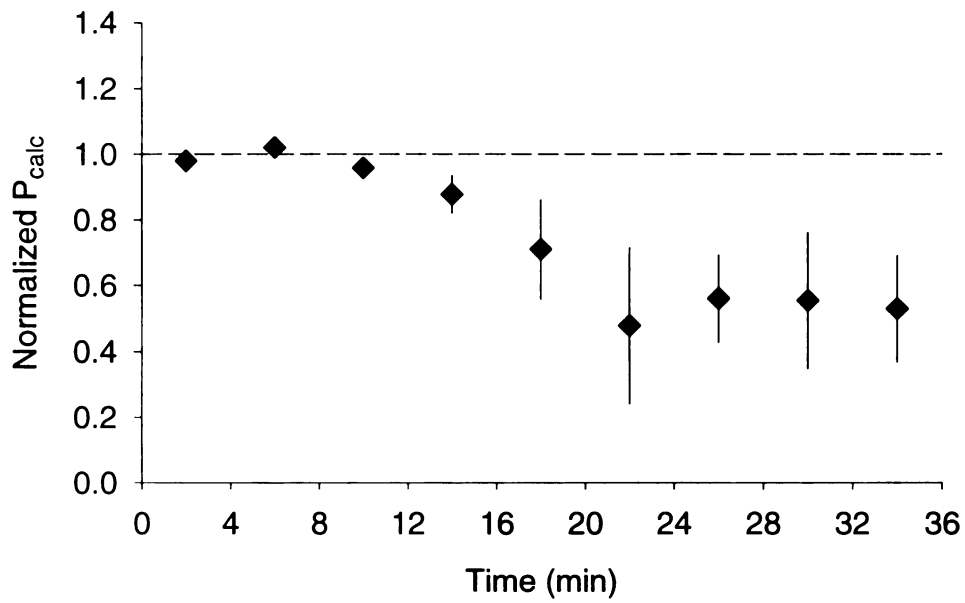
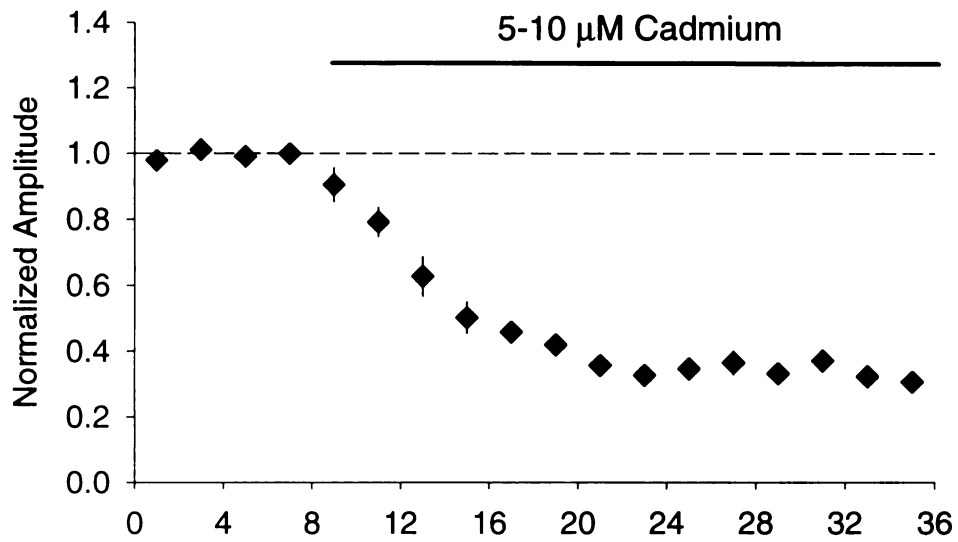


Figure 37. Application of 5-10 mM Cadmium decreases both the EPSC amplitude and

p_{calc} (n=4)



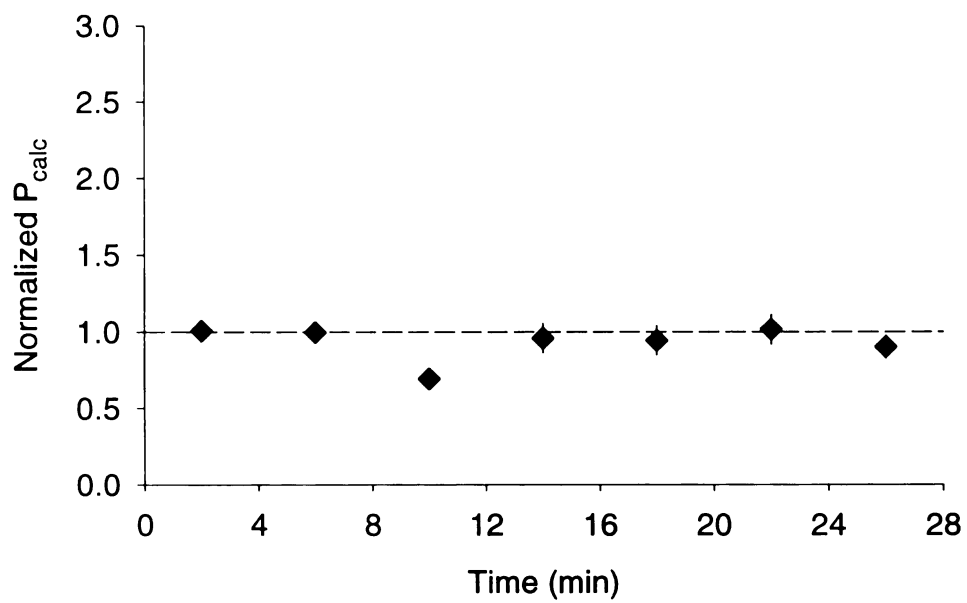
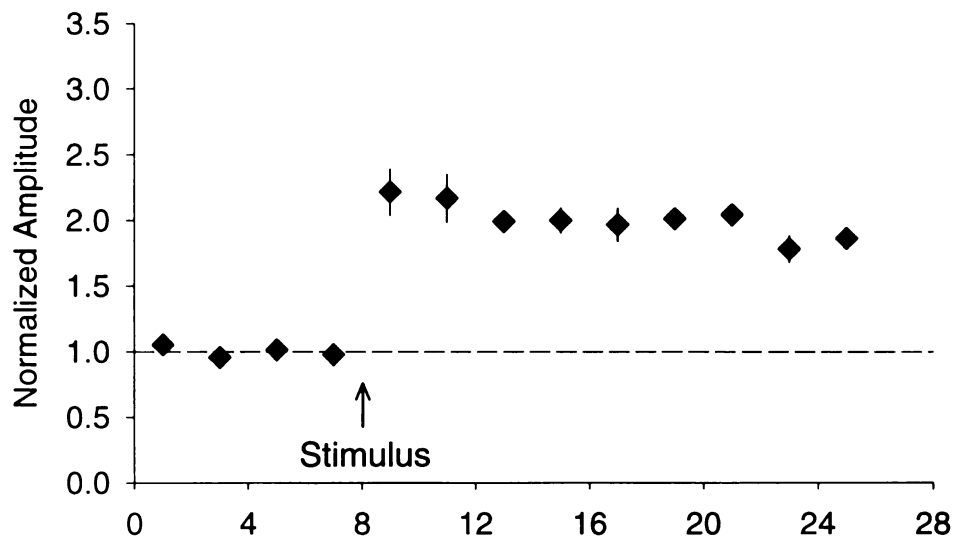


Figure 39. Application of 200 μM EGTA-AM, which decreases PPF causes a decrease in p_{calc} indicating that p_{calc} is not simply reflecting changes in PPF (n=4)

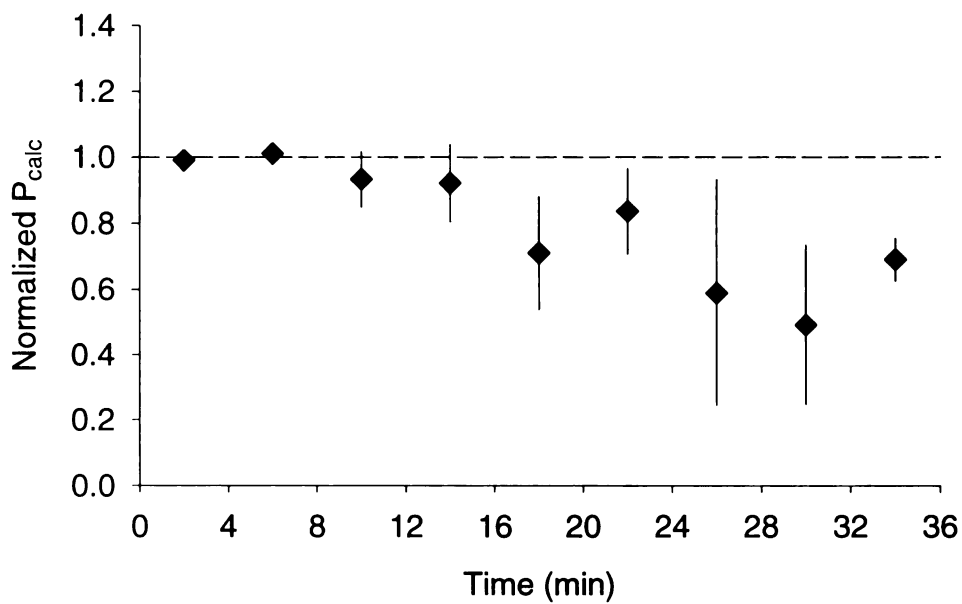
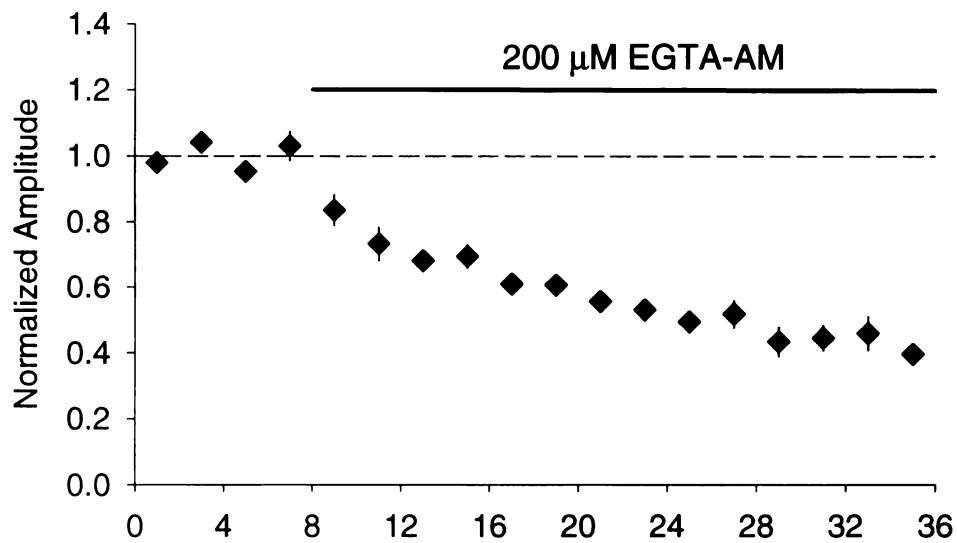


Figure 40. Long-term potentiation has no effect on p_{calc} .

A. Individual experiment showing changes in the amplitude of the initial EPSCs and the calculation of p_r following pairing induced LTP (100 stimuli at 1 Hz with the cell depolarized to 0 mv). The dashed lines give the average of all baseline data. Open squares are averages of 10 individual series of trial.

B. Average of six individual experiments shows changes in amplitude but not in p_{calc} following LTP induction. In two of these experiments LTP was induced by a 100 Hz tetanus with the cell held at 0 mv.

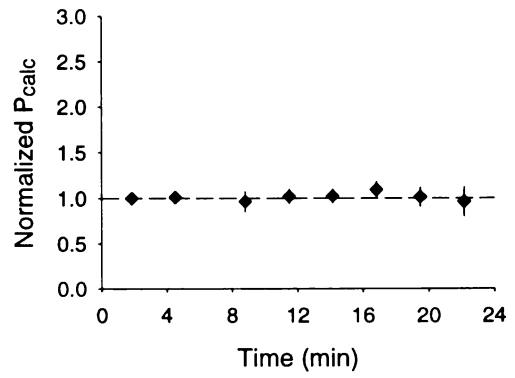
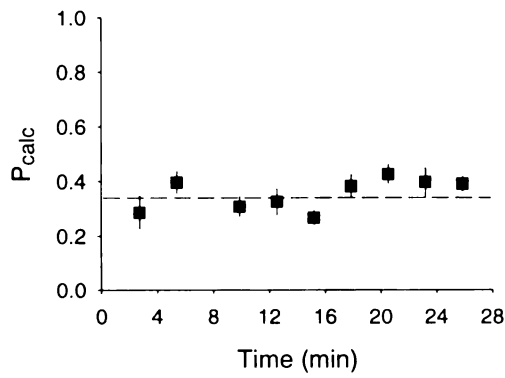
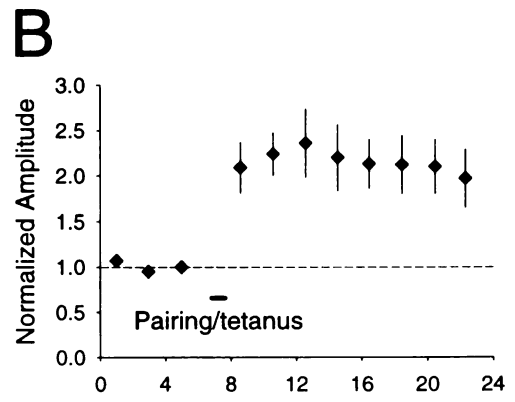
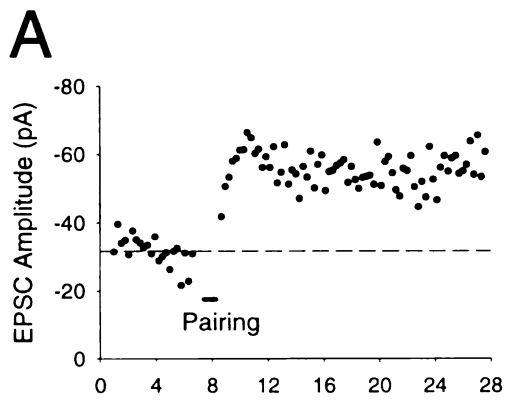


Figure 41. NMDA receptor-dependent long-term depression has no effect on p_{calc} .

A. Individual experiment showing changes in the amplitude of the initial EPSCs and calculation of p_r following LTD induced by prolonged low-frequency stimulation (5 minutes at 1 Hz) while the cell was held at -40 mv. Dashed lines are the average of all baseline data.

B. Average of six individual experiments shows changes in amplitude but not p_{calc} following induction of NMDA receptor-dependent LTD.

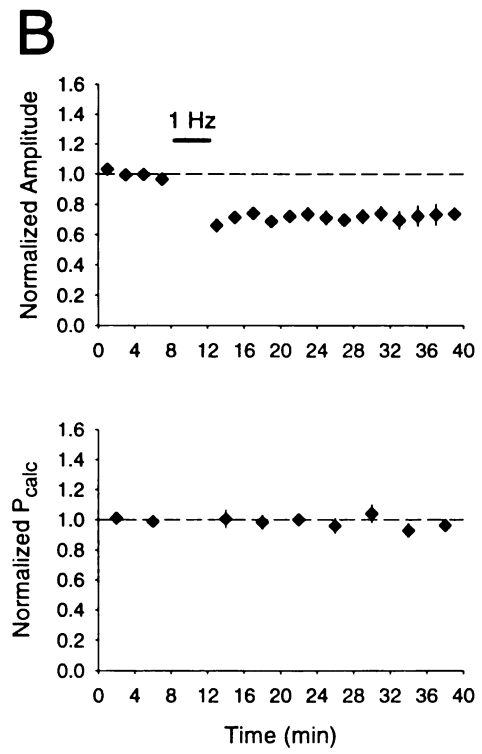
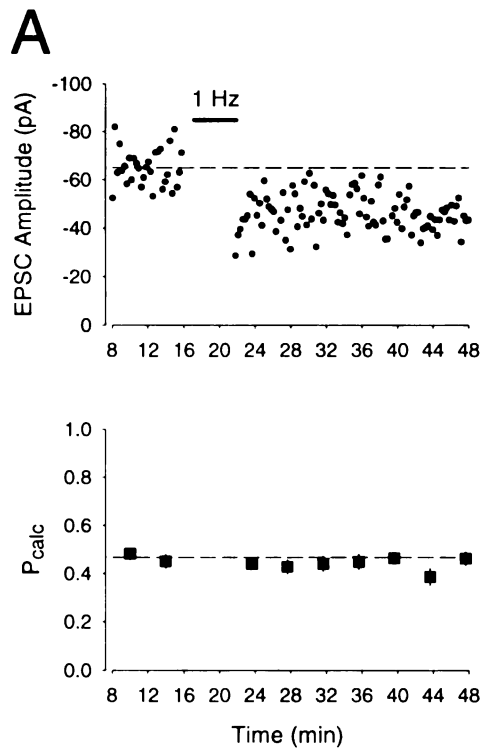


Figure 42. Summary of all manipulations plotted as the ratio of p_{calc} (following manipulation to baseline) to the ratio of EPSC amplitude. The dashed line is a linear regression through all individual control experiments where p_r was manipulated

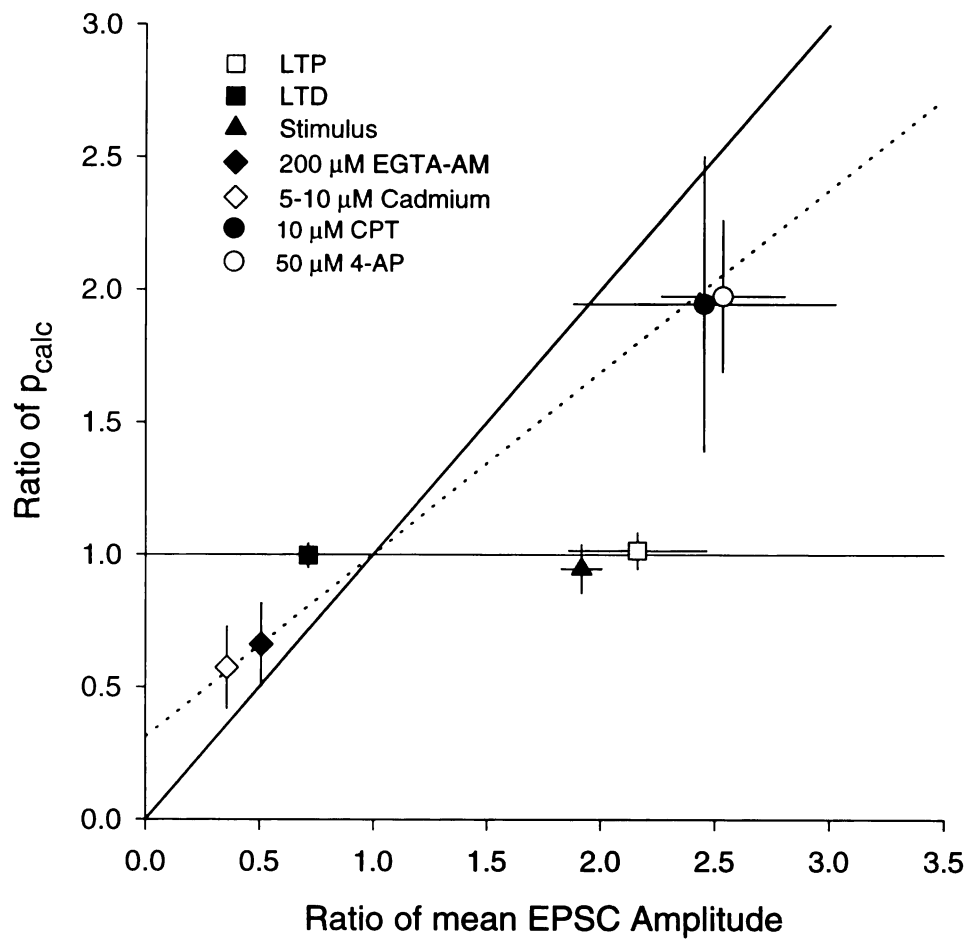
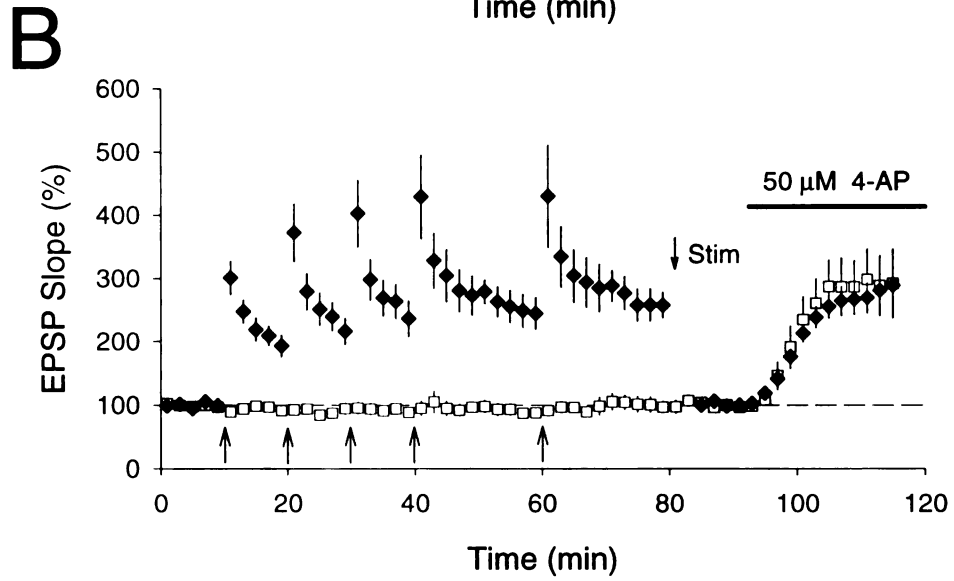
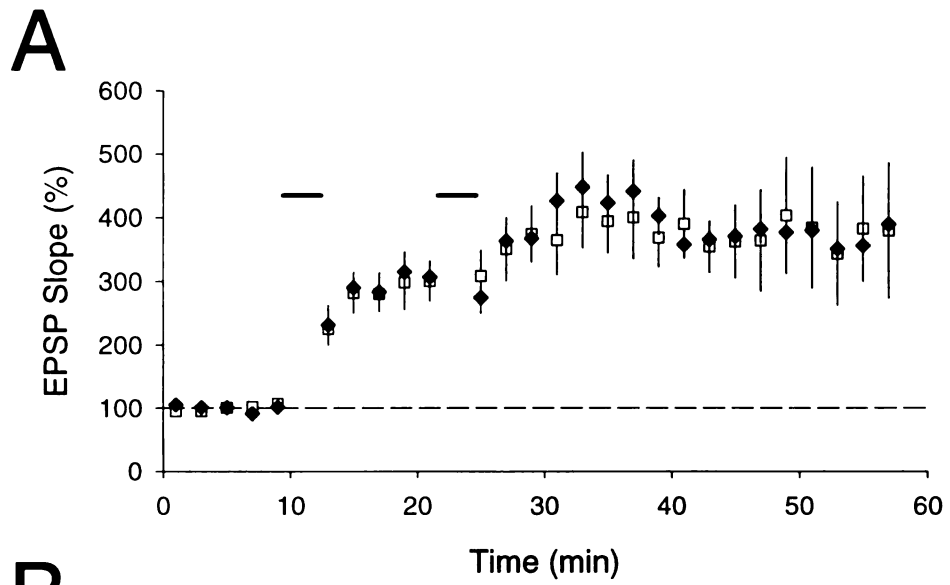


Figure 43. Long-term potentiation does not interact with a manipulation increasing p.

A. Using perforated patch recordings, a similar magnitude of LTP occurs under control conditions (open squares, n=4) and in the presence of 50 μ M 4-AP (filled diamonds, n=4). LTP was elicited with two episodes of pairing (100 stimuli at 1 Hz., cell depolarized to +10 mV).

B. A summary of six field experiments showing that application of 50 μ M 4-AP has a similar effect on a test pathway where LTP has been saturated and an independent control pathway. LTP was saturated by repeated 100 Hz tetani (each arrow is two 100 Hz tetani for 1 sec separated by 15 sec).



CHAPTER SEVEN

GENERAL CONCLUSIONS

The phenomenon of long-term potentiation provides a plausible biological mechanism to describe the changes that occur during learning and memory. Because of this, it is important to understand the specific mechanisms underlying LTP, as they may have a profound influence on our understanding of how the nervous system works.

Our work has concentrated on elucidating the particular quantal changes that underlie LTP. We have shown that while LTP can be associated with a change in the synaptic failure rate and the coefficient of variation, indicating that LTP is associated with an increase in quantal content, these changes are not easily compatible with an increase in the probability of release underlying LTP.

The comparison of LTP and LTD on the AMPA and the NMDA receptor-mediated currents indicates that these two currents do not change uniformly. This is most easily explained by separate post-synaptic mechanisms underlying the two processes (although it is important to add that simplicity—or for that matter parsimony—does not ensure that one's explanation is correct). The argument that spillover of glutamate from neighboring synapses occurs (Kullmann and Sieglebaum, 1995; Kullmann et al., 1996) has been used to explain the differential amounts of LTP on AMPA and NMDA receptors and the difference in $1/CV^2$ on the two components. Nevertheless, it does not explain the reversal of NMDA LTD (Figure 9) or the ability to depress the NMDA component in the absence of LTD of the AMPA component (Figure 12).

Injection of CaM kinase II into hippocampal CA1 pyramidal cells causes a potentiation that both mimics and occludes LTP. While we saw a decrease in the proportion of synaptic failures (Figures 15-16), we also observed an increase in the mEPSC amplitude and in the sensitivity to iontophoretically applied AMPA (Figure 17).

Furthermore, the increase to applied AMPA was similar in magnitude to the total amount of potentiation seen. One explanation of these data is that the change in failure rate was due to the uncovering of postsynaptic silent synapses (Liao et al., 1995; Isaac et al. 1995). Nevertheless, other explanations can be proposed. For instance, the iontophoresis data may be due, in part, to an increase in the sensitivity of extrasynaptic receptors, leaving room for an increase in p_r to explain the failure rate.

When recording from presumptive single sites, LTP could be induced without a concomitant reduction in synaptic failures (Figure 24), indicating that, at least in some cases, LTP was due solely to a change in the quantal amplitude. In those cases where a change in quantal content also occurred, it was inadequate to explain all of the potentiation that we observed. From this data, we clearly have evidence for a change in quantal amplitude, in part, underlying LTP. From these data alone, though, we cannot determine whether the change in quantal content is due to a change in probability of release or in the number of synapses being activated, although the analysis of paired-pulse potency indicated that the change occurred in n (Figure 26). We would propose that in some experiments we were recording from only a single release site, whereas in others, we were additionally stimulating a silent synapse, which was converted following the induction of LTP.

It is important to note that these data are inconsistent with two reports in the literature (Stevens and Wang, 1994; Bolshakov and Sieglebaum, 1995), which report that LTP at single sites is not accompanied by a change in potency, and therefore is exclusively due to an increase in p_r . There is no apparent explanation for this discrepancy between our laboratories—the two data sets do not appear to overlap (compare Figures 22

and 27 with Figure 4 from Stevens and Wang, 1994)—but it is plausible that some systematic bias, either in techniques or data analysis, is responsible for the discrepancy.

We attempted to circumvent this issue by utilizing a different approach. By analyzing the refractory period following synaptic stimulation, we have shown that LTP is not accompanied by an increase in the mean probability of release. This result is consistent with studies that observe no change during LTP in either paired-pulse facilitation (Manabe et al., 1993; Asztely et al., 1996; but see Schultz et al., 1994) or the use-dependent blockade of NMDA receptors with MK-801 (Manabe and Nicoll, 1994, but see Kullmann et al., 1996). While observing no change in p_r , our LTP was accompanied by a change in $1/CV^2$. Therefore, we would conclude that the change in quantal content observed with LTP is due to a change in the number of active synapses.

It should be noted that, aside from the iontophoresis data, from these results alone we are unable to distinguish a presynaptic change in n from a postsynaptic change in n . Furthermore, we cannot distinguish the difference in a presynaptic change in n from a presynaptic change in probability of release only at synapses with extremely low initial p_r . While the latter issue is basically semantic, the first issue of primary importance, and may be difficult to resolve. The fact that NMDA-only synapses can be potentiated so that AMPA responses are present where they were not before (Liao et al., 1995; Isaac et al., 1995) is difficult to resolve with a presynaptic mechanism, but it can be done (Kullmann and Sieglebaum, 1995; Malenka and Nicoll, 1997). This requires that one assumes there is spillover of glutamate onto NMDA receptors at neighboring synapses and that the silent synapse has a release probability of zero (or near zero). The spillover would

activate the NMDA receptor during pairing, which could then send a retrograde messenger to enhance the release probability at the synapse.

In conclusion, we find that LTP is associated with changes in two quantal parameters, q and n . Several hypotheses can explain these results by a single mechanism. For instance, LTP could occur by the addition of new AMPA receptors to synapses already containing receptors (resulting in a q change) or to postsynaptically silent synapses (resulting in an n change). Alternatively, a change in the affinity of the AMPA receptors at a given synapse may change during LTP, with silent synapses occurring when the initial affinity and/or the glutamate concentration is too low to cause receptor opening. On the other hand, there may be multiple mechanisms underlying the expression of LTP.

Ultimately, the answer to whether LTP is associated with a pre- versus a post-synaptic change will not be answered by quantal analysis, which can only implicate a specific parameter of synaptic transmission. Instead, direct evidence showing changes in the amount of neurotransmitter release or changes in the number or properties of AMPA channels during LTP will be required.

References

Abeliovich, A., Chen, C., Goda, Y., Silva, A. J., Stevens, C. F., and Tonegawa, S. (1993). Modified hippocampal long-term potentiation in PKC gamma-mutant mice. *Cell* 75, 1253-1262.

Allen, C., and Stevens, C. F. (1994). An evaluation of causes for unreliability of synaptic transmission. *Proc. Natl. Acad. Sci. USA* 91, 10380-10383.

Asztely, F., Wigstrom, H., and Gustafsson, B. (1992). The relative contribution of NMDA receptor channels in the expression of long-term potentiation in the hippocampal CA1 region. *Eur. J. Neurosci.* 4, 681-690.

Asztely, F., Xiao, M. Y., and Gustafsson, B. (1996). Long-term potentiation and paired-pulse facilitation in the hippocampal CA1 region. *Neuroreport*, 7,1609-1612.

Bear, M. F., Cooper, L. N., and Ebner, F. E. (1987). A physiological basis for a theory of synapse modification. *Science* 237, 42-48.

Bekkers, J. M., and Stevens, C. F. (1989). NMDA and non-NMDA receptors are co-localized at individual excitatory synapses in cultured rat hippocampus. *Nature* 341, 230-233.

Bekkers, J. M., and Stevens, C. F. (1990). Presynaptic mechanism for long-term potentiation in the hippocampus. *Nature* 346, 724-729.

Betz, W. (1970) Depression of transmitter release at the neuromuscular junction of the frog. *J. Physiol.* 206, 629-644.

Bienenstock, E. L., Cooper, L. N., and Munro, P. W. (1982). Theory for the development of neuron selectivity: orientation specificity and binocular interaction in visual cortex. *J. Neurosci.* 2, 32-48.

Blanton, M. G., Lo Turco, J. J., and Kriegstein, A.R. (1989) Whole cell recording from neurons in slices of reptilian and mammalian cerebral cortex. *J. Neurosci. Meth.* 30, 203-210.

Bliss, T. V. P., and Collingridge, G. L. (1993). A synaptic model of memory: long-term potentiation in the hippocampus. *Nature* 361, 31-39.

Bliss, T. V. P., and Lømo, T. (1973) Long-lasting potentiation of synaptic transmission in the dentate area of the anaesthetized rabbit following stimulation of the perforant path. *J. Physiol.* 232, 331-356.

Bolshakov, V. Y., and Siegelbaum, S. A. (1995). Regulation of hippocampal transmitter release during development and long-term potentiation. *Science* 269, 1730-1734.

Bolshakov, V. Y., and Siegelbaum, S. A. (1994). Postsynaptic induction and presynaptic expression of hippocampal long-term depression. *Science* 264, 1148-1152.

Bonhoeffer, T., Staiger, V., and Aertsen, A. (1989) Synaptic plasticity in rat hippocampal slice cultures: local "Hebbian" conjunction of pre- and postsynaptic stimulation leads to distributed synaptic enhancement. *Proc. Natl. Acad. Sci. U.S.A.* 86, 8113-8117.

Borst, J. G. G., and Sakmann, B. (1996). Calcium influx and transmitter release in a fast CNS synapse. *Nature* 383, 431-434.

Boyd, I. A., and Martin, A. R. (1956). The end-plate potential in mammalian muscle. *J. Physiol.* 132, 74-91.

Burgard, E. C., and Hablitz, J. J. (1993). NMDA receptor-mediated components of miniature excitatory synaptic currents in developing rat neocortex. *J. Neurophysiol.* 70, 1841-1852.

Calquohoun, D., Jonas, P., and Sakmann, B. (1992) Action of brief pulses of glutamate on AMPA/kainate receptors in patches from different neurones of rat hippocampal slices. *J. Physiol.* 458, 261-287.

Carmignoto, G., and Vicini, S. (1992). Activity-dependent decrease in NMDA receptor responses during development of the visual cortex. *Science* 258, 1007-1011.

Castillo, P. E., Salin, P. A., Weisskopf, M. G., and Nicoll, R. A. (1996). Characterizing the site and mode of action of dynorphin at hippocampal mossy fiber synapses in the guinea pig. *J. Neurosci.* 16, 5942-5950.

Chen, L., and Huang, L. Y. M. (1992). Protein kinase C reduces Mg^{2+} block of NMDA-receptor channels as a mechanism of modulation. *Nature* 356, 521-523.

Christie, B. R., and Abraham, W. C. (1992). Priming of associative long-term depression in the dentate gyrus by θ frequency synaptic activity. *Neuron* 9, 79-84.

Clark, K. A., and Collingridge, G. L. (1995). Synaptic potentiation of dual-component excitatory postsynaptic currents in the rat hippocampus. *J. Physiol.* 482, 39-52.

Clarke, E., and Dewhurst, K. (1972). An illustrated history of brain function. Berkeley: University of California Press.

Clarke, E., and O'Malley, C. D. (1996). The human brain and spinal cord: a historical study illustrated by writings from antiquity to the twentieth century. (2nd ed.) San Francisco: Norman Publishing.

Coan, E. J., Irving, A. J., and Collingridge, G. L. (1989). Low-frequency activation of the NMDA receptor system can prevent the induction of LTP. *Neurosci. Lett.* *105*, 205-210.

Collingridge, G. L., Kehl, S. J., and McLennan, H. (1983). Excitatory amino acids in synaptic transmission in the Schaffer collateral-commissural pathway of the rat hippocampus. *J. Physiol.* *334*, 33-46.

Crair, M.C. and Malenka, R.C. (1995). A critical period for long-term potentiation at thalamocortical synapses. *Nature* *375*, 325-328.

Davies, S. N., Lester, R. A. J., Reymann K. G., and Collingridge, G. L. (1989). Temporally distinct pre- and postsynaptic mechanisms maintain long-term potentiation. *Nature* *338*, 500-503.

Daw, N. W., Stein, P. S., and Fox, K. (1993). The role of NMDA receptors in information processing. *Ann. Rev. Neurosci.* *16*, 207-222.

del Castillo, J., and Katz, B. (1954a). Quantal components of the end-plate potential. *J. Physiol.* *124*, 560-573.

del Castillo, J., and Katz, B. (1954b). Statistical factors involved in neuromuscular facilitation and depression. *J. Physiol.* *124*, 574-585.

Descartes, R. (1931). The passions of the soul. In Haldane, E. S., and Ross, G. R. T., (Ed. and Trans.) The philosophical works of Descartes, volume I. New York: Dover (Original work published in 1649).

Dobrunz, L. E., and Stevens, C. F. (1997). Heterogeneity of release probability, facilitation and depletion at central synapses. *Neuron* 18, 995-1008.

Dudek, S. M., and Bear, M. F. (1992). Homosynaptic long-term depression in area CA1 of the hippocampus and effects of N-methyl-D-aspartate receptor blockade. *Proc. Natl. Acad. Sci. U.S.A.* 89, 4363-4367.

Dunwiddie, T. V., and Haas, H. L. (1985). Adenosine increases synaptic facilitation in the *in vitro* rat hippocampus: evidence for a presynaptic site of action. *J. Physiol.* 369, 365-377.

Edwards, F.A. (1991). LTP is a long-term problem. *Nature* 350, 271-272.

Engert, F., and Bonhoeffer, T. (1997). Synapse specificity of long-term potentiation breaks down at short distances. *Nature* 388, 279-284.

Faber, D. S., and Korn, H. (1991). Applicability of the coefficient of variation method for analyzing synaptic plasticity. *Biophys. J.* 60, 1288-1294.

Feng, T. P. (1941). Studies on the neuromuscular junction XXVI: the changes of the end-plate potential during and after prolonged stimulation. *Chinese J. Physiol.* *16*, 37-50.

Finger, S. (1994). *Origins of neuroscience: a history of explorations into brain function*. New York: Oxford University Press.

Foster, T. C., and McNaughton, B. L. (1991). Long-term enhancement of CA1 synaptic transmission is due to increased quantal size, not quantal content. *Hippocampus* *1*, 79-91.

Frerking, M., and Wilson, M. (1996). Effects of variance in mini amplitude and stimulus-evoked release: a comparison of two models. *Biophys. J.* *70*, 2078-2091.

Fujii, S., Saito, K., Miyakawa, H., Ito, K., and Kato, H. (1991). Reversal of long-term potentiation (depotentiation) induced by tetanus stimulation of the input to CA1 neurons of guinea pig hippocampal slices. *Brain Res.* *555*, 112-122.

Fukunaga, K., Stoppini, L., Miyamoto, E., and Muller, D. (1993). Long-term potentiation is associated with an increased activity of Ca²⁺/calmodulin-dependent protein kinase II. *J. Biol. Chem.* *268*, 7863-7867.

Gean, P. W., and Lin, J. H. (1993). D-2-amino-5-phosphonovalerate blocks induction of long-term depression of the NMDA receptor-mediated synaptic component in rat hippocampus. *Neurosci. Lett.* *158*, 170-172.

Grillner, S., Wallen, P., Brodin, L., and Lansner, A. (1991). Neuronal network generating locomotor behavior in lamprey: circuitry, transmitters, membrane properties, and simulation. *Ann. Rev. Neurosci.* *14*, 169-199.

Gustafsson, B., Huang, Y. Y., and Wigstrom, H. (1988). Phorbol ester-induced synaptic potentiation differs from long-term potentiation in the guinea pig hippocampus in vitro. *Neurosci. Lett.* *85*, 77-81.

Hebb, D. O. (1949). *The organization of behavior*. New York: John Wiley and Sons.

Hessler, N. A., Shirke, A. M., and Malinow, R. (1993). The probability of transmitter release at a mammalian central synapse. *Nature* *366*, 569-572.

Hestrin, S. (1992). Developmental regulation of NMDA receptor-mediated synaptic currents at a central synapse. *Nature* *357*, 686-689.

Hestrin, S., Perkel, D. J., Sah, P., Manabe, T., Renner, P., and Nicoll, R. A. (1990). Physiological properties of excitatory synaptic transmission in the central nervous system. *Cold Spring Harbor Symposia on Quantitative Biology* *55*, 87-93.

Heuser, J. E., Reese, T. S., Dennis, M. J., Jan, Y., Jan, L., and Evans, L. (1979). Synaptic vesicle exocytosis captured by quick freezing and correlated with quantal transmitter release. *J. Cell Biol.* *81*, 275-300.

Huang, Y. Y., Colino, A., Selig, D. K., and Malenka, R. C. (1992). The influence of prior synaptic activity on the induction of long-term potentiation. *Science* *255*, 730-733.

Hughes, J. R. (1958). Post-tetanic potentiation. *Physiol. Rev.* *38*, 91-113.

Hvalby, Ø., Hemmings, H. J., Paulsen, O., Czernik, A., Nairn, A., Godfraind, J., Jensen, V., Raastad, M., Storm, J., Andersen, P., and Greengard, P. (1994). Specificity of protein kinase inhibitor peptides and induction of long-term potentiation. *Proc. Natl. Acad. Sci. USA* *91*, 4761-4765.

Isaac, J. T. R., Hjelmstad, G. O., Nicoll, R. A., and Malenka, R. C. (1996). Long-term potentiation at single fiber inputs to hippocampal CA1 pyramidal cells. *Proc. Natl. Acad. Sci. USA* *93*, 8710-8715.

Isaac, J. T. R., Nicoll, R. A., and Malenka, R. C. (1995). Evidence for silent synapses: implications for the expression of LTP. *Neuron* *15*, 427-434.

Isaacson, J. S., and Hille, B. (1997). GABA_B-mediated presynaptic inhibition of excitatory transmission and synaptic vesicle dynamics in cultured hippocampal neurons. *Neuron* 18, 143-152.

Ito, I., Hidaka, H., and Sugiyama, H. (1991). Effects of KN-62, a specific inhibitor of calcium/calmodulin protein kinase II, on long-term potentiation in the rat hippocampus. *Neurosci. Lett.* 121, 119-121.

Izumi, Y., Clifford, D. B., and Zorumski, C. F. (1992). Inhibition of long-term potentiation by NMDA-mediated nitric oxide release. *Science* 257, 1273-1276.

James, W. (1890). *The principles of psychology vol. I.* New York: Henry Holt and Company.

Jonas, P., and Spruston, N. (1994). Mechanisms shaping glutamate-mediated excitatory postsynaptic currents in the CNS. *Curr. Opin. Neurobiol.* 4, 366-372.

Kamiya, H., Sawada, S., and Yamamoto, C. (1991). Persistent enhancement of transmitter release accompanying long-term potentiation in the guinea pig hippocampus. *Neurosci. Lett.* 130, 259-262.

Katz, B., and Miledi, R. (1968). The role of calcium in neuromuscular facilitation. *J. Physiol.* 195, 481-492.

Kauer, J. A., Malenka, R. C., and Nicoll, R. A. (1988). A persistent postsynaptic modification mediates long-term potentiation in the hippocampus. *Neuron* 1, 911-917.

Kelly, P. T., McGuinness, T. L., and Greengard, P. (1984). Evidence that the major postsynaptic density protein is a component of a Ca²⁺/calmodulin-dependent protein kinase. *Proc. Natl. Acad. Sci. USA* 81, 945-949.

Kelso, S. R., Nelson, T. E., and Leonard, J. P. (1992). Protein kinase C-mediated enhancement of NMDA currents by metabotropic glutamate receptors in *Xenopus* oocytes. *J. Physiol.* 449, 705-718.

Kennedy, M. B., Bennett, M. K., and Erondy, N. E. (1983). Biochemical and immunochemical evidence that the "major postsynaptic density protein" is a subunit of a calmodulin-dependent protein kinase. *Proc. Natl. Acad. Sci. USA* 80, 7357-7361.

Kolaj, M., Cerne, R., Cheng, G., Brickey, D. A., and Randic, M. (1994). Alpha subunit of calcium/calmodulin-dependent protein kinase enhances excitatory amino acid and synaptic responses of rat spinal dorsal horn neurons. *J. Neurophysiol.* 72, 2525-31.

Kombian, S. B., and Malenka, R. C. (1994). Simultaneous LTP of non-NMDA and LTD of NMDA-receptor-mediated responses in the nucleus accumbens. *Nature* 368, 242-246.

Korn, H., and Faber, D. S. (1991). Quantal analysis and synaptic efficacy in the CNS. *Trends Neurosci.* *14*, 439-445.

Korn, H., Mallet, A., Triller, A., and Faber, D. S. (1982). Transmission at a central inhibitory synapse. II. Quantal description of release, with a physical correlate for binomial n . *J. Neurophysiol.* *48*, 679-707.

Korn, H., Faber, D. S., Burnod, Y., and Triller, A. (1984). Regulation of efficacy at central synapses. *J. Neurosci.* *4*, 125-130.

Korn, H., Sur, C., Charpier, S., Legendre, P., and Faber, D. S. (1994). The one-vesicle hypothesis and multivesicular release. In *Molecular and Cellular Mechanisms of Neurotransmitter Release*, L. Stjärne, P. Greengard, S. Grillner, T. Hökfelt, and D. Ottoson, eds. (New York: Raven Press, Ltd.), pp. 301-322.

Kullmann, D. M. (1994). Amplitude fluctuations of dual-component EPSCs in hippocampal pyramidal cells: implications for long-term potentiation. *Neuron* *12*, 1111-1120.

Kullmann, D. M., and Siegelbaum, S. A. (1995). The site of expression of NMDA receptor-dependent LTP: New fuel for an old fire. *Neuron*, *15*, 997-1002.

Kullmann, D. M., Erdemli, G., and Asztely, F. (1996). LTP of AMPA and NMDA receptor-mediated signals: evidence for presynaptic expression and extrasynaptic glutamate spill-over. *Neuron* 17, 461-474.

Kullmann, D. M., Perkel, D. J., Manabe, T., and Nicoll, R. A. (1992). Ca^{2+} entry via postsynaptic voltage-sensitive Ca^{2+} channels can transiently potentiate excitatory synaptic transmission in the hippocampus. *Neuron* 9, 1175-1183.

Kullmann, D. M., and Nicoll, R. A. (1992). Long-term potentiation is associated with increases in quantal content and quantal amplitude. *Nature* 357, 240-244.

Larrabee, M. G., and Bronk, D. W. (1947). Prolonged facilitation of synaptic excitation in sympathetic ganglia. *J. Neurophysiol.* 10, 139-154

Larkman, A. U., and Jack, J. J. B. (1995). Synaptic plasticity: hippocampal LTP. *Curr. Opin. Neurobiol.* 5, 324-334.

Larkman, A., Hannay, T., Stratford, K, and Jack, J. (1992). Presynaptic release probability influences the locus of long-term potentiation. *Nature* 360, 70-73.

Liao, D., Hessler, N. A., and Malinow, R. (1995). Activation of postsynaptically silent synapses during pairing-induced LTP in CA1 region of hippocampal slice. *Nature* 375, 400-404.

Liao, D., Jones, A., and Malinow, R. (1992). Direct measurement of quantal changes underlying long-term potentiation. *Neuron* 9, 1089-1097.

Lieberman, D. N., and Mody, I. (1994). Regulation of NMDA channel function by endogenous Ca^{2+} -dependent phosphatase. *Nature* 369, 235-239.

Linden, D. J., and Routtenberg, A. (1989). The role of protein kinase C in long-term potentiation: a testable model. *Brain Res. Rev.* 14, 279-296.

Lipton, S. A., and Rosenberg, P. A. (1994). Excitatory amino acids as a final common pathway for neurologic disorders. *N. Engl. J. Med.* 330, 613-622.

Lisman, J. E. (1985). A mechanism for memory storage insensitive to molecular turnover: a bistable autophosphorylating kinase. *Proc. Natl. Acad. Sci. USA* 82, 3055-3057.

Lisman, J. (1994). The CaM kinase II hypothesis for the storage of synaptic memory. *Trends Neurosci.* 17, 406-412.

Lisman, J. E., and Harris, K. M. (1993). Quantal analysis and synaptic anatomy-integrating two views of hippocampal plasticity. *Trends Neurosci.* 16, 141-147.

Lledo, P.-M., Hjelmstad, G. O., Mukherji, S., Soderling, T. R., Malenka, R. C., and Nicoll, R.A. (1995). Calcium/calmodulin-dependent kinase II and long-term potentiation enhance synaptic transmission by the same mechanism. *Proc. Natl. Acad. Sci. USA* 92, 11175-11179.

Llinás, R., Walton, K., and Bohr, V. (1976). Synaptic transmission in squid giant synapse after potassium conductance blockage with external 3- and 4-aminopyridine. *Biophys. J.*, 16, 83-86.

Lloyd, D. P. C. (1949). Post-tetanic potentiation of response in monosynaptic reflex pathways of the spinal cord. *J. Gen. Physiol.* 33, 147-170.

Lynch, G., Larson, J., Kelso, S., Barrionuevo, G., and Schottler, F. (1983). Intracellular injections of EGTA block induction of hippocampal long-term potentiation. *Nature* 305, 719-721.

Magleby, K. L., and Miller, D. L. (1981). Is the quantum of transmitter release composed of subunits? A critical analysis in the mouse and frog. *J. Physiol.* 311, 262-287.

Malenka, R. C. (1994). Multiple forms of NMDA receptor-dependent synaptic plasticity in the hippocampus. In *Long-Term Potentiation, Volume 2*, M. Baudry and J.L. Davis, eds. (Cambridge, M.I.T. Press), pp. 121-142.

Malenka, R. C., and Nicoll, R. A. (1993). NMDA-receptor-dependent synaptic plasticity: multiple forms and mechanisms. *Trends Neurosci.* *16*, 521-527.

Malenka R. C., and Nicoll, R. A. (1997). Silent synapses speak up. *Neuron* *19*, 473-476.

Malenka, R. C., Kauer, J. A., Zucker, R. S., and Nicoll, R. A. (1988). Postsynaptic calcium is sufficient for potentiation of hippocampal synaptic transmission. *Science* *242*, 81-84.

Malenka, R. C., Kauer, J. A., Perkel, D. J., Kelly, P. T., Nicoll, R. A., and Waxham, M. N. (1989). An essential role for postsynaptic calmodulin and protein kinase activity in long-term potentiation. *Nature* *340*, 554-557.

Malinow, R. (1991). Transmission between pairs of hippocampal slice neurons: quantal levels, oscillations, and LTP. *Science* *252*, 722-724

Malinow, R., and Mainen, Z. F. (1996). Long-term potentiation in the CA1 hippocampus *Science* *271*, 1604-1605.

Malinow, R., and Tsien, R. W. (1990). Presynaptic enhancement shown by whole-cell recordings of long-term potentiation in hippocampal slices. *Nature* *346*, 177-180.

Malinow, R., Schulman, H., and Tsien, R. W. (1989). Inhibition of postsynaptic PKC or CaMKII blocks induction but not expression of LTP. *Science* 245, 862-866.

Manabe, T., and Nicoll, R. A. (1994). Long-term potentiation: evidence against an increase in transmitter release probability in the CA1 region of the hippocampus. *Science* 265, 1888-1892.

Manabe, T., Renner, P., and Nicoll, R.A.(1992). Postsynaptic contribution to long-term potentiation revealed by the analysis of miniature synaptic currents. *Nature* 355, 50-55.

Manabe, T., Wyllie, D. J. A., Perkel, D. J., and Nicoll, R. A. (1993). Modulation of synaptic transmission and long-term potentiation: effects of paired pulse facilitation and EPSC variance in the CA1 region of the hippocampus. *J. Neurophysiol.* 70, 1451-1459.

Markram, H., and Segal, M. (1992). Activation of protein kinase C suppresses responses to NMDA in rat CA1 hippocampal neurones. *J. Physiol.* 457, 491-501.

Mayford, M., Wang, J., Kandel, E. R., and O'Dell, T. J. (1995). CaMKII regulates the frequency-response function of hippocampal synapses for the production of both LTD and LTP. *Cell* 81, 891-904.

McBain, C., and Dingledine, R. (1992). Dual-component miniature excitatory synaptic currents in rat hippocampal CA3 cells. *J. Neurophysiol.* 68, 16-27.

McGlade-McCulloh, E., Yamamoto, H., Tan, S. E., Brickey, D. A., and Soderling, T. R. (1993). Phosphorylation and regulation of glutamate receptors by calcium/calmodulin-dependent protein kinase II. *Nature* 362, 640-642.

Miller, S. G., and Kennedy, M. B. (1986). Regulation of brain type II Ca²⁺/calmodulin-dependent protein kinase by autophosphorylation: a Ca²⁺-triggered molecular switch. *Cell* 41, 861-870.

Mukherji, S., Brickey, D. A., and Soderling, T. R. (1994). Mutational analysis of secondary structure in the autoinhibitory and autophosphorylation domains of calmodulin kinase II. *J. Biol. Chem.* 269, 20733-20738.

Mulkey, R. M., and Malenka, R. C. (1992). Mechanisms underlying induction of homosynaptic long-term depression in area CA1 of hippocampus. *Neuron* 9, 967-975.

Mulkey, R. M., Herron, C. H., and Malenka, R. C. (1993). An essential role for protein phosphatases in hippocampal long-term depression. *Science* 261, 1051-1055.

Mulkey, R. M., Endo, S., Shenolikar, S., and Malenka, R. C. (1994). Involvement of a calcineurin/inhibitor 1 phosphatase cascade in hippocampal long-term depression. *Nature* 369, 486-488.

Muller, D., and Lynch, G. (1988). Long-term potentiation differentially affects two components of synaptic responses in the hippocampus. *Proc. Natl. Acad. Sci. USA* 85, 9346-9350.

Muller, D., and Lynch, G. (1989). Evidence that changes in presynaptic calcium currents are not responsible for long-term potentiation in hippocampus. *Brain Res.* 479, 290-299.

Muller, D., Turnbull, J., Baudry, M., and Lynch, G. (1988). Phorbol ester-induced synaptic facilitation is different than long-term potentiation. *Proc. Natl. Acad. Sci. U.S.A.* 85, 6997-7000.

Murthy, V. N., Sejnowski, T. J., and Stevens, C. F. (1997). Heterogeneous Release Properties of Visualized Individual Hippocampal Synapses. *Neuron* 18, 599-612.

Neveu, D., and Zucker, R. S. (1996) Long-lasting potentiation and depression without presynaptic activity. *J. Neurophysiol.* 75, 2157-2160.

Nicoll R. A., and Malenka, R. C. (1995). Contrasting properties of two forms of long-term potentiation in the hippocampus. *Nature* 377, 115-118.

O'Conner, J. J., Rowan, M. J., and Anwyl, R. (1995). Tetanically induced LTP involves a similar increase in the AMPA and NMDA receptor components of the excitatory

postsynaptic current: investigations of the involvement of mGlu receptors. *J. Neurosci.* *15*, 2013-2020.

O'Dell, T. J., Kandel, E. R., and Grant, S. G. N. (1991). Long-term potentiation in the hippocampus is blocked by tyrosine kinase inhibitors. *Nature* *353*, 558-560.

Oliet, S. H. R., Malenka, R. C., and Nicoll, R. A. (1996). Bidirectional control of quantal size by synaptic activity in the hippocampus. *Science* *271*, 1294-1297.

Perkel, D. J., and Nicoll, R. A. (1993). Evidence for all-or-none regulation of neurotransmitter release: implications for long-term potentiation. *J. Physiol.* *471*, 481-500.

Pettit, D. L., Perlman, S., and Malinow, R. (1994). Potentiated transmission and prevention of further LTP by increased CaMKII activity in postsynaptic hippocampal slice neurons. *Science* *266*, 1881-1885.

Prince, D. A., and Stevens, C. F. (1992). Adenosine decreases neurotransmitter release at central synapses. *Proc. Natl. Acad. Sci. U.S.A.* *89*, 8586-8590.

Rae, J., Cooper, K., Gates, P., and Watsky, M. (1991). Low access resistance perforated patch recordings using amphotericin B. *J. Neurosci. Methods* *37*, 15-26.

Raastad, M. (1995). Extracellular activation of unitary excitatory synapses between hippocampal CA3 and CA1 pyramidal cells. *Eur.J.Neurosci.* 7, 1882-1888.

Raastad, M., Storm, J. F., and Andersen, P. (1992). Putative single quantum and single fibre excitatory postsynaptic currents show similar amplitude range and variability in rat hippocampal slices. *Eur. J. Neurosci.* 4, 113-117.

Raastad, M., and Lipowski, R. (1996). Diversity of postsynaptic amplitude and failure probability of unitary synapses between CA3 and CA1 cells in the rat hippocampus. *Eur. J. Neurosci.* 8, 1265-1274.

Rosenmund, C., and Westbrook, G. L. (1993a). Rundown of N-methyl-D-aspartate channels during whole-cell recording in rat hippocampal neurons: role of Ca^{2+} and ATP. *J. Physiol.* 470, 705-729.

Rosenmund, C., and Westbrook, G. L. (1993b). Calcium-induced actin depolymerization reduces NMDA channel activity. *Neuron* 10, 805-814.

Rosenmund, C., Clements, J. D., and Westbrook, G. L. (1993). Non-uniform probability of glutamate release at a hippocampal synapse. *Science* 262, 754-757.

Schulz, P. E. (1997). Long-term potentiation involves increases in the probability of neurotransmitter release. *Proc. Natl. Acad. Sci. (USA)* 94, 5888-5893.

Schulz, P. E., Cook, E. P., and Johnston, D. (1994). Changes in paired-pulse facilitation suggest presynaptic involvement in long-term potentiation. *J. Neurosci.* *14*, 5325-37.

Selig, D. K., Hjelmstad, G. O., Herron, C., Nicoll, R. A., and Malenka, R. C. (1995). Independent mechanisms of long-term depression of AMPA and NMDA responses. *Neuron* *15*, 417-426.

Sherrington, C. (1906) *The integrative action of the nervous system*. New York: C. Scribner's sons.

Schuman, E. M., and Madison, D. V. (1994) Locally distributed synaptic potentiation in the hippocampus. *Science* *263*, 532-536.

Silva, A. J., Stevens, C. F., Tonegawa, S. & Wang, Y. (1992) Deficient hippocampal long-term potentiation in alpha calcium-calmodulin kinase II mutant mice. *Science* *257*, 201-206.

Sorra, K. E., and Harris, K. M. (1993). Occurrence and three-dimensional structure of multiple synapses between individual radiatum axons and their target pyramidal cells in hippocampal area CA1. *J. Neurosci.* *13*, 3736-3748.

Spruston, N., Jaffe, D. B., Williams, S. H., and Johnston, D. (1993). Voltage-clamp and space-clamp errors associated with the measurement of electronically remote synaptic events. *J. Neurophysiol.* *70*, 781-802.

Stern, P., Edwards, F. A., and Sakmann, B. (1992). Fast and slow components of unitary EPSCs on stellate cells elicited by focal stimulation in slices of rat visual cortex. *J. Physiol.* *449*, 247-278.

Stevens, C. F., and Wang, Y. (1994). Changes in reliability of synaptic function as a mechanism for plasticity. *Nature* *371*, 704-707.

Stevens, C. F., and Wang, Y. (1995). Facilitation and depression at single central synapses. *Neuron* *14*, 795-802.

Stricker, C., Field, A. C., and Redman, S. J. (1996a). Statistical analysis of amplitude fluctuations in EPSCs evoked in rat CA1 pyramidal neurones *in vitro*. *J. Physiol.* *490*, 419-441.

Stricker, C., Field, A. C., and Redman, S. J. (1996b). Changes in quantal parameters of EPSCs in rat CA1 neurons *in vitro* after the induction of long-term potentiation. *J. Physiol.* *490*, 443-454.

Tong, G., and Jahr, C. E. (1994). Regulation of glycine-insensitive desensitization of the NMDA receptor in outside-out patches. *J. Neurophysiol.* 72, 754-761.

Tong, G., Shepherd, D., and Jahr, C. E. (1995). Synaptic desensitization of NMDA receptors by calcineurin. *Science* 267, 1510-1512.

Triller, A., and Korn, H. (1985). Activity-dependent deformations of presynaptic grids at central synapses. *J. Neurocytol.* 14, 177-192.

Urushihara, H., Tohda, M., and Nomura, Y. (1992). Selective potentiation of N-methyl-D-aspartate-induced current by protein kinase C in *Xenopus* oocytes injected with rat brain RNA. *J. Biol. Chem.* 267, 11697-11700.

Walmsley, B. (1995). Interpretation of 'quantal' peaks in distributions of evoked synaptic transmission at central synapses. *Proc. R. Soc. Lond. [Biol.]* 261, 245-250.

Wang, J.-H., and Feng, D.-P. (1992). Postsynaptic protein kinase C essential to induction and maintenance of long-term potentiation in the hippocampal CA1 region. *Proc. Natl. Acad. Sci. USA* 89, 2576-2580.

Wang, J. H., and Kelly, P. T. (1995) Postsynaptic injection of CA2+/CaM induces synaptic potentiation requiring CaMKII and PKC activity. *Neuron* 15, 443-452.

Wang, Y. T., and Salter, M. W. (1994). Regulation of NMDA receptors by tyrosine kinases and phosphatases. *Nature* 369, 233-235.

Wexler, E. M., and Stanton, P. K. (1993). Priming of homosynaptic long-term depression in hippocampus by previous synaptic activity. *Neuroreport* 4, 591-594.

Wyllie, D. J. A., and Nicoll, R. A. (1994). A role for protein kinases and phosphatases in the Ca²⁺-induced enhancement of AMPA receptor-mediated synaptic responses in the hippocampus. *Neuron* 13, 635-643.

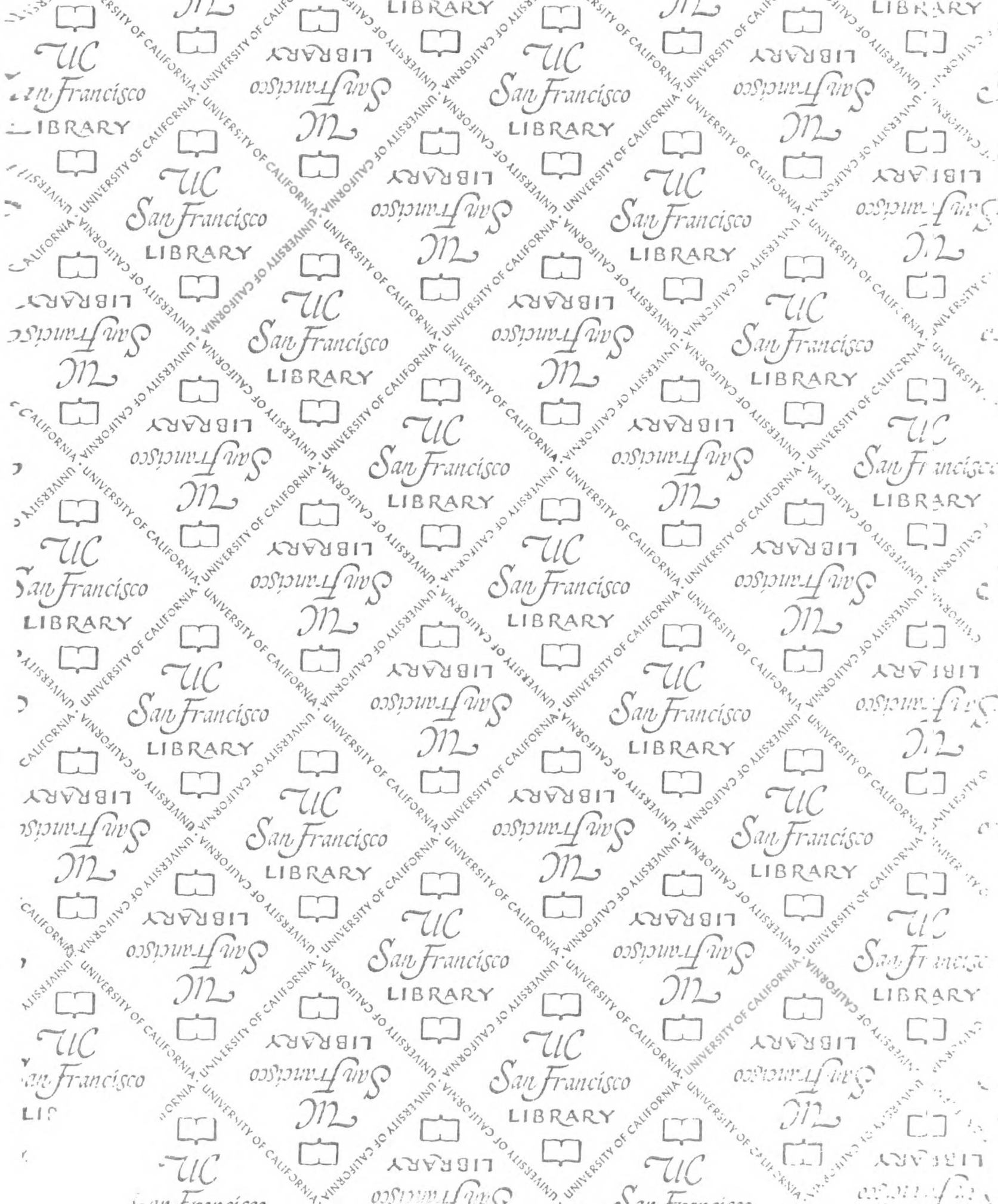
Xiao, M.-Y., Wigstrom, H., and Gustafsson, B. (1994). Long-term depression in the hippocampal CA1 region is associated with equal changes in AMPA and NMDA receptor-mediated synaptic potentials. *Eur. J. Neurosci.* 6, 1055-1057.

Xie, X., Berger, T. W., and Barrioneuvo, G. (1992). Isolated NMDA receptor-mediated synaptic responses express both LTP and LTD. *J. Neurophysiol.* 67, 1009-1013.

Yakel, J. L., Vissavajhala, P., Derkach, V. A., Brickey, D. A., and Soderling, T. R. (1995). Identification of a Ca²⁺/calmodulin-dependent protein kinase II regulatory phosphorylation site in non-N-methyl-D-aspartate glutamate receptors. *Proc. Natl. Acad. Sci. USA* 92, 1376-80.

Yang, X. D. and Faber, D. S. (1991). Initial synaptic efficacy influences induction and expression of long-term changes in transmission. *Proc. Natl. Acad. Sci. U.S.A.* 88, 4299-4303.

Zucker, R. S. (1989). Short-term synaptic plasticity. *Ann. Rev. Neurosci.* 12, 13-31.



For reference

Not to be taken from the room.



